UNCLASSIFIED

SECURITY CLASSIFICATION OF THIS PAGE (When Data Entered)

(1)

REPORT DOCUMENTATION PAGE		READ INSTRUCTIONS BEFORE COMPLETING FORM
1. REPORT NUMBER AFIT/CI/NR 88-107	2. GOVT ACCESSION NO.	3. RECIPIENT'S CATALOG NUMBER
4. TITLE (and Subtitle) THE ROLE OF A LID IN THE 31 MAY 1985 TORNADO OUTBREAK		5. TYPE OF REPORT & PERIOD COVERED MS THESIS 6. PERFORMING ORG. REPORT NUMBER
7. AUTHOR(s) ROBERT J. FARRELL, JR.		8. CONTRACT OR GRANT NUMBER(s)
9. PERFORMING ORGANIZATION NAME AND ADDRESS AFIT STUDENT AT: PENNSYLVANIA STATE UNIVERSITY		10. PROGRAM ELEMENT, PROJECT, TASK AREA & WORK UNIT NUMBERS
11. CONTROLLING OFFICE NAME AND ADDRESS		12. REPORT DATE 1988 13. NUMBER OF PAGES
14. MONITORING AGENCY NAME & ADDRESS(if different from Controlling Office) AFIT/NR Wright-Patterson AFB OH 45433-6583		15. SECURITY CLASS. (of this report) UNCLASSIFIED 15a. DECLASSIFICATION/DOWNGRADING SCHEDULE

16. DISTRIBUTION STATEMENT (of this Report)

DISTRIBUTED UNLIMITED: APPROVED FOR PUBLIC RELEASE

17. DISTRIBUTION STATEMENT (of the abstract entered in Block 20, if different from Report)

SAME AS REPORT

18. SUPPLEMENTARY NOTES

Approved for Public Release: IAW AFR 190-1
LYNN E. WOLAVER
Dean for Research and Professional Development
Air Force Institute of Technology
Wright-Patterson AFB OH 45433-6583

19. KEY WORDS (Continue on reverse side if necessary and identify by block number)

20. ABSTRACT (Continue on reverse side if necessary and identify by block number)

ATTACHED

DD FORM 1 JAN 73 1473 EDITION OF 1 NOV 65 IS OBSOLETE

UNCLASSIFIED

SECURITY CLASSIFICATION OF THIS PAGE (When Data Entered)

ABSTRACT

The Carlson-Ludlam Conceptual Model is useful for predicting severe convective outbreaks. Central to the entire model is the presence of an elevated mixed layer that caps and then helps focus the release of built-up latent instability in a concentrated area. An historical review of the the model's development and a thorough discussion of the concepts involved is presented. It is concluded that it is very successful at explaining many of the processes which produce severe convection. Subjective analysis necessary to use this model, however, is much too time consuming for operational forecasting. Therefore, a computer application is presented that objectively delineates lid involvement.

The 31 May 1985 Tornado Outbreak occurred in the NE United States. Analysis reveals that there were four critical factors in the pre-storm environment responsible for the severity of the outbreak: (1) the presence of a lid and the resulting build-up of a high wet-bulb potential temperature in the boundary layer, (2) readily available soil moisture, (3) underrunning, and (4) forced ascent associated with baroclinic forcing from a migrating short wave. Because vigorous short waves move across the NE United States several times each Spring and such outbreaks rarely occur, it is concluded that the lid was the most critical factor. This conclusion is supported by a climatological analysis which found two important relationships: (1) the frequency of lid days highly parallels the frequency of tornado occurrences throughout the nation, and (2) lids have a significant impact on the value of wet-bulb potential temperature, particularly in the north during the Spring.

The Pennsylvania State University

The Graduate School

Department of Meteorology

THE ROLE OF A LID IN THE 31 MAY 1985 TORNADO OUTBREAK

A Thesis in

Meteorology

by

Robert J. Farrell, Jr.

Submitted in Partial Fulfillment
of the Requirements
for the Degree of

Master of Science

May 1988

I grant The Pennsylvania State University the nonexclusive right to use this work for the University's own purposes and to make single copies of the work available to the public on a not-for-profit basis if copies are not otherwise available.

Robert J. Farrell, Jr.

We approve the thesis of Robert J. Farrell, Jr..

Date of Signature:

Toby N. Carlson — 7 March 1988
Professor of Meteorology
Thesis Advisor

Gregory S. Forbes — 4 March 1988
Associate Professor of Meteorology

William Frank — 7 March 1988
Associate Professor of Meteorology
Head of the Department of Meteorology

ABSTRACT

Because severe convective systems are normally on the mesoscale and the available data is on the macroscale (synoptic scale), accurate prediction of these systems continues to elude the meteorological community. The Carlson-Ludlam Conceptual Model (Carlson and Ludlam, 1968) has been proven insightful at filling this gap, and consequently, useful for predicting the location of severe convective development. Central to the entire model is the production of a warm, dry, elevated mixed layer that caps and then helps focus the release of built-up latent instability in a concentrated area.

An historical review of the model's development and a thorough discussion of the concepts involved is presented. It is concluded that this conceptual model is very successful at explaining the processes which produce much of the severe convective storm activity in many parts of the world. Subjective analysis necessary to use this conceptual model, however, is much too time consuming for operational forecasting. Therefore, a computer application was developed to objectively delineate lid involvement. This application and the ideas discussed are used to both analyze a major tornadic event and develop a climatology of the lid and its attendant parameters.

The 31 May 1985 Tornado Outbreak occurred in eastern Ohio, Western Pennsylvania, New York State, and Ontario. It is the worst tornado outbreak, in terms of damage and death, to strike the United States since the super outbreak of 3-4 April 1974. Analysis reveals that there were four critical factors in the pre-storm environment responsible for the severity of the outbreak: (1) the presence of a strong lid and the resulting build-up of a high wet-bulb potential temperature (θ_w) in the planetary boundary layer (PBL), (2) readily available soil moisture, (3) underrunning, and (4) forced ascent associated with baroclinic forcing resulting from a migrating short wave.

Because vigorous short-wave troughs move across the northeastern United States several times each spring and such outbreaks rarely occur, it is concluded that the lid must have been the most critical factor. This conclusion is supported by the climatological analysis which found three important relationships: (1) in the northeastern United States, lids are as rare an event as tornadic outbreaks, (2) the frequency of lid days highly parallels the frequency of tornado occurrences throughout the nation, and (3) lids have a significant impact on the value of θ_w in the PBL, particularly in the north during the Spring.

TABLE OF CONTENTS

TABLE OF CONTENTS (continued)

LIST OF TABLES

LIST OF FIGURES

LIST OF FIGURES (continued)

LIST OF SYMBOLS

Symbol	*Description*
API	Antecedent Precipitation Index
CCL	Convective Condensation Level
EML	Elevated Mixed Layer
ζ	Relative vorticity
f	Coriolis Force
GMT	Greenwich Mean Time
LCL	Lifted Condensation Level
LFC	Level of Free Convection
LI	Lifted Index
L.I.D.	Lid Involvement Delineator
LSI	Lid Strength Index
MCL	Mixing Condensation Level
NWS	National Weather Service
PBL	Planetary Boundary Layer
POR	Period of Record
q	Specific Humidity
θ	Potential Temperature
θ_w	Wet-bulb Potential Temperature
θ_{bw}	The maximum ("best") 50 mb-thick layer-averaged Wet-bulb Potential Temperature in the planetary boundary layer
θ_{sw}	Saturation Wet-bulb Potential Temperature
θ_{sw5}	Saturation Wet-bulb Potential Temperature at 500 mb
θ_{swl}	The maximum Saturated Wet-bulb Potential Temperature from the "reference level" up to 500 mb (see Section 3.1)

θ_{wsfc}	Wet-bulb Potential Temperature at the surface
$\Delta\theta_{bw}$	The difference between the average θ_{bw} when a lid is present and the average θ_{bw} with *no conditions*
SBT	Surface Buoyancy Term
T	Dry-bulb Temperature
Td	Dewpoint Temperature
Tdd	Dewpoint Depression
t	Time in GMT
w	Mixing Ratio

ACKNOWLEDGMENTS

I would first like to express my heartfelt gratitude to Professor Toby Carlson, my thesis advisor, for his invaluable guidance and for imparting his enthusiasm throughout the course of both my research work and the preparation of this thesis. It was particularly difficult in this case because I completed this work in absentia. Dr. Carlson's persistence and patience is deeply appreciated.

I thank Professor Gregory Forbes for his review of this manuscript and his encouraging comments; I thank Barry Lynn for contributing his analysis of soil moisture which is integrated into Chapter 4; and I thank the United States Air Force for their financial support through the Air Force Institute of Technology, and their research support through Grant No. AFOSR-83-0064.

I am also very grateful to my parents who taught me the worth of dedication to education. My deepest appreciation is given to my wife and best friend, Kim, whose support and endearing patience made the whole endeavor possible. Special recognition must go to my children: daughter, Heather, for her contributions to my map analyses and son, Bobby, for breaking up the monotony by showing up in the middle of it all. I thank God every day for these aforementioned blessings.

Chapter 1

INTRODUCTION

The last 45 years have seen a great increase in the understanding of the initiation and evolution of severe, organized, mid-latitude, convective systems and their dynamic and thermodynamic structures. Accurate prediction of these systems, however, continues to elude us. With the destructive winds, hail, flash flooding, and the relative suddenness of these storms, it is obvious that these severe convective systems are the most threatening weather events to human life, property and operations. Therefore, new insights into the forecasting of these systems continue to be desirable.

Most severe convective storms in mid-latitudes are mesoscale phenomena. The term mesoscale refers to an intermediate scale between the microscale and macroscale (synoptic scale). This scale encompasses phenomena that occur horizontally, extending between 2 and 2,000 km and with a period ranging from a few hours to a few days (Orlanski, 1975). Currently, a major problem in the analysis and prediction of these convective storms is the fact that the rawinsonde network is on the synoptic scale. Development of methods to effectively predict areas of severe convection, using this current synoptic scale data network, would be of significant operational value. One such method which has been proven insightful involves the analysis of synoptic scale environments using a conceptual model first introduced by Carlson and Ludlam in 1968. This model helps explain how a stratification, favorable for the development of severe weather, is created. Central to the entire conceptual model is the production of an anomalously warm, elevated mixed layer which caps and then helps focus the release of latent instability in a concentrated area. In keeping with current terminology, this capping inversion will henceforth be referred to as the "lid."

1.1 Purpose

The purpose of this thesis is fourfold:

(1) to encapsulate, as much as possible, the development of the conceptual model. Since its introduction, there have been a lot of improvements in the understanding of the physical processes involved. It is intended here to review these physical processes in a form suitable for undergraduate course work. This topic is addressed in Chapter 2.

(2) to present an objective analysis routine which is adequate at determining the location and areal extent of existing lids. Subjective analysis is much too time consuming for operational forecasters. Therefore, some type of computer-generated output is needed to help diagnose lid involvement. This issue is addressed in Chapter 3.

(3) to present a case study showing the applicability of the conceptual model in predicting the occurrence of severe convection. It is also shown that one can track the lid over two days or more, and that the lid affects other parts of the nation besides the Great Plains. The 31 May 1985 Tornado Outbreak is used as illustration. This study is presented in Chapter 4.

(4) to present a climatology of lid occurrences over the United States to show the prevalence of lids and to suggest their importance in severe weather production. Most, if not all, current severe storm analysis and forecasting methods do not incorporate the lid concept. Therefore, it is hoped that this study will further underscore the importance of the lid. This climatology is presented in Chapter 5.

Although several authors have published articles reviewing many of the advancements leading up to the introduction of the conceptual model (e.g., Carlson et al., 1983; Lanicci, 1984b), it is useful to consider, for completeness, the following historical review.

1.2 Historical Review

Throughout most the the 19th century, scientific literature on severe convection in the United States consisted mainly of statistics and descriptions of storm damage. By the close of the century, however, attention moved to the observed structure of the atmosphere. Finley (1885) reported that severe thunderstorms were related to the large scale synoptic patterns. Ferrel (1895) and Finley (1890) observed that unstable equilibrium (warm, moist air lying below cold, dry air) was a necessary condition for tornado development. This indicated that the southeastern quadrant of a low pressure area or the warm sector, when using frontal theory (Bjerknes, 1919; and Bjerknes and Solberg, 1922) was the preferred zone for tornadic storms.

Using kites and hot air balloons, Varney (1926) found that a capping inversion and a vertical wind shear preceded severe thunderstorms. Varney's article is the earliest known documentation of these phenomena. Humphreys (1926) attempted to explain this inversion as a result of subsidence. Although this explanation has since been proven incorrect, it remains a common misconception (e.g., Hoxit and Chappell, 1975). It has been determined that Humphreys was also the first to document the hypothesis that geographically favored areas for tornadic storms are linked to topography. This was later noted by others (e.g., Fulks, 1951; Fawbush et al., 1951; and Palémen and Newton, 1969, p. 401).

In the 1930's, the introduction of radiosonde observations advanced the study of severe convective environments. Lloyd (1942) used these soundings to follow the trajectories of air that formed the capping inversion. He referred to the air above the inversion nose as a "dry superior air mass." The *Glossary of Meteorology* (Huschke, 1959) defines a superior airmass as:

> An exceptionally dry mass of air formed by subsidence and usually found aloft but occasionally reaching the earth's surface during extreme subsidence processes. It is often found above mT [marine tropical air], bounded by the trade-wind inversion. (p. 556)

Lloyd claimed that this air is marine polar air to the west which subsides as it travels eastward and eventually overruns the marine tropical air from the Gulf of Mexico. Berry et al. (1945, p. 627) claimed that the origin of this "superior air" was inconclusive. It is shown in Chapter 2 that the origin of this "superior air" is actually from a deep mixed layer over the desert regions of the southwest United States and northern Mexico and not the result of subsidence. Berry et al. are the earliest known to have referred to this capping inversion as a "lid." Later investigators also used "lid" to describe the inversion (Means, 1952, p. 173; Petterssen, 1956b, p. 55; Sugg and Foster, 1954, p. 139).

Research done during the 1930's and 1940's began to link severe thunderstorms and tornadoes with individual features in the atmosphere; however, a comprehensive method of prediction had yet to be developed. In March 1948, without any prior warning, a severely damaging tornado struck Tinker AFB, Oklahoma. Lt. Col. E.J. Fawbush and Capt. R.C. Miller were asked to study the feasibility of forecasting such occurrences. They used semi-empirical research methods to develop the needed forecasting techniques.

The first publication of Fawbush and Miller's research (Fawbush et al., 1951) appeared in the Bulletin of the American Meteorological Society. This article was based on their accumulated experiences throughout the 1940's, which they only began to apply in 1949. It dealt mainly with synoptic relationships to severe thunderstorm occurrences. Presented were six conditions which they felt were necessary for tornadoes to occur:

> (1) A layer of moist air near the earth's surface must be ... [capped] by a deep layer of dry air.
>
> (2) The horizontal moisture lapse rate within the moist layer must exhibit a distinct maximum along a relatively narrow band (i.e., a moisture wedge or ridge).

(3) The horizontal distribution of winds aloft must exhibit a maximum of speed along a relatively narrow band at some level between 10,000 and 20,000 feet (3 and 6 km), with the maximum speed exceeding 35 kt.

(4) The vertical projection of the axis of wind maximum must intersect the axis of the moisture ridge.

(5) The temperature lapse rate of the air column as a whole must be such as to indicate conditional instability.

(6) The moist layer must be subjected to appreciable lifting. (pp. 4-5)

They noted that other researchers had individually expressed or implied some of these rules: Jakl (1944), Lemons (1939), Humphreys (1940, pp. 218-224), Lloyd (1942), and especially Showalter and Fulks (1943) who discussed most of these concepts. Fawbush et al., however, were the first to emphasize that, "successful forecasting depends on consideration of the complete set ... which must be satisfied simultaneously at the time of the first appearance of ... [severe storms]." It is shown in Chapter 2 that the first five of these conditions are consistent with the processes associated with the conceptual model, while the sixth is a misconception.

A year later, Fawbush and Miller (1952) published a paper which presented a mean sounding of the tornado "airmass." The sounding was compiled using 72 soundings, from 1948 to 1952, which were taken within 6 hours and 200 miles of confirmed tornado occurrences. They compared their results with earlier work done by Showalter and Fulks (1943) and found insignificant differences. In 1954 they published a refinement to the composite by considering 155 additional soundings. They also introduced the typing of tornado "airmasses" and designated the original mean sounding as being of Type I. Two other types were described but are not relevant to this discussion. (A fourth type was added by Miller in 1967).

The Type I composite sounding has two strata, both in the troposphere and separated by an inversion. Each stratum has a conditionally unstable lapse rate (Figure 1.1). The

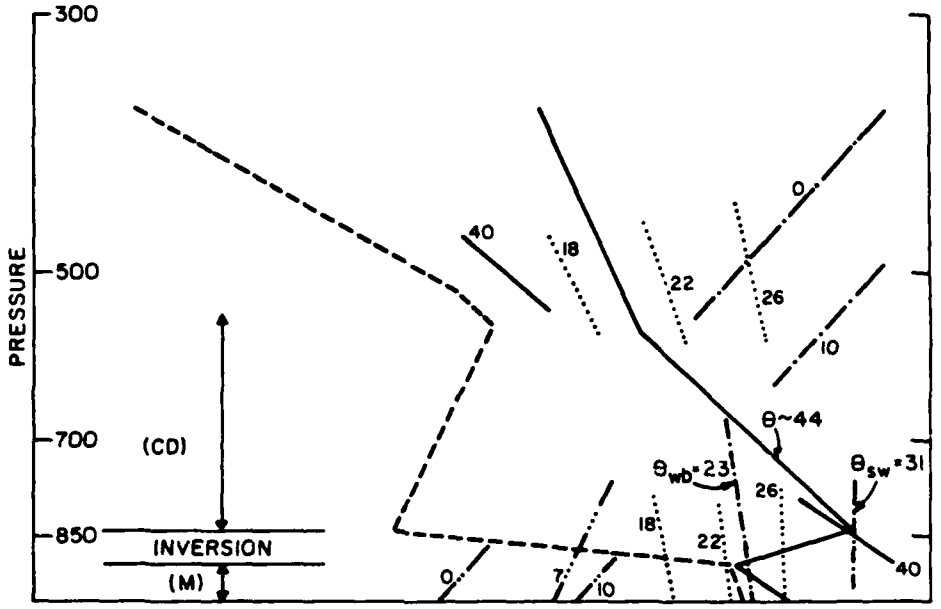

Figure 1.1: Schematic lid sounding on a Skew-T Log-p diagram. The vertical temperature profile is indicated by the solid line and the dewpoint profile is indicated by the dashed line. The dashed double-dotted line segments slanting upward and toward the right are portions of isotherms. The dashed triple-dotted line segment slanting less sharply toward the right than the isotherms is a portion of a saturation mixing ratio line. The solid line slanting upward and to the left is a portion of a dry adiabat. The dotted lines slanting less sharply to the left than the dry adiabats are moist adiabats. The dashed single-dotted lines are moist adiabats representing the maximum or "best" 50-mb layeraveraged wet-bulb potential temperature (θ_{bw}; discussed in Chapter 3) and the saturation wet-bulb potential temperature at the nose of the inversion (θ_{swI}). The potential temperature (θ) of the well mixed layer above the inversion is also indicated. A low-level moist layer (M) and a mid-level well mixed layer (CD) are highlighted to the left. (Adapted from Goldman, 1981).

lower stratum possesses a high relative humidity, usually over 65%, and a dewpoint over 55°F (12.7°C). This layer is capped by an inversion (which at the time was attributed to subsidence). At the inversion base, the relative humidity is 82% (range: 62-100%). The moisture mixes vertically from the surface but is trapped by the capping inversion and increases with time below the inversion. The depth of this layer averages 5200 feet (1.6 km) (range: 2100 to 9000 feet/ 0.6 to 2.7 km).

The upper stratum is anomalously warm and very dry with a relative humidity of 38% (range: "Motor-boating" to 65%). This layer has a temperature lapse rate that is nearly dry adiabatic (static stability, $-T\theta^{-1}(\partial\theta/\partial p)$, is 3.5°C per 100 mb) and a mixing ratio that is nearly constant with height, all of which is consistent with a well mixed layer. As a consequence of the slowly increasing potential temperature and the nearly constant mixing ratio with height, the relative humidity increases with height, slightly at first, then *more rapidly above approximately 550 mb.* Also, as a result of this stratification, the atmosphere as a whole is conditionally unstable with a lifted index of -6°C.

Winds were found to veer and increase with height suggesting warm air advection. Sugg and Foster (1954) shows that during a tornado outbreak on 1 May, 1954 there was warm advection "to great heights" above the moist layer at the surface. This contradicts the hypothesis that subsidence produces the inversion. At 850 mb the wind is southwesterly at 15.5 ms^{-1} (30 kt); at 500 mb the wind is west-southwesterly at 26 ms^{-1} (50 kt). The flow of dry air above the inversion has a component of at least 15.5 ms^{-1} (30 kt) perpendicular to the flow in the lower layer. This fact supports the discussion of the dryline in section 2.1.2.

Fawbush and Miller (1952) noted that the typical tornado "airmass" structure shows no great variation with the seasons; when tornadoes do occur in the "off season," the structure is the same. However, the frequency of occurrence of this structure fluctuates with the seasons. This observation supports the discussion in Chapter 5.

Carlson and Ludlam (1965), looking at soundings taken from pre-severe storm environments over the Great Plains of the United States, also found the structure which Fawbush and Miller (1954) reported as a Type I sounding (Figure 1.1 on page 6). They analyzed the vertical structure of those "airmasses" and found as others had (James, 1951; Warner, 1963) that several layers could be distinguished. Each of the layers is characterized by particular lapse rates of potential temperature and mixing ratio. Using an isentropic analysis method designed by Green et al. (1965 and 1966), they were able to show that the different layers are due to the juxtaposition of synoptic-scale airstreams of strikingly different origin and character. From this information, a conceptual model describing the creation of the pre-severe storm environment was designed and presented by Carlson and Ludlam in 1968.

Chapter 2

THE CARLSON-LUDLAM CONCEPTUAL MODEL

The foundation of the Carlson-Ludlam Conceptual Model is that a unique combination of geography and atmospheric flow patterns produce the extreme stratification which is observed (Figure 1.1 on page 6 discussed in Section 1.2). The ideal combination is to have low-level flow from a large moisture source onto low plains, mid-level flow, originating over an elevated arid region, and a short-wave trough approaching the area. The Great Plains of the United States, with the Gulf of Mexico to the south, the deserts of the Mexican Plateau to the west and southwest, and frequent transient upper-level, short-wave troughs, is but one area of the world which has the potential to produce such stratification.

Many investigators have documented the existence of such stratification over many other parts of the world: Ramaswamy (1956) observed it over South Africa, Brazil, India, Australia, Uruguay, and northeast Argentina; Colon (1964) over India, and the Arabian Sea; Both Carlson and Ludlam (1968), and Wessels (1968) over Spain and France; Weston (1972) over India; Carlson and Prospero (1972, 1973) and Diaz et al. (1976) over the trade-wind region of the equatorial Atlantic Ocean; Peterson (1979) over Australia; Silberstein (1983) over Persia; both Goldman (1981) and Carlson and Farrell (1983) over the upper Mississippi and Ohio Valleys, Kentucky and Tennessee; Whitney and Miller (1956) over Michigan; and Penn et al. (1956) over Massachusetts! Most of these areas are noted by Ludlam (1963) as having the propensity for severe thunderstorms.

The model's synoptic airstream pattern which leads to such a stratification is illustrated in the schematic of Figure 2.1. Although this figure depicts the scenario over the Great Plains of the United States, the basic pattern is applicable to all of the locations mentioned above.

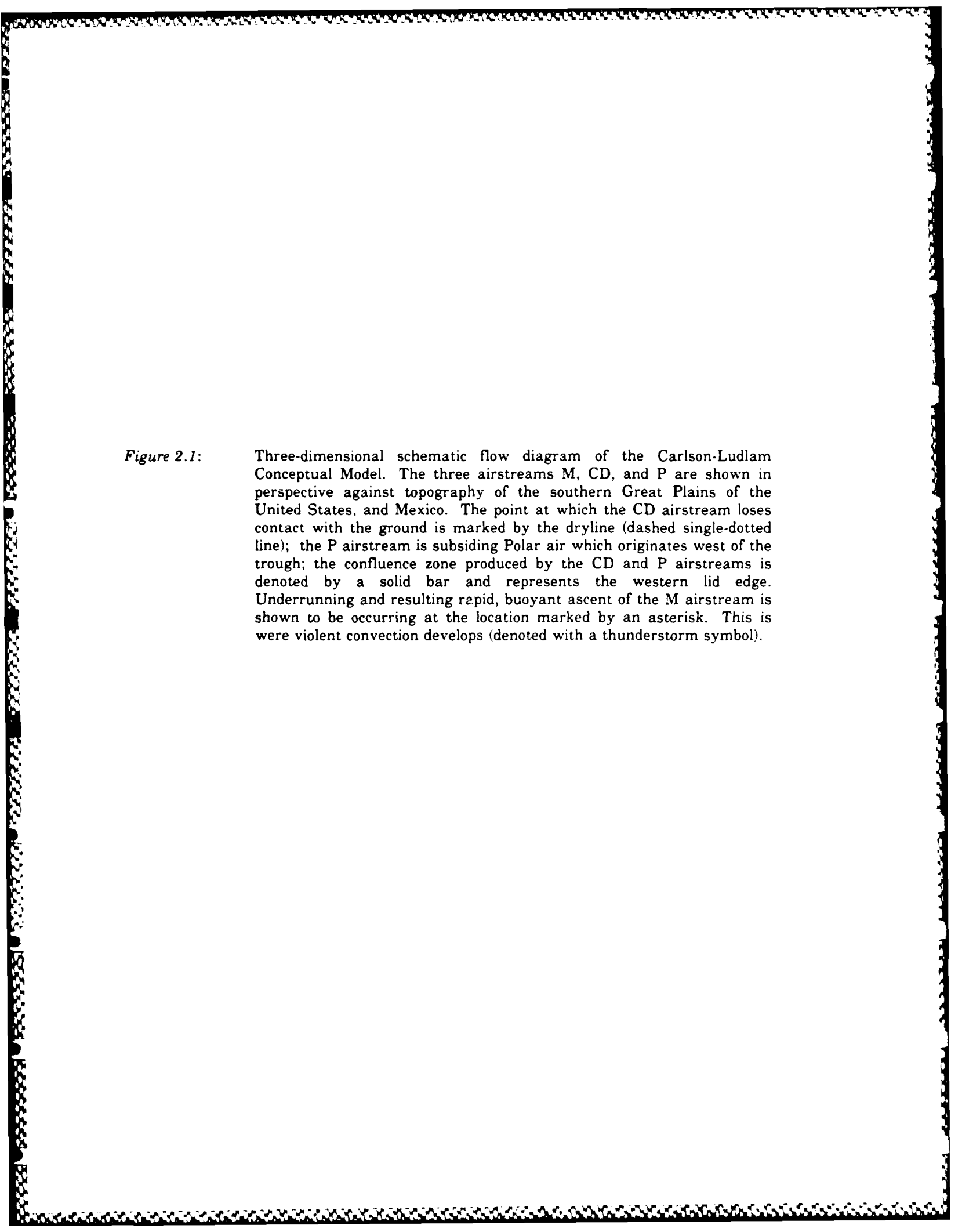

Figure 2.1: Three-dimensional schematic flow diagram of the Carlson-Ludlam Conceptual Model. The three airstreams M, CD, and P are shown in perspective against topography of the southern Great Plains of the United States, and Mexico. The point at which the CD airstream loses contact with the ground is marked by the dryline (dashed single-dotted line); the P airstream is subsiding Polar air which originates west of the trough; the confluence zone produced by the CD and P airstreams is denoted by a solid bar and represents the western lid edge. Underrunning and resulting rapid, buoyant ascent of the M airstream is shown to be occurring at the location marked by an asterisk. This is were violent convection develops (denoted with a thunderstorm symbol).

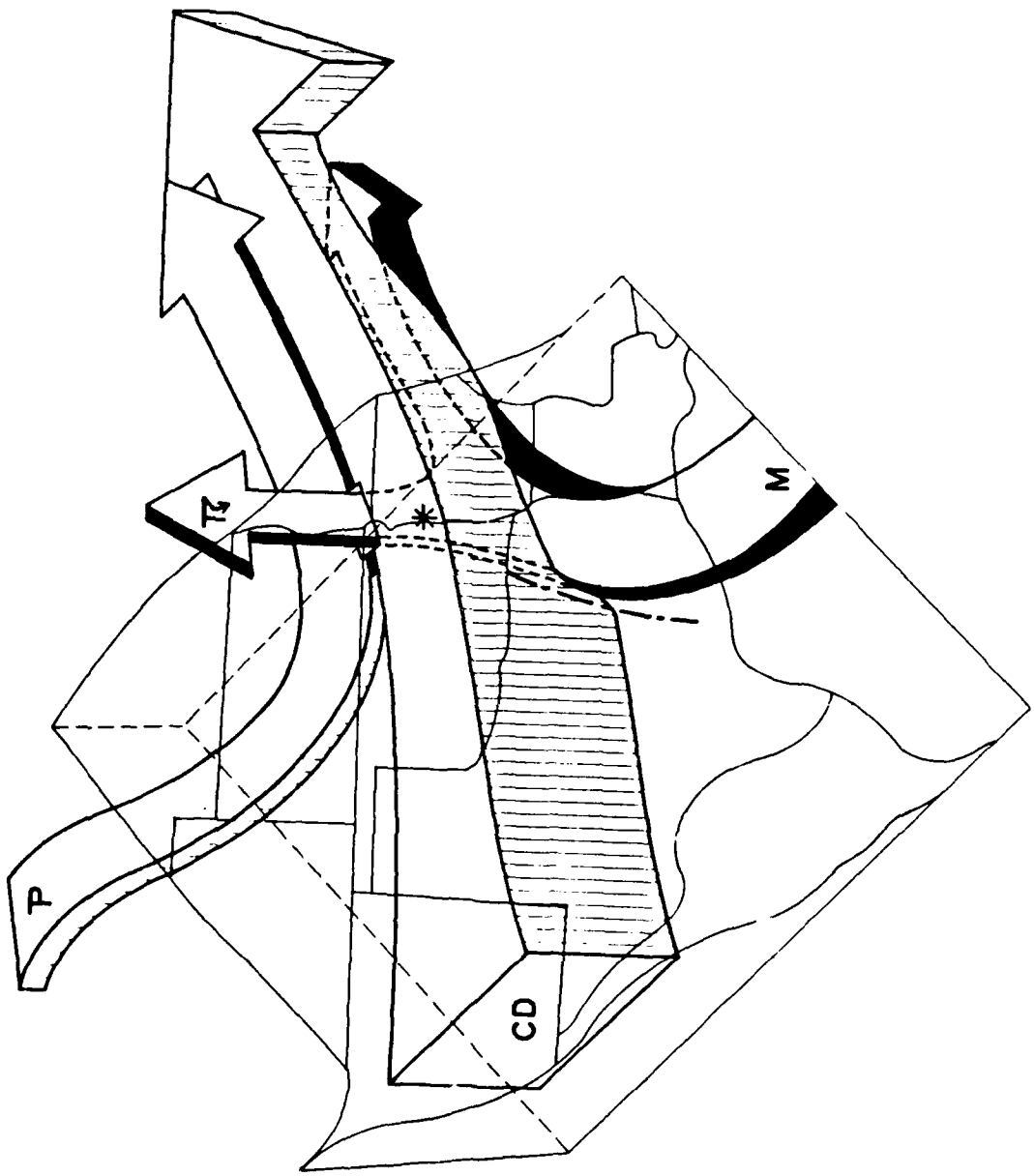
M
P
CD

This pattern is very similar to the tornado producing synoptic patterns introduced by Miller (1959) and refined by Miller (1967 and again in 1972); however, Miller failed to mention how these patterns produce the observed stratification (Type I sounding, i.e. lid, Section 1.2) and consequently misinterprets many of the causes and effects.

The sequence of events leading to the development of severe convection over the Great Plains frequently begins with the approach, from the west, of a short wave disturbance in the mid- and upper-troposphere. In response to the falling surface pressures ahead of the trough, low-level southerly flow from off the Gulf of Mexico is established and advects warm, moist (maritime tropical) air with high θ_w ($\simeq$22°C; see Section 5.2) northward (labeled M in Figure 2.1 on page 11).

In association with the warm air advection ahead of the trough and the maintenance of geostrophic balance, the winds veer with height. As a result, the winds at higher altitudes (800-700 mb) are southwesterly. This flow (labeled CD in Figure 2.1 on page 11) advects a hot, dry, well-mixed (continental tropical) plume with high θ (above 40°C; Carlson and Ludlam, 1968) from the higher elevations of the Mexican Plateau and the desert southwest, over the cooler ($\theta \simeq$30°C; Carlson and Ludlam, 1968), layer to the [illegible].

The base of this now elevated plume is anomalously warm for the levels at which it is found and therefore constitutes a strong inversion. This "lid" is very effective at capping deep convection which may have otherwise originated in the cool, moist air. It confines any resulting small-scale convection to a shallow layer within which θ_w can then rise to values considerably above the saturation wet-bulb potential temperature (θ_{sw}) aloft. The latent instability therefore increases far beyond that which is possible without the presence of the lid.

The third airstream depicted in Figure 2.1 on page 11, labeled P, is cool, dry (continental polar) air which originates from the western side of the trough and becomes

confluent with the hot, dry air from the mixed layer. This confluence zone creates a sharp transition between a stratification which effectively caps deep convection, and a stratification that can not. Therefore, this zone effectively acts as a lateral edge to the lid. This edge is a preferential site for the development of severe weather (Carlson and Ludlam, 1968; Carlson et al., 1980; Benjamin and Carlson, 1982; Carlson and Farrell, 1983; Carlson et al., 1983; Lanicci, 1984b; Keyser and Carlson, 1984; Lakhtakia and Warner, 1987; Benjamin and Carlson, 1986).

Several important thermodynamic and dynamic processes occur simultaneously during the evolution of the severe storm environment. They work in tandem to suddenly and violently release the built-up latent instability into a very concentrated area along the lid edge. The processes involved, and the salient features of the conceptual model are discussed in more detail in the following sections.

2.1 The Evolution of the Elevated Mixed Layer (EML)

2.1.1 The Formation of the Mixed Layer

The crux of the entire conceptual model is that a deep, hot, dry, mixed layer needs to form on the windward side of a large moisture source. For such a layer to form, two things have to happen.

First, available insolation has to rapidly increase the layer's potential temperature. When insolation heats the surface, some of the radiant energy is stored in the soil, some returns to the atmosphere as sensible heat flux, and the remainder returns as latent heat flux introduced by evaporation from the surface. The ratio of sensible to latent heat flux, the Bowen ratio, depends on the availability of moisture in the soil (Monteith, 1973). Over arid regions, the Bowen ratio is quite large. Accordingly, most of the insolation is in the

form of sensible heat flux and hence the potential temperature at the surface increases. Super-adiabatic lapse rates develop in the surface layer and convective overturning begins. This mixing occurs within a layer which deepens with time. The more arid a region, the more efficiently the surface layer is heated, and hence the deeper the mixed layer can become (Halstead, 1954, p.358; Dyer, 1961).

Secondly, the mixing has to occur for several days; the longer the duration of heating of air near the surface across the source region, the deeper the mixed layer can become. If an arid region is sufficiently large and the rate of movement of the air column relatively slow, the mixed layer may grow to very great depths. The net result is the formation of a very deep mixed layer with near constant potential temperature (approximately dry adiabatic lapse rate).

Because the Sahara and the deserts of northern India are so expansive and the weather patterns are relatively stagnant much of the time, air in these regions can remain over the desert for several days. As a result, mixed layers over Africa have been observed to reach 5-7 km in altitude (Diaz et al., 1976; Karyampudi, 1979). Mixed layers of 4-5 km altitude have been observed over the deserts of northern Mexico and the southwest United States (Fujita et al., 1970; McCarthy and Koch, 1982; Carlson et al., 1983).

During the process of mixing, dry thermals overshoot their equilibrium level and become cooler than the surrounding environment. Entrainment leads to the cooling of the layer above. Compensating downward mixing of potentially warmer air produces a layer of downward heat flux. This flux contributes to the heating of the layer below. Both observational and theoretical studies suggest that the ratio of downward to surface sensible heat flux is about 0.2, although the exact value may depend a little on the magnitude of the surface heating (Tennekes, 1973). The result is an inversion, the mixing inversion, which acts as an upper boundary to the mixed layer. This inversion is usually

relatively weak, with an equivalent of one or two degrees difference in potential temperature between the layers above and below the inversion. The magnitude of this inversion tends to be larger the stronger the net heating from below.

Marht (1976), using data from the National Hail Research Experiment, studied the lapse rates of potential temperature and moisture in the heated boundary layers over the high plains region of the United States. He shows that the lower troposphere is well mixed in terms of potential temperature, θ, but not in terms of specific humidity, q.

The reason q doesn't remain constant with height through the layer is because drier air, originating above the mixing inversion, is able to pass through the inversion and entrain with the air below. Ball (1960) has shown that although material beneath an inversion cannot penetrate it, material above an inversion can readily pass down through it. This mixing decreases q below the inversion and thereby increases the lapse rate.

Marht also found that the lapse rate of q is substantially greater on days with strong positive vertical wind shear (wind speeds increasing with height) than on days with strong negative vertical wind shear (wind speeds decreasing with height). This occurs because positive shear contributes to turbulent mixing which enhances the total mixing through the inversion.

As a result, the depth of the well-mixed moisture layer may not be the same as the depth of the well-mixed thermal layer. Since the upward transfer mechanisms for both moisture and sensible heat are virtually identical (Dyer, 1967), the ratio of heights of the well-mixed moisture and thermal layers should indicate whether there is active mixing down through the inversion. Using an energy budget analysis, Carson (1973) showed that the ratio, R, the depth of the layer affected only by thermals rising out of the surface layer (C) to the depth of the adiabatic layer (H), is related to the ratio, A, the downward heat flux through the inversion to that out of the surface contact layer, by the relationship:

$$R = C/H = 1 + A/(1 + 2A) \qquad (1).$$

Theoretical estimates of A are available in the literature. Ball (1960) hypothesized that the upward flux from the surface balanced the downward flux through the inversion; in this case A would equal 1 and R would equal 2/3. If no entrainment through the inversion is assumed (Lilly, 1968), A would equal 0 and R would equal 1. When R equals 1, the lapse rate of q is zero and the mixed layer is quite uniform; however, as R decreases, mixing increases and forces the lapse rate of q to increase. Carson (1973), examining the 1953 O'Neill Nebraska data found that A varied from 0 to 1/2 making R vary from 1 to 3/4. Schaefer (1976), analyzing boundary layer data collected from an instrumented TV tower in Oklahoma, found that 33% of his sample showed Lilly's minimum entrainment condition (R=1), while 56% of the sample showed active entrainment with an R value of approximately 4/5. Schaefer shows that for 89% of his cases, mixing through the mixing inversion was small. Therefore, it can be assumed that the lapse rate of q in the mixed layer is near zero most of the time (i.e. q is constant through the layer).

Because the temperature decreases with height while the specific humidity remains relatively constant, the relative humidity, which combines the effects of both temperature and specific humidity, increases with height. This increase is slight at first then becomes more rapid two-thirds of the way up (Fawbush and Miller, 1954). In essence, the mixing condensation level is approached as the mixed layer grows with time. Consequently, deep mixed layers, even though they form in arid regions, may still reach saturation in a layer near its top. This layer is frequently visible as a haze layer; however, when saturation occurs, thin layer cloud may form, often as altocumulus or altocumulus castellatus. The latter cloud-forms have been reported originating from this layer by many investigators (e.g., Means, 1952, p. 174; Carlson and Ludlam, 1968; Fujita et al., 1970).

The relative humidity at the bottom of the well-mixed layer tends to be a minimum, whereas a maximum in relative humidity occurs just below the base of the mixing inversion. Above the inversion, the relative humidity rapidly decreases. For this reason, relative humidity profiles are particularly useful in estimating mixed layer depths. However, if the entrainment through the mixing inversion is sufficiently rapid (R approximately 1/2), the lapse rate of q becomes quite large. In these cases, the relative humidity profiles are not as helpful.

The formation of a deep mixed layer, with its near neutral lapse rate, allows momentum to be transferred down from mid-levels to the surface (Saucier, 1955, p. 247). It is plausible that zonal momentum in a mid-tropospheric jet stream could be entrained through the top of the mixed layer, then transported down to the surface by means of turbulent mixing (Danielsen, 1974a). This produces gusty winds at the surface. As a result of the arid soils, these gusty winds often pick up large amounts of dust and distribute it throughout the mixed layer. This phenomena has been reported by several researchers (e.g., Fujita, 1958, Schaefer, 1973[1]; Fujita et al., 1970; McCarthy and Koch, 1982).

Fujita et al. (1970) noted that dust reached to the top of a mixed layer, 2.8 km deep, which existed over much of the south central United States during the Palm Sunday tornado outbreak of 11 April 1965. McCarthy and Koch (1982) noted that a dust layer reached to the top of a mixed layer, 4.1 km deep, over northern Texas during a tornado outbreak on 9 June 1974. They found that all of their observations are consistent with the hypothesis that turbulent mixing carries zonal momentum down from the upper-level jet through the mixed layer to the surface. Danielsen (1974b) also found a relationship

---

[1] This reference is a NOAA Technical Memo which Schaefer later published in 1974a and 1974b. For sake of convenience, unless the text is specifically directed to one of the later publications, only the original work is referenced.

between duststorms and tornadogenesis; however, he points out that this relationship is a symptom not a cause.

Wind directions throughout the mixed layer vary by no more than 10°: a necessary requirement if momentum is redistributed efficiently by vertical mixing. The surface winds tend to deviate more towards the direction of the flow aloft, approaching the mass-weighted mean of the layer as the mixed layer grows. Thus, through time, surface winds become super-geostrophic (McCarthy and Koch, 1982). One point to keep in mind for later discussion is that the flow near the top of the mixed layer slows and becomes sub-geostrophic. As the surface flow acquires a stronger zonal component, a zone of confluence forms where it meets with the meridional flow from off the Gulf of Mexico. This zone has been labeled the dryline.

2.1.2 The Dry Line

The dryline is a sharp low-level (1 to 3 km deep) discontinuity between the cool, moist air to the east and the hot, dry air to the west. It is a common feature of extratropical cyclones in the Great Plains. It typically intersects the cold front at or near the low's center, forming what is often referred to as a "triple point" (Doswell, 1982). However, it is not a front in the sense of a discontinuity in density. The gradient of virtual temperature is near zero because of the opposing effects of moisture and temperature. Both the moisture and temperature fields, however, have strong gradients. The moisture gradients observed with mesoscale networks can be enormous, with mixing ratio changes of 5 gkg-1 over distances of 1 km (Fujita, 1958; McGuire, 1962; Sanders in NSSP Staff, 1963). Beebe (1958) reported an average dewpoint gradient of 9°C km^{-1} across the dryline. The temperature (or potential temperature) gradients are similar to active polar fronts. Drylines are easily recognizable surface features, and remain so until the synoptic

scale pattern changes or eliminates the mixed layer. Schaefer (1973) determined that the dryline is usually positioned within a band in the mixing ratio field ranging from 6-12 gkg^{-1}. He reports that the 9 gkg^{-1} (median) isopleth is a good estimator of the dryline position.

Many investigations of the dryline consist of observational studies: Beebe (1958), Fujita (1958), Miller (1959), McGuire (1962), the NSSP Staff (1963), Rhea (1966), Schaefer (1973 and 1974a), and McCarthy and Koch (1982). From these studies, it was determined that the dryline is regional in character and generally confined to the Great Plains, west of the Mississippi River and south of the Dakotas. This is generally recognized to be the result of topography.

As moisture flows from the Gulf of Mexico on to the Great Plains (M in Figure 2.1 on page 11), it is deflected by the high terrain of the Rocky Mountains and the Texas escarpment and is channeled northward (Wexler, 1961; Carlson and Ludlam, 1968; Schaefer, 1973). Thus, a natural tendency exists for the development of a north-south boundary separating the dry, well-mixed air from the moist air. A climatological study by Dodd (1965) shows a definite gradient in mean dewpoint over western Texas. This gradient strengthens during the spring and weakens by mid-summer.

The role of differential surface heating in dryline intensification has been discussed and numerically modeled by Schaefer (1973 and 1974b). In regions, such as eastern Texas, where there is a strong horizontal gradient in soil moisture, there is a strong horizontal gradient in the Bowen ratio. As such, there is a strong horizontal gradient in the sensible heat flux (Penman, 1956; Brooks et al., 1963, p. 74). The resulting variation in heating across the natural north-south boundary further enhances the existing temperature gradient which in turn increases the moisture gradient via accentuated soil evaporation on the side of the dryline with greater moisture. Hence, as insolation

increases through the spring, the gradient of dewpoint increases. However, by mid-summer, as a result of increased rainfall along and west of the dryline, the gradient in the Bowen ratio decreases. This leads to a weakening of the gradient in sensible heat flux which in turn leads to a weakening of the dryline. This is in agreement with Dodd's observations. Besides the sensible heating gradient, there are several other gradient enhancement processes which act in the region of the dryline.

The low level flow patterns in the south central United States create a deformation field which is frontogenetic. Hence, geostrophic confluence tightens the gradients of both temperature and moisture. In response to this geostrophic forcing, ageostrophic motions set in which also help to enhance the gradients. This feedback process can be adequately modeled using the kinematic frontogenetic function of Petterssen (1956a) and Eliassen (1962); however, investigators using the geostrophic momentum approximations have had better success (Shapiro, 1982; Anthes et al., 1982). Anthes et al. (1982), showed that geostrophic deformation contributes to the increase of the moisture gradient along the dryline. They found that both confluence and shearing deformation contributed during the SESAME II 25-26 April 1979 case, but that only confluent deformation was involved during the SESAME I 10 April 1979 case. Nevertheless, geostrophic deformation as a whole was shown to be an important gradient enhancement process.

Schaefer (1975) shows that in a nonlinear biconstituent system possessing certain necessary boundary conditions, diffusion can act to create and intensify gradients. He shows that the dryline is one boundary in the atmosphere that possesses those necessary conditions. The resulting circulation from this second-order effect produces confluent deformation which thereby increases the moisture gradient.

Once formed, the dryline has a diurnal east-west oscillation. Its westernmost extent is reached in the morning; its easternmost extent is reached by early evening. The

behavior of the dryline is affected by the nature of its structure, which is influenced by diurnal variations in mixing. The dryline usually begins the day as an almost horizontal boundary intersecting the sloping terrain at higher elevations. This inversion is usually enhanced by the presence of a nocturnal inversion. The dryline ends the day farther east with a slope on the order of 1:30, which is much steeper than classical polar fronts (Fujita, 1958, McGuire, 1962; NSSP Staff, 1963; Schaefer, 1973). There are several processes which have been found which work together to cause this translation (McNider and Pielke, 1981).

One process is the mixing of dry, hot air through the low-level inversion and breaking it down. This is observed as an apparent translation of the dryline. During the day, solar heating and the resultant mixing destroy the moist surface layer and the dryline "jumps" eastward. As a result of the sloping terrain, the depth of the moist layer increases to the east. The speed at which the moist layer is destroyed varies with the depth of the moist layer. Therefore, the farther eastward the dryline goes, the deeper the moist layer is, and the slower the translation becomes (Schaefer, 1973). Hence, its motion is not temporally uniform during the day.

Another process, which was previously discussed, is the advection of the hot, dry air eastward by the zonal ageostrophic winds produced by the turbulent mixing in the mixed layer west of the dryline. The momentum exchange may occasionally cause surface winds to gust as high as 25 ms^{-1} or more (Doswell, 1982). However, surface heating produces a thermal low over the arid region which, in turn, intensifies the lee trough. This intensification strengthens the easterly wind component on both sides of the dryline. This easterly wind component opposes both mixing and advection of the dryline eastward, and may slow or even reverse its eastward translation (Benjamin and Carlson, 1986).

At sunset, several processes begin which act to reverse the translation of the dryline. When the surface begins to cool the mixing loses its intensity and a nocturnal inversion forms at the surface west of the dryline. Because moisture retards surface radiative cooling, the air at the surface east of the dryline does not cool as fast as the air at the surface west of the dryline (Staley, 1965). Hence, the easterly component of the air east of the dryline remains relatively constant while the opposing westerly component of the air west of the dryline weakens considerably.

This net easterly component is also enhanced by the diurnal variation of the surface geostrophic wind. This oscillation, which is caused by variations in the diurnal pressure wave, gives a minimum westerly (maximum easterly) component to the pressure force immediately after sunset (Bonner and Paegle, 1970).

With little density discontinuity present, the dryline is forced westward, translating at a uniform rate proportional to the speed of the net advective winds in the cool, moist air. Through the night, the dryline moves up the sloping terrain until either the slope of the dryline becomes horizontal again or the dry air becomes denser than the moist air as a result of continued cooling (Schaefer, 1973). From this time until insolation again induces eastward motion, the dryline remains nearly stationary.

The location and movement of the dryline is important because the dryline is a favorable location for the development of severe weather (Fawbush et al., 1951; Miller, 1959; Rhea, 1966). A four year study of radar echo formation showed that when convective cells existed within 200 n mi either side of the dryline, 78% of the first echoes developed within 10 n mi of the dryline position (Rhea, 1966). Such mechanisms as sub-synoptic upper-level trough interactions (Williams, 1971; Bluestein and Thomas, 1984), inland sea breeze effects (Sun and Ogura, 1979), gravity waves (Ogura and Chen, 1977; Ogura et al., 1982), nonlinear biconstituent diffusion effects (Schaefer, 1975), frontogenetic

ageostrophic flows (Anthes et al., 1982; Shapiro, 1981 and 1982; Koch and McCarthy, 1982; Keyser and Carlson, 1984; Lakhtakia and Warner, 1987), and symmetric instabilities (Ogura et al., 1982), to name just a few, have been used to help explain the causes for the frequent development of severe weather along the dryline.

2.1.3 The Elevation of the Mixed Layer

Besides forming the dryline at the surface, the hot, dry mixed layer air also loses contact with the sloping terrain and flows up over the cool, moist air. This, now elevated, mixed layer (henceforth to be referred to as the EML) forms the lid. This overflow has been observed by many investigators (e.g., Fujita, 1958; Carlson and Ludlam, 1968; Fujita et al., 1970; Schaefer, 1973; Danielsen 1974a; and McCarthy and Koch, 1982).

Schaefer (1973) recognized that the upper boundary of moist air east of the dryline was a capping inversion, above which the air resembles that in the mixed layer west of the dryline. He used a chi-squared statistical test to support this claim. Danielsen (1974a) specifically attributes the creation of the "southern Plains low-level inversion" to differential advection of the deep, high-plateau mixed layer over moist flow from the Gulf.

Using sensitivity studies in the PSU/NCAR mesoscale numerical model, Benjamin (1983) determined that a strong gradient of soil moisture is necessary for a lid to form. He showed that lids formed without elevated terrain as long as there was differential heating created by a gradient in soil moisture. Therefore, drought stricken lowlands may become source regions for lids. Carlson and Ludlam (1965) showed that, in 1958, a drought-stricken France acted as a source region for lids. Several undocumented cases show that the Great Plains have also acted as a source region during times of severe drought.

During the winter months, northern Mexico is under the affects of a weak winter monsoon. As a result, the region gets very little precipitation (Aleman and Garcia, 1974). Understandably, the region is very arid. The surface-level mixing ratios average only around 8 gkg^{-1} (Lanicci, 1984a). Therefore, this area acts as a good source region for lids which are found over the United States during the Spring. By mid-summer, however, the summer monsoon is fully established and the soil moisture content over northern Mexico increases. The surface-level mixing ratios average above 14 gkg^{-1} (Lanicci, 1984a) (a 6 gkg^{-1} increase). As a result, this area is no longer capable of producing deep mixed layers and, as such, no longer constitutes a favorable source for lids.

On the other hand, the Rockies in the United States receive a lot of snow during the winter months. Spring insolation melts and evaporates the snow instead of heating the air (i.e. a very low Bowen ratio). As a consequence, mixed layers do not form over that part of the country until the snow cover is eliminated and the soil drys out. The snow is usually gone by early May (Figure 2.2) (Court, 1974). Consequently, this is the first time that mixed layers can, and do, form over the Rockies. Gates (1961) shows that the environment is very stable over the Rockies in January but that by July there is a very deep well mixed layer extending over most the the mountain range (Figure 2.3). Hence, the source region for lids spreads northward, behind the retreating snow line and, as circumstances have it, behind the retreating polar jet. By August, the summer monsoon is established over the desert southwest (Roe and Vederman, 1952) and the soil moisture content increases. As in the case of Mexico, this eliminates the desert southwest as a source region for lids. Consequently, both the maximum in lid occurrences and the seasonal maximum in severe convection (e.g., Fawbush et al., 1951) progress northward. (See Section 5.1 for further discussion).

Figure 2.2: Average annual date of last snow cover of 2.5 cm or more, 1950-1960. Dashed lines give percent of years without snow cover. (Prepared by Donald Larson; from Court, 1974).

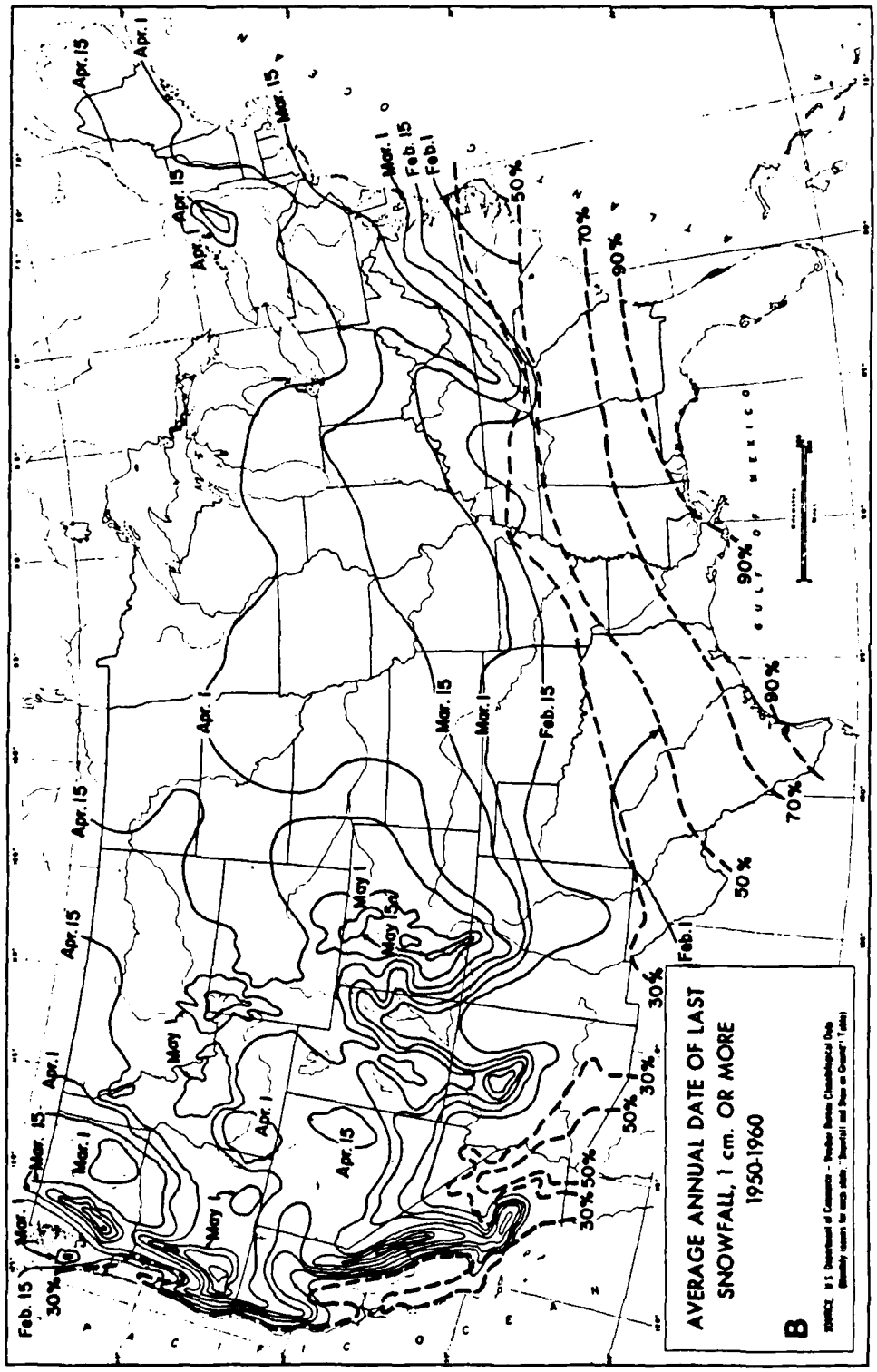
AVERAGE ANNUAL DATE OF LAST
SNOWFALL, 1 cm. OR MORE
1950-1960
B
Feb. 15
Mar. 1
Mar. 15
Apr. 1
Apr. 15
May 1
30%
50%
70%
90%
MEXICO
GULF OF

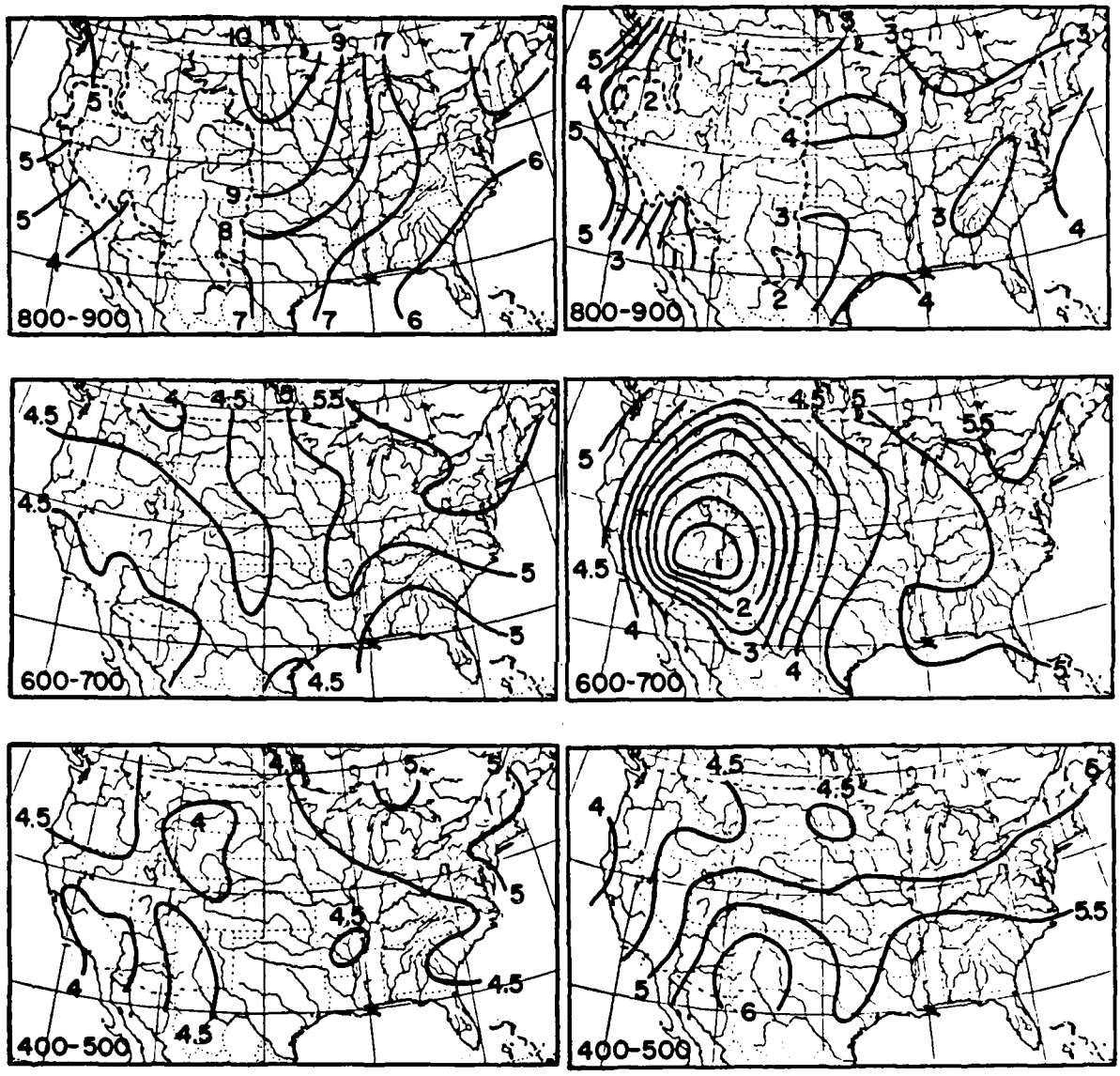

Figure 2.3: The horizontal variation of the static stability, $-T\theta^{-1}(\partial\theta/\partial p)$ [°C decibar^{-1}], in selected isobaric layers denoted in the bottom left of each map for January (a) and July (b). The dashed line on the 800 to 900 mb map indicates intersection of the ground. (From Gates, 1961).

Several investigators have documented the location of source regions of elevated mixed layers which were involved in the development of severe weather over the United States. These studies are summarized in Table 2.1. Many of the physical processes resulting from the presence of the lid are discussed in more detail in the following section.

Table 2.1: Source Region Locations; North America

Investigator	Case	Source Region
Goldman (1981)	3 APR 1981	Mexican Plateau
Lanicci (1984b)	3-4 APR 1981	Mexican Plateau
Anthes et al. (1982)	10 APR 1979	Desert SW
Carlson et al. (1980)	10-11 APR 1979	Desert SW
Fujita et al. (1970)	11 APR 1965	Desert SW
Carlson et al. (1983)	25-26 APR 1979	Desert SW
Carlson & Ludlam (1965)	4 MAY 1961	Mexican Plateau
Carlson et al. (1983)	9 MAY 1979	Mexican Plateau
Goldman (1981)	10 MAY 1979	Desert SW
Carlson & Farrell (1983)	13 MAY 1981	Desert SW
Carlson & Ludlam (1968)	26 MAY 1962	Mexican Plateau
Caracena & Fritsch (1983)	2 AUG 1978	Saharan Desert!

2.2 The LID

The winds in the middle levels (≈700 mb) advect the EML along with the flow. In conjunction with the warm air advection ahead of the approaching trough, the EML rises downwind and therefore cools dry adiabatically. Hence, the EML eventually reaches a point downstream where it no longer constitutes an inversion with sufficient strength to cap deep convection. The place where this occurs can be considered a downstream edge to the lid.

In barotropic regimes where this along-stream ascent is minimal, however, the characteristics of the EML persist recognizably for a long time. Carlson and Ludlam (1965, 1968) presented a case (26 May 1962) in which they identified an EML, with origins over northern Mexico, residing over Charleston, South Carolina (approximately 2500 km downstream from Mexico). Assuming that the EML is advected at only 9 ms^{-1} (17.5 kt) it can travel approximately 800 km per day. Therefore, the EML must have lasted in excess of three days! Lids originating from the mixed layers of the Saharan Desert have been observed to persist as recognizable entities from 7 to 10 days (Karyampudi, 1979, 1986).

When a feature persists this long, radiational effects become important. There are two notable processes that result. First, when a moisture discontinuity coincides with an inversion, as in the case of a lid, the resulting discontinuity in optical thickness makes the effects of longwave radiational cooling important. Staley (1965) showed this by applying the formula relating radiational flux divergence to the clear-air cooling rate of inversions with a variety of moisture distributions. He found that cooling tends to destroy inversions with little moisture discontinuity across them, whereas it tends to actually increase the strength of inversions which coincide with the sharp mixing ratio lapse rate. This occurs because the cooling is maximized at the inversion base. This radiational cooling also causes the air in the PBL to loose buoyancy. Consequently, the strength of the lid oscillates diurnally, stronger in the morning than in the evening. This was noted by Graziano and Carlson (1987) in a statistical study of the lid strength (see Section 3.1).

Secondly, as the EML flows downstream, a marginal radiative equilibrium is maintained throughout the layer as a whole. Radiative warming, resulting from the absorption of short-wave radiation by dust trapped in the EML (see Section 2.1.1) is almost balanced by longwave radiational cooling (Carlson and Benjamin, 1980). The net

warming helps to preserve the EML by counteracting the adiabatic cooling. Over the several days in which an EML can persist, however, the potential temperature near the top of the layer may actually cool 2°C to 3°C due to radiative losses. This has been noted by several researchers (e.g., Carlson and Ludlam, 1965; Karyampudi, 1979, 1986; Benjamin and Carlson, 1986).

It has been suggested that this cooling is associated with a sinking of the EML's top via the increase in density. A more correct explanation is that this cooling enhances the vertical mixing up through the mixing inversion topping the EML which in turn brings the warmer air above the inversion down. The net effect of this mixing is a lowering of the mixing inversion. This resultant lowering of the EML top, in conjunction with the rising base of the EML, decreases the depth (or thickness) of the EML along the direction of flow. This suggests that potential vorticity plays a role.

Potential vorticity, $(\zeta+f)\partial\theta/\partial p$, is conserved only if the flow is isentropic. Even though the top of the EML sinks as a result of diabatic cooling, the change in θ ($\simeq$3°C) is a small fraction of the change in thickness ($\simeq$300 mb; i.e. almost a 100% difference!). Therefore, potential vorticity should be conserved in this case. When the EML flows northward, the thickness of the layer decreases and the Coriolis parameter increases; both contribute toward a decrease in relative vorticity. Consequently, it might be concluded that the flow should curve anticyclonicly; however, this turning is rarely observed. Dutton (1976, pp. 344-345) notes that a crucial assumption for making such a conclusion is that the horizontal shear must remain constant. As will be discussed in Section 2.3, many investigators have observed a strong mid-level jet along the western edge of the EML. The presence of this jet reflects strong anticyclonic shear. Therefore, it is suggested here that it is an increase in anticyclonic horizontal shear, not curvature, which balances the changes in the thickness and Coriolis parameter to conserve potential vorticity.

The lid base (i.e. the boundary between the cool, moist air and the EML) is not of uniform height. It has been shown that the lid base has mesoscale undulations (NSSP Staff, 1963; Palmén and Newton, 1969, p. 400). Palmén and Newton have hypothesized that these undulations reflect the presence of gravity waves, which are initiated at the dryline, and propagate downstream. These propagating gravity waves are ducted by the lid (Balachandran, 1980) and can travel a considerable distance. As they propagate: they can produce organized cumulus cloud patterns under the lid (cloud along the ascending sections and clear skies along the descending sections of the waves); they can propagate out from under the restraining effects of the lid and initiate severe convection (Matsumoto and Akiyama, 1970; Uccellini, 1975; Feteris, 1978; Koch, 1979; Balachandran, 1980; Hung et al., 1980; Koch and McCarthy, 1982); and, the resulting upward vertical velocities can create seams of weakened stability. These seams can sometimes become weak enough to allow moist convection to penetrate.

Seams of weakened stability can also form as a result of the diurnal variations of surface heating within the source region of the EML (Section 2.1.1). The mixing of momentum over the source region during the day actually decreases the advection of air eastward by slowing the winds near the top of the mixed layer (Benjamin and Carlson, 1986); however, during the night, a forward acceleration of the winds occurs as a result of an inertial oscillation (Blackadar, 1957). The potential temperature of the air near the top of the mixed layer does not vary diurnally, as do the advective winds. Hence, the flux of the hot, dry air up over the cool, moist air varies diurnally.

This process creates pulses of hot, dry air within the EML which produce gradients of temperature. These gradients depend on the phase differences between the diurnal heating cycle and residence period of the air over the source region. This period is roughly equal to L/U, where L is the width of the source region and U is the mean cross-source-

region wind speed (Benjamin and Carlson, 1986). These temperature gradients create spatial fluctuations, or seams, in the strength of the lid. This effect was observed by Lanicci (1984b, pp. 31-50). He shows that two distinct "bubbles" in the lid strength were evident during a severe storm outbreak on 3-4 April, 1981. The case study presented in Chapter 4 also exhibits this characteristic.

An interesting side note is the response of thunder to the presence of the lid. Because of the strong temperature inversion, and the fact that sound is refracted downward at an angle proportional to the strength of the positive vertical temperature gradient, loud sounds like thunder (i.e. explosions) are refracted very sharply and become ducted. As a result, these sounds can be heard for great distances (Humphreys, 1940, pp. 427-430). Thunder is also noted to rumble more than usual. This may occur because the efficiency of "retransmitting" terrain-induced echoes increases (Humphreys, 1940, p. 441).

Electromagnetic propagation (e.g., radar) is also affected by the presence of the lid. The vertical gradient of refractivity associated with the lid is such that a beam passing through the inversion will be superrefracted (i.e. bent toward the ground more than normal; Petterssen, 1956b, p. 57), and passing through the EML will be subrefracted (i.e. bent less than normal; Petterssen, 1956b, p. 58). The beam becomes so contorted that a radar, peering through a lid, will misinterpret the distance and echo heights of targets. In strong lid events this contortion may even create shadows or "holes" in the radar's coverage.

Another problem created by the presence of the lid is that, as a radar beam passes through the lid, the beam width broadens more than usual. Consequently, the resolution of targets and the power reaching them decreases significantly more than usual (Doviak and Zrnić, 1984, pp. 16-17). The deterioration in resolution enhances the commonly observed effect of the distant "solid" line of thunderstorms breaking up into separate cells

as it comes closer. This gives the false impression that the line is dissipating. The reduction in power density results in the underestimation of the reflectivity of thunderstorms at a distance from the radar. Obviously, these effects pose significant problems for operational forecasting and should therefore always be considered.

Furthermore, if the lid base is strong enough it will create an elevated duct (defined as a vertical refractivity gradient of -157 N-units km^{-1}) which, if low enough, can severely impact microwave transmissions. GTE Sylvania has done extensive climatological studies of elevated ducts (Miller et al., 1979; Ortenburger et al., 1985). From their results it can be seen qualitatively that the percent frequency of elevated ducts is well correlated with the frequency of lid occurrences (see Section 5.1). This reveals that lids not only have an important impact on severe weather production, they also have an important impact on electronic communications!

If the mixing condensation level (MCL) is below the lid base, stratus forms in the morning. If the MCL is above the lid base, no stratus forms. Often, however, the MCL is well below the lid base. Many investigators have noted the presence of morning stratus under a lid (e.g., Carlson and Ludlam, 1968; Carlson et al., 1980; Anthes et al., 1982; Carlson et al., 1983) and both an inversion and morning stratus preceding severe storm events (e.g., Fawbush et al., 1951; Fawbush and Miller, 1954; Beebe and Bates, 1955; Fujita et al., 1970; Miller, 1972).

Benjamin and Carlson (1986) showed that this morning stratus/stratocumulus enhances the dryline and the strength of the lid by enhancing the differential heating across the cloud edge (see Section 2.1.2). It is well known that subsidence inversions help to maintain decks of stratocumulus by limiting the size of eddies which entrain dry air from above the moist layer. Benjamin and Carlson suggest that lids act in the same way. As a result, stratus/stratocumulus can persist long enough into the day to have a significant impact on the lid's strength.

If stratus does form, it eventually burns off by late morning but skies remain hazy. As the day's heating continues, shallow convection develops in the moist layer beneath the lid. If the convective condensation level (CCL) is above the lid base, cumulus clouds do not form; however, if the CCL is below the lid, cumulus clouds form. If clouds do form, the tops barely penetrate the lid base. Kelvin-Helmholtz waves sometimes become observable at cloud top levels. The resulting billows never last very long, however, because the cloud evaporates rapidly due to entrainment of the very dry air in the EML. Kelvin-Helmholtz waves develop on a boundary separating two fluids of differing densities if the condition is stable and the shear across the boundary is large enough. Hence, the lid base, with its large stability and strongly veering winds, is highly conducive to Kelvin-Helmholtz wave generation.

The vertical advection of moisture by convective clouds results in a cooling at the lid base due to the evaporation of cloud into the dry air. This leads to a diffusion of the boundary between the cool, moist and hot, dry air. Over the course of several days, it may even lead to the destruction of the lid itself (Estoque, 1968).

2.3 The Polar Airstream (P) Contribution

As mentioned earlier, flow from west of the trough axis becomes confluent with the EML and thereby forms a lateral edge to the lid. This flow sinks approximately 200 mb as it crosses the trough axis (Carlson and Ludlam, 1968; Carlson et al., 1980). As it does, it: sinks and warms adiabatically, flows along the surface, is heated somewhat due to its convective contact with the ground, and eventually becomes confluent with the EML. Despite the increase in potential temperature, this air remains cooler than the EML. As a result, it usually does not form effective lids, contrary to Lloyd's (1942) conclusions.

Several investigators, however, have determined that there are cases where this flow does produce secondary lids alongside of the EML (Goldman, 1981; Carlson et al., 1983; Lakhtakia, 1985). These seconday lids are much weaker and, as such, are usually not as well defined.

Lakhtakia and Warner (1987), using the PSU/NCAR mesoscale numerical model, have confirmed that the trajectories of the polar airstream in the SESAME IV (9-10 May 1979) case do agree with those described in the conceptual model. They also show that there is a wind maximum along the zone of confluence. Several investigators have observed this feature (Fawbush et al., 1951; Sugg and Foster, 1954; Miller, 1959; Carlson and Ludlam, 1968; Fujita et al., 1970; Wills, 1969; Feteris, 1978; Ogura et al., 1982; and McCarthy and Koch, 1982). This induced jet streak plays a vital role in severe weather production by contributing the necessary low level vertical wind shear (Weisman and Klemp, 1982). Weisman and Klemp have suggested that low level wind shear is much more important than upper-level shear. The shear associated with the confluence zone is a maximum in the lower troposphere (850-700 mb)!

Keyser and Carlson (1984) show that the lateral edge to the lid acts as a baroclinic zone. Geostrophic confluence contributes to a thermally direct circulation with rising motion directed up the isentropes. This circulation pattern is reinforced by an indirect cell, centered in the upper portion of the EML, which is forced by anticyclonic shear in the presence of a potential temperature gradient. The magnitude of the diagnosed vertical motions (on the order of 2 cm s^{-1}) indicates that these ageostrophic circulations should not be expected to play a direct role in the outbreak of severe convection; however, these mesoscale circulations help to enhance the gradient along the edge of the EML, making the lid edge even sharper. This circulation acts favorably by inducing upward motion along the lid edge, thereby diminishing the strength and increasing the height of the lid along its

edge, while the compensating subsidence reinforces the strength of the lid over the lid. Furthermore, these ageostrophic circulations can be expected to act in a cooperative sense with mechanisms involved in producing underrunning (see following section). Ogura et al. (1982) have proposed that an induced "inland sea-breeze" circulation produces similar effects.

2.4 Differential Advection and Underrunning

Severe convection "explodes" when buoyant energy is suddenly released in an area where the lid is eliminated or the moist lowlevel air flows out from underneath it. These two processes tend to be present in the same area simultaneously, making it very difficult to study their effects separately. Early investigators who noticed the presence of an inversion in the pre-severe-storm environment concluded that the inversion layer must be subjected to forced lifting in order to weaken it enough to allow convection to develop (e.g., U.S. Weather Bureau, 1939; Lloyd, 1942; Fulks, 1951; Fawbush et al., 1951; Sugg and Foster, 1954; Beebe and Bates, 1955). The stratification existing in a lid situation is potentially unstable ($\partial\theta_w/\partial z < 0$). As a result, the EML base (lid) cools more quickly than does the moist air below, and eventually loses its capability to cap moist convection (i.e. the lid is destroyed by lifting). Petterssen (1956b, pp. 184-186) schematically illustrates this process associated with the lid but fails to recognize the true origin of the lid.

Lloyd (1942) and Fulks (1951) hypothesized that upper-level fronts produced the necessary lifting. Fawbush et al. (1951) concluded that approaching surface frontal systems were needed to produce the necessary lifting. Beebe and Bates (1955) proposed that transverse circulations associated with upper tropospheric jet streaks (four cell model of Riehl et al., 1954) created the needed lifting.

Carlson et al. (1980), Anthes et al. (1982), Carlson et al. (1983) and Lakhtakia and Warner (1987) show that moist air flowing out from under the lid into a region of much lower stability results in the elimination of the lid's affects much more efficiently than lifting. This process has been termed "underrunning." These investigators have shown that underrunning is the most important and most prevalent process that results in severe weather production.

Other investigators such as Lloyd (1942), Means (1944), Whitney and Miller (1956), House (1959), and Crumrine (1965) imply that underrunning occurs when they cite the importance of horizontal differential advection. Miller (1955) defines differential advection as, "... any vertical variation of the horizontal transport of heat and humidity which decreases the vertical stability of the air column." McNulty (1980) provides a more complete historical review of the differential advection concept in severe storm research. Means (1952, p. 188) was the first to specifically use the term "underrunning" to refer to stability change via differential advection with respect to the low-level air parcels flowing out from under a "stationary hub of warm air." Many other investigators (e.g., Fawbush et al., 1951; Sugg and Foster, 1954; Porter et al., 1955; and Miller, 1959) emphasized the importance of this crossing flow. Newton (1963) schematically illustrated the roles of the M and the P airstreams (Figure 2.1 on page 11) in destabilizing the environment by tracking their trajectories through the trough.

This Lagrangian perspective on destabilization, which is central to the Carlson-Ludlam conceptual model, was also taken by Fujita et al. (1970) in their use of "material differential advection" as a forecasting tool. This process is discussed further and mathematically formulated within the stability change equation by Anthes et al. (1982). They show that the rate of destabilization via underrunning (differential advection) can be large because of the strong stability and thermal gradients created by the confluence of the

two different airstreams (CD and P in Figure 2.1 on page 11) along the lid edge. Whitney and Miller (1956) showed that:

> If the stability decreases slowly [leaks], updrafts of lesser intensity will have time to break out and release the latent energy at a relatively slow rate long before it has reached extreme values. But if the destabilization is rapid [underrunning], the available latent energy may become quite large before an updraft is set off to release it. (p. 224)

Sugg and Foster (1954) expressed the opinion that:

> Perhaps the most severe tornadoes should be expected in air that has built up a large amount of potential energy by dry-over-moist structure before the "triggering mechanism"...[releases it]. (p. 139)

Even Miller (1959) stated that:

> The development of convective activity is retarded until the airmass is triggered, when the latent instability is released with explosive violence. (p. 467)

In essence, underrunning enables the latent instability which builds-up below the lid, to be suddenly and violently released in a concentrated area. This is perhaps one of the reasons why the Great Plains of the United States has such spectacular occurrences of severe convective storms.

The underrunning favors violent convection in three ways (Whitney and Miller, 1956):

> 1) It decreases the amount of work required to lift the air.
>
> 2) It decreases the height through which the air must be lifted before it will rise freely.
>
> 3) It increases the amount of energy available to the convective system aloft. (p. 224)

The first two of these effects permit the convection to be initiated more easily. This happens because, with the increase of low-level θ_w due primarily to latent heat flux at the surface, the lifted condensation level (LCL) is lowered and hence so is the level of free convection (LFC) (i.e. the negative area decreases). Fawbush et al. (1951) also stressed the importance in the height of the LCL/LFC. They pointed out that as θ_w increases and the LFC lowers, the positive area increases.

Many investigators (e.g., Fawbush et al., 1951; Means, 1952; Sugg and Foster, 1954; Whitney and Miller, 1956) found that severe convection developed on the "high height" side of the maximum gradient in the LFC distribution, on the windward side with respect to the upper-level winds, to the left of the low-level flow along the gradient. This observation is consistent with the conceptual model. Noting that the LFC is indirectly proportional to θ_w, and that θ_w is a maximum under the lid but quickly decreases at the edge, it can be concluded that the maximum LFC gradient is along the the lid edge. Consequently, low-level flow turned across this gradient from low to high height values is merely a reflection of the underrunning process. Clearly, low-level differential advection is an important process to consider when forecasting severe convection (Whitney and Miller, 1956).

Unfortunately, most of the investigators who have used differential advection in their studies did not consider whether their trajectories remained with the same "airmasses" or not (e.g., Whitney and Miller (1956) and McNulty (1980) advected on constant pressure surfaces; Fujita et al. (1970) advected on constant heights). Because the lid base follows isentropic surfaces, trajectories on either pressure or height surfaces would sometimes change airstreams. For example, the 850 mb pressure surface near the dryline would most probably be in the EML, whereas farther downstream the surface would be in the moist air. For this reason, it is advisable to use isentropic surfaces when considering differential advection.

Anthes et al. (1982) refer to the fact that Lagrangian differential advection is accomplished by the ageostrophic component only. Although differential advection is frequently observed on daily upper air weather charts, it may also be inferred that if winds are geostrophic at all levels, the differential advection is only recreating stability profiles which previously existed upstream. Therefore, in order to diagnose regions of

underrunning, ageostrophic circulations must be inferred from, among other things, a knowledge of the circulations associated with fronts and jet streaks.

2.5 Ageostrophic Circulations

Lakhtakia and Warner (1987) show that differential heating across the dryline results in an ageostrophic component to the flow and hence produces underrunning. This component advects moist air from under the lid and allows moist convection to develop at the lid's edge. Subsequent moist convective heating then induces a stronger low-level convergence that strengthens the underrunning, which further enhances the convection (i.e. a feedback is set up). Feteris (1978) also shows that once convection is established at the edge of the "barrier [lid]," the induced circulations also enhance the differential advection by processes similar to those reported by Keyser and Carlson (1984). (See the discussion in the previous section). Hence, diabatic contributions are an important consideration in differential advection.

Another important contribution to underrunning is the transverse ageostrophic circulation established by jet streaks. Jet streaks are defined here as regions of isotach maxima (Palmén and Newton, 1969, p. 199). There is much literature on the influence of both the upper and lower jet streaks on severe storm production. For good reviews of the roles of tropospheric jet streaks in the development of severe storms, see: Petterssen (1956a, pp. 112-118), Reiter (1963), Ludlam (1963), Newton (1963 and 1967), Cahir (1971), Danielsen (1974b), Uccellini and Johnson (1979), Burkhart (1980), and Shapiro (1981, 1982). It is very clear that there is a large impact of the upper- and lower-level jet streak couplet on the production of severe weather. Beebe and Bates (1955) used the resulting circulations to explain the presence of the "necessary" lifting of the lid; however,

they overlooked the contribution of this circulation to enhancing the underrunning of the low-level flow.

The transverse ageostrophic circulation which couples the upper and lower jet streaks provides a means to simultaneously view the vertical and horizontal differential advective processes of destabilization in a lid situation (Uccellini and Johnson, 1979). One point to note is that the strength of these transverse circulations is dependent on the static stability (Eliassen, 1951; Benjamin and Carlson, 1986). As an upper-level jet streak moves in the vicinity of an EML, whose static stability is inherently low, the circulation becomes much stronger. Two important things happen when this occurs. First, the jet streak's propagation is slowed considerably, which allows it to affect a given area for a longer time. Second, the low-level jet streak component (underrunning) strengthens very rapidly.

The ageostrophic wind can be separated into three components: inertial advection, *isallobaric, and frictional* (Shapiro, 1982). In the upper-levels of a jet streak, inertial advection dominates; in the lower levels the isallobaric component dominates (Uccellini and Johnson, 1979). Uccellini and Johnson's numerical results verify that the lower tropospheric branches of the ageostrophic transverse circulation, forced by a two-layer mass adjustment accompanying the propagation of the upper-level jet, is adequately represented by the surface isallobaric winds.

Therefore, it can be assumed that the isallobaric wind is a good approximation of the low level ageostrophic wind component. As such, the isallobaric wind can be used to calculate the lower-level advection component when determining differential advection. Because the isallobaric wind is largest near the surface (Anthes et al., 1982) and because the upper and lower level transverse circulations are in opposite directions, there is significant directional shear in the ageostrophic wind. Consequently, significant differential advection exists in the vicinity of transverse circulations of the jet streak (Brill et al., 1985).

Along with favorable differential advection, favorable upperlevel dynamics are needed to sustain severe convection (Palmén and Newton, 1969, p. 394). Shapiro (1981, 1982) describes how upper and lower geostrophic forcings can couple to form favorable or unfavorable circulations for severe weather development depending on their vertical orientation. For sake of illustration, two different vertical alignments of the exit region of an upper-level jet front with a surface cold front and low-level jet at its leading edge are presented (Figure 2.4 and Figure 2.5; from Shapiro, 1982).

When geostrophic stretching deformation (diffluence) of an upperlevel jet exit region is situated to the west of a shearing deformation zone (cold front) and low level jet (Figure 2.4a), the thermally indirect circulation in the upper jet exit region overlies the direct circulation of the surface front and low level jet (Figure 2.4b). This situation suppresses deep convection at the leading edge of the surface front for two reasons. First, mid-tropospheric divergence is created where the descending branch of the upper circulation impinges upon the shallow ascent at the surface front. Second, the convectively stable stratification of the upper front acts to inhibit the vertical development of deep convection.

When the upper-level jet exit region is situated to the east of the cold front and low level jet (Figure 2.5a), the upper and lower circulations are vertically aligned (Figure 2.5b). This allows a deep, narrow plume of ascending motion near the leading edge of the surface front to form. This ascent would also be located near the edge of the lid. Hence, this situation is highly favorable for severe weather production because strong low-level underrunning, upper-level cold air associated with the upper-level front, strong low-level shear associated with the low-level jet, and ascent are all coupled together in one region!

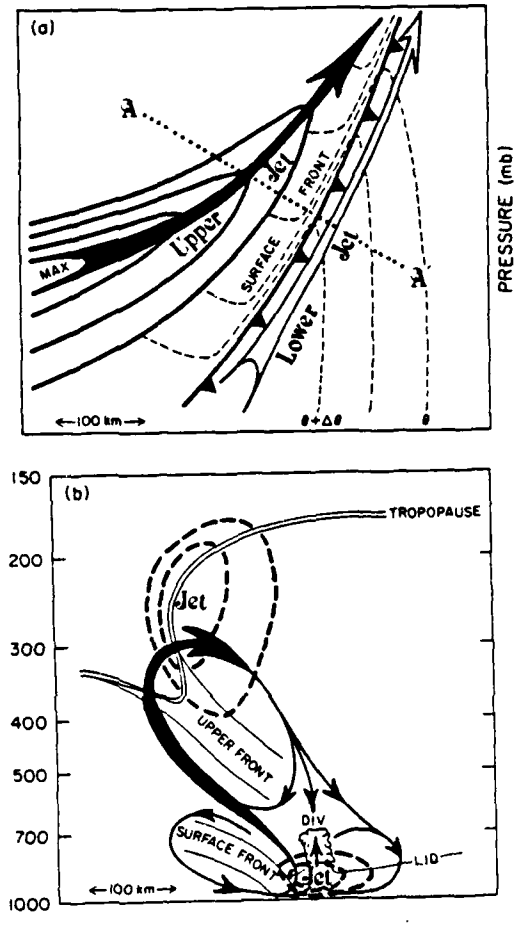

Figure 2.4: Vertically uncoupled upper and lower tropospheric jet-front systems and their associated secondary circulations (Unfavorable). (a) Upper jet-front exit region displaced to the west of a surface front and low-level jet. Upper jet (isotachs, heavy solid lines), upper-jet axis, solid arrow; lower jet axis, open arrow; surface potential temperature, thin dashed line; line AA', projection for cross section. (b) Cross section along the line AA' in (a). Upper and lower jet isotachs, heavy dashed line; potential vorticity tropopause, double thin lines; upper- and lower-level frontal surfaces, thin solid lines; moist layer, stippled area; streamlines with heavy arrows forced secondary circulation.

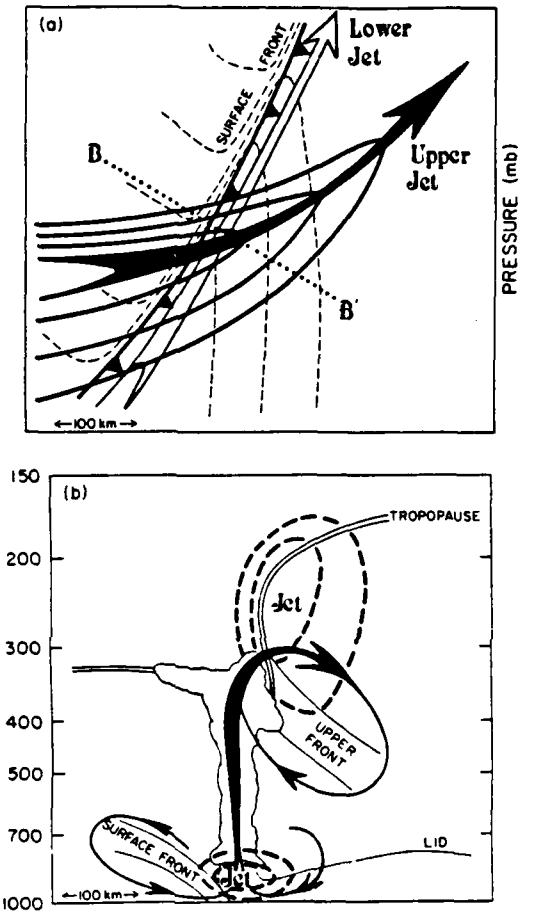

Figure 2.5: Vertically uncoupled upper and lower tropospheric jet-front systems and their associated secondary circulations (Favorable). (a) Upper jet-front exit situated above the surface front and lowlevel jet. Line BB', projection for (b). (b) Cross section along the line BB' in (a). Symbol conventions same as Figure 2.4 on page 43.

2.6 Summation

Several severe weather case studies, drawn from the data-dense 1979 SESAME field program (Carlson et al., 1980; Goldman, 1981; Carlson et al., 1983) and studies drawn from the standard NWS rawinsonde network (Goldman, 1981; Carlson and Farrell, 1983; Lanicci, 1984b), have demonstrated that the Carlson and Ludlam Conceptual Model is realistic in positioning observed outbreaks of severe convection.

The concepts involved with the Conceptual Model help give physical explanation to many of the methods and rules which have been employed by operational forecasters for many years (some since World War II). The model has been proven effective in supplementing, or fine tuning, the methods currently employed. As such, it deserves attention and possible integration into current methodologies; however, subjective analysis of the necessary number of upper-air soundings is much too time consuming for operational use. Therefore, a computer application was developed in an attempt to make the conceptual model operational. A discussion of that application follows.

Chapter 3

OBJECTIVE LID EDGE DETERMINATION

Goldman (1981) designed a preliminary operational technique to recognize the shape and areal extent of existing lids. The 700 mb chart was his primary tool. Lanicci (1984b, pp. 20-22) presented a subjective analysis technique in a form suitable for incorporation into Air Weather Service operational procedures. Although subjective analysis of mandatory pressure level charts has been proven useful, it does have a major weakness. Because the EML follows isentropic surfaces and not pressure surfaces, it can rise above a given pressure level but still remain effective at capping deep convection. Therefore, even though the EML "disappears" from the analysis, it still has impact on the environment downstream; how far downstream is impossible to tell using pressure surfaces alone.

For this reason, Carlson and Farrell (1983) developed an objective computer analysis routine using significant level data to determine the existence and areal extent of lids. They then used the 700 mb chart and selected soundings to verify the analysis. Because of the problems using mandatory level data and the fact that subjective analysis of sounding data is prohibitively time-consuming, a computer application is stressed here. A refinement of the computer application developed by Carlson and Farrell is presented in this chapter.

The computer application, named L.I.D. [Lid Involvement Delineator], is based on the values of the two terms in the Lid Strength Index (LSI) (Carlson et al., 1980) and several other criteria derived from subjective inspections of many decided lid soundings. A discussion of these criteria and their implications follow; however, a description of the LSI and its individual terms is required first.

3.1 The Lid Strength Index

Quantitative prediction of severe convective storms is aided by the use of a multitude of stability indices. For example: Showalter Index (Showalter, 1953); Lifted Index (Galway, 1956); K Index (George, 1960); Total Energy Index (Darkow, 1968); Potential Buoyancy Index (Wills, 1969); Tornado Likelihood Index (Wills, 1969); Sweat Index (Bidner, 1970); Potential Wet-Bulb Index (David and Smith, 1971); Total Potential Instability, or LAPOT Index (Harley, 1971); and the Total Totals (Miller, 1972). Most of these indices use the difference between upper level temperatures and temperatures of parcels lifted from a lower level. None of these, however, are sensitive to low level inversions, like the lid.

An index was developed by Carlson et al. (1980) which is sensitive to those low level inversions. They called it the Lid Strength Index (LSI) even though it is sensitive to inversions produced by any mechanism. Wet-bulb potential temperature is used in the index rather than temperature because it is proportional to energy and hence, more representative of the actual physics involved (Darkow, 1968; Madden and Robitaille, 1970; Levin, 1972; Betts, 1974). The index has had several changes since its inception (Carlson et al., 1983; Carlson and Farrell, 1983; Graziano and Carlson, 1987). It is defined in this work as:

$$LSI = \underbrace{(\theta_{sw5} - \theta_{bw})}_{A} + \underbrace{(\theta_{swl} - \theta_{bw})}_{B} \qquad (2)$$

where:

> θ_{sw5} is defined as the saturated wet-bulb potential temperature at 500 mb. This was done to be compatible with customary versions of the Lifted Index, although it could be defined as the average saturated wet-bulb potential temperature from a predetermined reference level up to 500 mb to better represent the actual energy involved.

θ_{bw} is the maximum (or best) of the individual 50 mb-thick layer-averaged wet-bulb potential temperatures in the Planetary Boundary Layer (PBL), which is defined here to pertain to a layer extending from the surface up to either the reference level or 100 mb above the surface, whichever is lower in height.

θ_{swl} is the maximum saturated wet-bulb potential temperature from the reference level up to 500 mb.

As such, term A quantifies the convective instability, or the buoyancy, of air parcels originating from the PBL. Term A, therefore, is labeled the Buoyancy Term. This term is very similar to the Lifted Index currently used by the National Weather Service, but is approximately half the numeric value. Term B quantifies the strength of any low level inversions and its capabilities in suppressing convection. Term B, therefore, is labeled the Lid Strength Term. A sample calculation is presented in Figure 3.1.

The index was first designed to use the lifted condensation level (LCL) as a reference level for calculation of the terms (Carlson et al., 1980). It was determined by Carlson and Farrell (1983) that this wasn't a consistent enough reference because the position of the LCL varied with respect to the lid base, from sounding to sounding (Section 2.2). In some cases, the LCL is below the lid base and calculated terms are representative. In other cases, however, the LCL is above the lid base and calculated terms are not at all representative. In those cases, the layer used to calculate the PBL θ_w component extends into the dry air. As a consequence, the calculated value is much less than that which is likely to be found in the buoyant thermals present in the PBL. For this reason, Carlson and Farrell used the top of the surface-based moist layer as the reference level.

The top of this layer is marked by a sharp transition from high to low relative humidities. This transition is almost a discontinuity (i.e. a zero-order break) in relative humidity. Carlson and Farrell considered a 30% difference between reported contiguous significant level data points as the critical value for the relative humidity break to mark the top of the moist layer. They labeled this the level of the relative humidity break

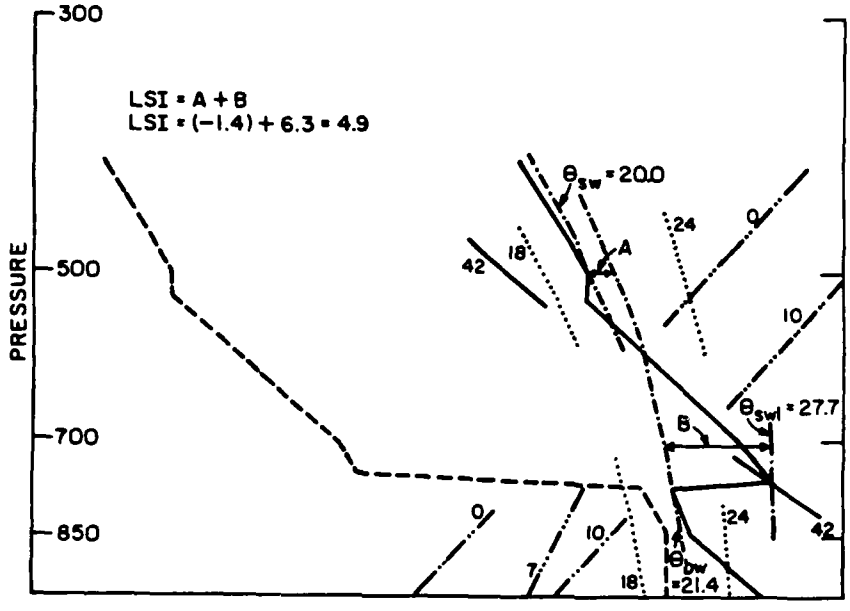

Figure 3.1: Conceptual lid sounding showing the Buoyancy Term (A) and Lid Strength Term (B) of Equation 2. A sample calculation of the LSI is shown.

(LRHBRK). Graziano (1985) and Lanicci (1984b) used a change of 40% per mb over a 40 mb layer (1% per mb) to find LRHBRK. As Heppner (1984) pointed out, their value is too restrictive because it incorrectly excludes actual lid soundings. Recent empirical studies have shown that 35% over 40 mb (0.87% per mb) is more satisfactory. If such an LRHBRK is not present within a sounding, the reference level used for the calculation of the Buoyancy Term (A) is set at 100 mb above the surface and the Lid Strength Term is set to zero.

A representative average wet-bulb potential temperature in the PBL has been the most difficult variable in the LSI to calculate, and unfortunately the most important for two reasons. First, most severe storms have been found to be associated, not with an abnormally low θ_{sw} aloft, but with an abnormally high θ_w in the PBL (Newton, 1963; Ludlam, 1963; Carlson and Ludlam, 1965). The results presented in Section 5.3 supports this contention. Second, this variable appears twice in the LSI's definition. Not only does an increase in θ_w increase the potential buoyancy, but it also renders any existing lid less effective at capping convection. As a consequence, small changes in θ_w create large changes in the stability.

Because of this difficulty, there have been several attempts at redefining this variable to make it as representative of the actual available potential energy as possible. It was first defined as the average θ_w in the lowest 50 mb (Schwartz, 1980). Goldman (1981), however, showed that this value is much too dependent on surface layer diurnal effects in a manner which produces misleading results. He proposed that the maximum θ_w in the lowest 100 mb be used instead. Carlson and Farrell (1983) used this definition with good results.

Convection has been shown to be dependent on an average θ_w within a moisture-source layer and not on the somewhat higher values obtained from afternoon screen-level

readings (Carlson and Ludlam, 1965). It has also been determined that the vertical moisture gradient in the PBL complicates determination of the LCL and the more important level of free convection (LFC) (Petterssen, 1956b; Malkus, 1958; Warner, 1963; Betts, 1974). Therefore, using the maximum θ_w in the lowest 100 mb frequently misrepresents the actual LFC and in turn the convective instability.

Graziano and Carlson (1987) used the average θ_w in a layer bounded by a top 80 mb above the surface and a bottom 30 mb above the surface. They did this to avoid the troublesome surface layer and its diurnal effects, while at the same time incorporating the layer averaging benefits. Unfortunately, however, this definition encounters similar problems when using the LCL as the reference level (i.e. their calculated average θ_w could be much less than that which is actually available). Hence, both their Buoyancy Terms (A) and their Lid Strength Terms (B) could be larger (more positive) than what may actually be present. Consequently, they could both underestimate the convective instability and overestimate the strength of inversions.

In an earlier attempt to deal with this problem of determining a representative θ_w in the PBL, Fujita et al. (1970) introduced the Best Lifted Index. They found that calculating average θ_w's in 50 mb-thick layers incremented every 10 mb and using the maximum of those values gave them the "best" (i.e. most unstable) representative value of the lifted index. Not only did they find that this method was representative but they showed that this value was relatively conservative with respect to time of day, which makes it an easier parameter to forecast and thus the best indicator of θ_w in the PBL. Hence, their definition is adopted here.

Another change to the original definition is that the sign convention has been reversed (Carlson and Farrell, 1983). Since the LSI is a "stability" index, positive values should indicate stability and negative values should indicate instability, as suggested by

Showalter (1953). Therefore, positive LSI indicates areas of stable environments; negative LSI indicates areas of unstable environments. This also made it compatible with the sign convections of the Lifted Index.

A positive Lid Strength Term shows that an inversion is present (stable lapse rate). The more positive the term, the stronger the inversion. Because the Lid Strength Term does not physically contribute to the buoyancy, the term is set to zero if it becomes negative (Carlson and Farrell, 1983). Therefore, the Buoyancy Term remains as the only possible contributor of negative values to the LSI. When the Buoyancy Term is positive, the LSI is positive and the environment is stable. When the Buoyancy Term is negative, the environment may be convectively or potentially unstable. The Lid Strength Term determines which. If the Lid Strength Term is positive, the environment is potentially unstable. If the Lid Strength Term is zero, the environment is convectively unstable.

Graziano and Carlson (1987), found that there was only a small statistical significance when using both LSI terms added together to delineate between areas of convection and no convection, but that there was a large statistical significance when using the terms separately. They determined that under the condition of a negative Buoyancy Term, there is a critical value of the Lid Strength Term which can be used to delineate areas that can support convective activity from those that can not. This critical value varied with sounding time. At 0000 GMT, the critical value was determined to be +3. At 1200 GMT, the critical value was determined to be +2. The diurnal variation is thought to be the result of the definition of the depth over which the PBL θ_w was determined.

A Lid Strength Term value greater than this critical value signifies that an inversion exists that can effectively suppress convection. Therefore, as Graziano and Carlson have shown, convection may only develop in areas where the Buoyancy Term is less than or equal to zero, but may be confidently ruled out in areas where the Lid Strength Term is

greater than the critical value regardless of the value of the Buoyancy Term. The example in Figure 3.1 on page 49 shows that even though the sounding is latently unstable with a Buoyancy Term of - 1.4°C (Lifted Index of -2.2°C), the Lid Term of +6.3°C rules out any possibility of convection. Thus, the lid strength limits the areas of possible convective development. Limiting the forecasting area to regions where convection is possible is a concept recognized by Fawbush et al. (1951). Therefore, using the Lid Strength Term in conjunction with the Buoyancy Term has a large advantage over the currently used Lifted Index.

3.2 L.I.D.

To develop the Lid Involvement Delineator, criteria are required for separating lid soundings from non-lid soundings. Figure 1.1 on page 6 depicts the typical sounding found in a lid situation. From this composite and the discussions in Sections 1.2 and 2.1.1, most of the criteria, although developed empirically, can be easily identified. These criteria are:

(1) A relative humidity discontinuity (sharp decrease, or break (RHBRK)) should be present at a level below 500 mb.

(2) A layer, in which the lapse rate of the saturation wet-bulb potential temperature (θ_{sw}) has a maximum (i.e. inversion) or is zero (i.e. constant with height), must exist within 100 mb of the level of the RHBRK (LRHBRK).

(3) The Lid Strength Term must be equal to or greater than the critical value determined by Graziano (1985).

(4) The Buoyancy Term must be less than 0.5°C.

(5) The static stability, $-T\theta^{-1}(\partial\theta/\partial p)$, above an existing inversion (within the EML) must be less than 4.5°C per 100 mb.

(6) The relative humidity above the inversion must increase with height.

The first criteria, if met, would mean that a boundary separates moist air below from dry air above. This follows from the fact that the EML is exceptionally warm and dry (i.e. very low relative humidity) and traps moisture below it within potentially cooler air (i.e. high relative humidity). The critical break in relative humidity presented in the previous section also applies here (0.87% per mb within a 40 mb layer). The requirement that this RHBRK be present below 500 mb stems from the observation that inversions above this level are ineffective at capping deep convection.

The second criteria pertains to the fact that the EML is potentially warmer than the layer below. This does not necessarily mean that the temperatures are higher. Rather, it means that the potential temperature, or saturation wet-bulb potential temperature (θ_{sw}) is higher in the EML than that below it. This is an important point because it was found that in several lid cases, the temperature lapse rate reversed before the θ_{sw} lapse rate did. This often led to an incorrect positioning of the lid base. The requirement that a θ_{sw} inversion be present within 100 mb of the RHBRK follows from the fact that the potentially warm air must coincide with the dry air in order to remain consistent with the definition of the EML. Using a finite depth of 100 mb allows for mixing through the boundary and dilution of the gradients.

The third criteria, requires the existence of an inversion at midlevels that is capable of suppressing convection. A sounding with a Lid Strength Term greater than or equal to +2 at 0000 GMT or +3 at 1200 GMT is considered to have a lid; a Lid Strength Term less than those values but greater than or equal to +1 is considered to lie near the lid edge; and a Lid Strength Term less than +1 is considered lid free (Graziano and Carlson, 1987).

The fourth criteria requires the presence of latent instability. The absence of latent instability suggests that, either the lid hasn't been around long enough to affect an

increase of θ_w, or some other mechanism, such as subsidence, may have produced the inversion. In either case, the sounding would be ruled out because convection can not develop. A value of 0.5°C is used as the critical value instead of 0°C, as might be expected, in order to compensate for small errors in the reported data and/or calculation truncation.

The fifth criteria is introduced to delineate, as much as possible, between inversions created by EMLs and subsidence. An empirical study was conducted to determine a threshold value between the lapse rate of a mixed layer and the lapse rate above a subsidence inversion. The value 4.5°C per 100 mb was found to be the best; this value excludes most subsidence inversions but not all. This value falls within values determined in previous studies. Fawbush and Miller's (1952) composite sounding has a static stability of 3.5°C per 100 mb in the layer above the inversion; Karyampudi (1986) used a value of 4.0°C per 100 mb in his study of the Saharan Air Layer; Gates (1961) found that the static stability in the mixed layers over the Great Plains fell below 5°C per 100 mb by July (see Figure 2.3 on page 27).

The sixth and final criteria was derived from past studies, which found that the relative humidity increases with height near the top of most mixed layers (Fawbush and Miller, 1954; Marht, 1976; Schaefer, 1976). This criteria has been found to exclude many of the subsidence inversions that are not eliminated by the fifth criteria. The relative humidity in most subsidence inversions decreases rapidly and continually with height; however, there are three notable problems with this last criteria.

First, once the dewpoint depression exceeds 30°C, the rawinsondes often fail to recover if the dewpoint depression rebounds. Second, current convention requires that dewpoint depressions (Tdd) in excess of 30°C are reported as 30°C (ESSA, 1981). Hence, a Tdd of 45°C rebounding to 31°C, for example, is not reported. The special soundings

taken during the SESAME projects showed that the Tdd did indeed decrease near the top of the existing mixed layers (Carlson et al., 1980). Finally, the change in relative humidity often doesn't meet any of the criteria for selecting significant levels (ESSA, 1981).

As with any objective computer analysis, L.I.D. is affected adversely by data transmission errors and very erratic soundings. Several validators were designed in an attempt to retrieve some of the affected soundings. Note that the following items represent either errors or anomalies in the data.

(1) Elevated (i.e. not in contact with the surface), super-adiabatic layers deeper than 20 mb are not allowed. If such layers exist, they are converted to adiabatic layers.

(2) Gross fluctuations of temperature in layers less than 5 mb deep are smoothed out.

(3) Dewpoints are checked to see if there are any sharp or chaotic fluctuations between significant data levels. If the dewpoint between two contiguous levels changes by more than 30°C, it is corrected to a more representative value. If within any 100 mb layer, the dewpoint of two contiguous levels changes by more than 15°C and the dewpoint in the next significant level above that is only 5°C different from the lowest level, the middle significant level value is corrected to a massweighted average of the two bounding significant levels.

(4) When changing both temperature and dewpoints independently, it is necessary to check to make sure that the dewpoints are not greater than the temperature. If a dewpoint does become larger than the temperature, it is set equal to the temperature.

(5) Reported pressures are checked to make sure that they decrease with height. If they don't the sounding is discarded.

(6) If more than half of the significant levels are found to have errors, the sounding is discarded.

Once these problems are corrected, L.I.D. checks the significant level data at each station to determine if the data meets the six criteria. If it does, the sounding is flagged as containing a lid (when the Lid Strength Term is greater than or equal to the critical value), or near the lid's edge (when the Lid Strength Term is less than the critical value but

greater than 1). Each of these criteria is necessary but none are sufficient alone to flag a sounding as a lid sounding. Upon doing this, a map may be produced which delineates the position and areal extent of any existing lids. This routine takes only a few minutes to execute. L.I.D. is used in the analysis of the case study presented in Chapter 4 and is used to compile statistics for the climatological study presented in Chapter 5.

Chapter 4

THE CASE STUDY

The purpose of this chapter is to present a case study showing the applicability of the Conceptual Model. The 31 May 1985 Tornado Outbreak was chosen because it was a major tornado outbreak in which a lid was found to play a major role. The following discussion concerns the lid and its interaction with an upper-level jet streak which initiated an underrunning process.

4.1 Outbreak Statistics

On the last day of May 1985, the worst tornado outbreak to strike the United States, since the super outbreak of April 3-4, 1974 (Hoxit and Chappell, 1975), devastated parts of Ohio, Pennsylvania, New York State, and Ontario between Lake Ontario and Georgian Bay (Taggart et al., 1985; Farrell and Carlson, 1988). The statistics of the outbreak are presented in Table 4.1 and a map of the tornado paths is presented in Figure 4.1a. Figure 4.1b shows the location of the inception areas of each of the families noted in Table 4.1. The data were adapted from Forbes (1985).

They are based upon aerial and ground surveys, interviews, and newspaper accounts, on behalf of the National Weather Service Disaster Survey Team and the National Academy of Sciences National Research Council Survey Team. Aerial and ground surveys in the United States were preformed by Dr. Forbes (Penn State University) and Mr. Duane Stiegler (University of Chicago). Aerial and ground surveys in Ontario were preformed by Ontario Weather Centre, Atmospheric Environment Service and Mr. Brian Smith (University of Chicago). The map was prepared by the University of Chicago.

Table 4.1: Tornado List -- 31 May 1985 Outbreak

Times are from late on 31 May to early on 01 June. Superscripts in Tornado Name column reference numbering in Figure 4.24b. The Fujita Scale (F), Path Length (P_L), and Path Width (P_W) classifications are by category (see Table 4.2). The convection 9(18) in the path length column indicates a track continuous for 9 km and partly aloft for 9 more, for a total path length of 18 km. D is number of deaths reported; I is number of injuries reported. * indicates 10 in OH and 8 in PA. Adapted from Forbes (1985).

No.	Tornado Name	$F/P_L/P_W$	Length km	Width m	Times GMT	D/I
1	Rush Cove[1]	2/1/1	4	30	1900-1903	0/0
	BARRIE FAMILY[2]					
2	Hopeville	3/3/3	17	200	2010-2024	0/0
3	Corbetton	3/3/3	25(35)	200	2017-2045	0/?
4	Borden	2/3/2	9(18)	150	2050-2104	0/?
5	Essa	1/0/3	1	75	2057-2058	0/0
6	Barrie	4/2/3	9	250	2100-2107	8/144
	GRAND VALLEY FAMILY[3]					
7	Grand Valley	4/4/3	86(102)	300	2015-2127	4/?
8	Wagner Lake	1/1/2	5	100	2140-2144	0/?
9	Reavoro	1/2/2	9	100	2205-2211	0/?
	ALMA FAMILY[4]					
10	Alma	3/3/2	7(33)	150	2015-2040	0/?
11	Ida	2/2/3	9	200	2215-2222	0/?
12	Rice Lake	3/2/3	7(14)	200	2220-2230	0/?
13	Minto	1/0/0	1	13	2235-2236	0/?
14	Norfolk NY	1/2/1	8	40	0130-0140	0/0
	ALBION FAMILY[5]					
15	Albion PA	4/3/3	23	375	2059-2117	12/82
16	Corry PA	4/3/3	45	425	2125-2155	0/16+
17	Busti NY	3/3/2	21	175	2225-2245	0/10
	CENTERVILLE FAMILY[6]					
18	Dorset OH	2/3/2	16	150	2128-2141	0/15
19	Linesville PA	2/2/3	6	200	2110-2115	1/0
20	Saegertown PA	3/3/3	29(37)	250	2123-2155	0/?
21	Centerville PA	3/2/3	13	400	2212-2223	2/10
22	Thompson Run PA	1/2/3	8	200	2230-2237	0/0

(continued)

Table 4.1 (continued)

No.	Tornado Name	F/PL/Pw	Length km	Width m	Times GMT	D/I
	ATLANTIC FAMILY[7]					
23	Mesopotamia OH	3/3/3	24	425	2105-2120	0/30
24	Atlantic PA	4/4/3	90	350	2117-2230	16/125
25	Tionesta PA	4/3/4	48	800	2230-2310	7/30
26	Lamont PA	2/3/3	33	300	2250-2335	0/?
	KANE FAMILY[8]					
27	Tidioute PA	3/3/4	27	800	2330-2355	0/8
28	Kane PA	4/3/4	46	950	0000-0040	4/40
	MOSHANNON FAMILY[9]					
29	Moshannon State Forest	4/4/4	105(115)	1000	2335-0100	0/1!
30	Watsontown PA	4/3/4	34	850	0125-0215	6/60
31	Hollenback Twp	1/3/3	16	400	0245-0300	0/0
43	Tobyhanna PA	1/-/0	<1	15	0305-0306	0/0
	WHEATLAND FAMILY[10]					
32	Wheatland PA	5/4/3	75	425	2230-2335	18*/310
33	Big Bend PA	2/2/2	10	130	2354-0003	0/2
34	Emlenton PA	0/2/1	8	30	2356-0003	0/0
	BEAVER FALLS FAMILY[11]					
35	Middleton OH	2/3/3	24	200	2335-2355	0/20
36	Big Beaver PA	3/4/3	63	250	0010-0105	9/120
37	Penn Run PA	0/2/1	10	25	0153-0202	0/0
38	East Sparta OH[12]	1/-/1	<1	50	0105-0106	0/0
	UTICA FAMILY[13]					
39	Utica OH	3/3/2	45	150	2315-2345	1/20
40	Cooperdale OH	1/3/2	18	70	2350-0010	0/5
41	London OH[14]	1/0/1	1	50	2306-2307	0/0
42	West Union OH[15]	1/1/2	3	70	0105-0108	0/0
43	Tobyhanna PA (See Moshannon Family)					

Figure 4.1: The 31 May 1985 Tornado Outbreak. (a) The dark lines indicate the relative position, length, and width of each individual tornado path. Major metropolitan areas are indicated. The numbering is defined in Table 4.1 on page 59 (b) Indicates inception points of decided tornado families. Numbering is defined with superscripts in Table 4.1 on page 59 (adapted from Forbes, 1985).

UNITED STATES-CANADA TORNADO OUTBREAK of MAY 31, 1985

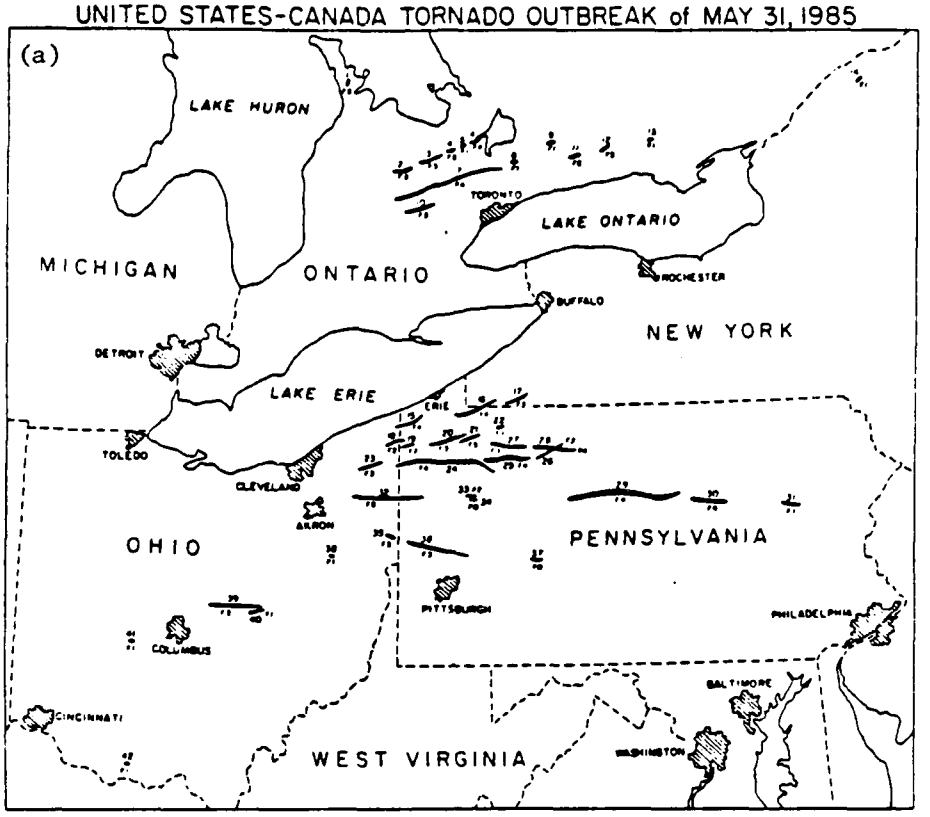

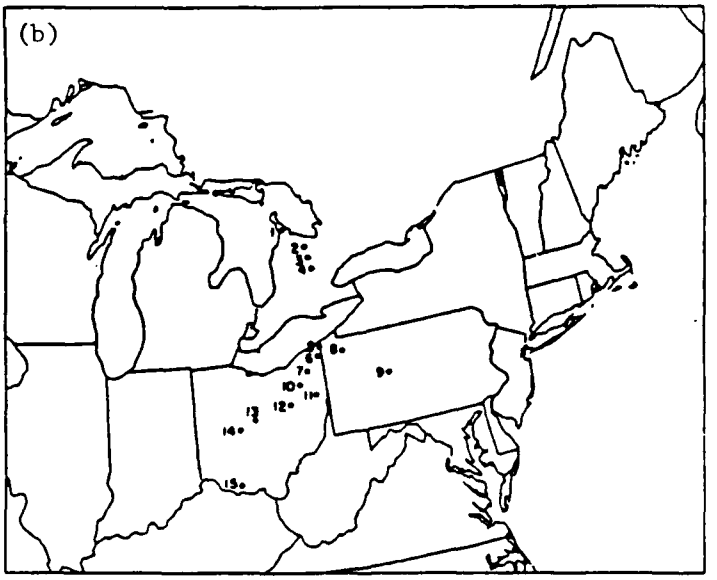

Table 4.2: Classification Key

The Fujita-Pearson (FPP) Tornado Scale. The values of wind speed, path length and width are computed from the equations below. Most tornadoes can be expressed by the FPP scale ranging between 0,0,0 and 5,5,5. Higher values are possible but unlikely. (Fujita, 1971).

F Scale	Maximum Windspeed	Expected Damage		Path Length	Path Width
F0:	<73 mph	Light	P0:	<1.0 mi	<18 yd
F1:	73-112	Moderate	P1:	1.0-3.1	18-55
F2:	113-157	Considerable	P2:	3.2-9.9	56-175
F3:	158-206	Severe	P3:	10-31	176-356
F4:	207-260	Devastating	P4:	32-99	.3-.9 mi
F5:	261-318	Incredible	P5:	100-315	1.0-3.1

Equations:

$$V = 14.1(F+2)^{3/2} \quad \text{Velocity in mph} \quad (1)$$

$$L = 10^{1/2(P_L-1)} \quad \text{Path length in miles} \quad (2)$$

$$W = 10^{1/2(P_w-5)} \quad \text{Path width in miles} \quad (3)$$

Much of the Climatological data which follows was taken from Ferguson et al. (1986, 1987).

At 1900 GMT on the 31st, the first tornadoes developed in Ontario along a warm frontal boundary. Within the next four hours, 13 tornadoes were spawned killing 12 people and injuring 450. Table 4.3 presents an approximate toll of the outbreak for Ontario and each of the three states affected. In order to focus this case study, however, the remainder of the discussions deal only with the outbreak in the United States.

At 2059 GMT, explosively developing thunderstorms formed just south of Lake Erie two miles west of the Pennsylvania border, and produced the first tornado of the outbreak in the United States (#15 in Table 4.1 on page 59 and Figure 4.1a). This tornado moved

Table 4.3: The Approximate 31 May 1985 Outbreak Toll

Tornado total shown here is greater than the outbreak total because of stateline crossings. D is number of deaths reported: I is the number of injuries reported. Adapted from Forbes (1985) and Taggart et al. (1985).

Region	Tornado Count	D/I	Homes Destroyed	Damage Losses
Pennsylvania	21	65/707	1009	$ 376,367,000
Ohio	11	11/340	300	$ 100,000,000
New York	3	0/16+	21	$ 4,000,000
Ontario	13	12/450	300	$ 150,000,000
TOTAL	48	88/1513+	1630	$ 630,367,000

ENE into Pennsylvania where it strengthened to F-4 intensity (see Table 4.2) just before it struck the town of Albion. Nine were killed (three in nearby Cranesville), and 82 were injured. It produced a 23 km (14 n mi) long path of destruction.

In less than 6 hours, 30 tornadoes produced a total path length of 863 km (540 n mi), killing 76 people (11 in Ohio and 65 in Pennsylvania) and injuring at least 1063 (See Table 4.1 on page 59). Twelve (40%) of the tornadoes were strong (F-2 and F-3) in intensity, and eight (27%) were violent (F-4 and F-5). Ten of the thirty tornadoes were killer storms. This was the highest death toll from one storm ever recorded in Pennsylvania, and was the worst to strike this section of the country since June 23, 1944 when 147 people were killed in West Virginia (103) and Pennsylvania (44) (Ferguson et al., 1986).

The most deadly tornado was also the most powerful one of the outbreak. It was registered as an F-5. It first touched down a few kilometers west of Newton Falls, OH, moved eastward at 20 ms^{-1} (39 kt/45 mph) for 75 km (47 n mi) through Wheatland Pennsylvania, and dissipated 22 km (14 n mi) east of the Pennsylvania border, near

Mercer. Eighteen people were killed (10 in Niles and Hubbard, Ohio; 7 in Wheatland and 1 near Mercer, Pennsylvania). This storm was the most powerful tornado in 1985 and only the third since 1977 to reach F-5.

The storms subsided just before midnight (0306 GMT) with a final total of 21 tornadoes in Pennsylvania (4 entered from Ohio), 11 in Ohio, and 3 in New York State (1 entered from Pennsylvania). Needless to say, several records were broken during this outbreak.

The 21 reported tornadoes in Pennsylvania broke the state single outbreak record of 5 set in 1983. Pennsylvania never reported more than 10 in any month. It was third in total number of tornadoes reported in all of 1985 with 21 (Both Texas and South Dakota reported 27). There were 181 total for the nation in May (26 above average). In contrast, there were eight months below normal in total tornadoes. A total of 82 tornadoes in June was the lowest monthly count since 73 were reported in 1959. A total of 51 tornadoes in July was the lowest monthly count since 42 were reported in 1960. On the other hand, August had more than twice its 35 year 1950-1984 mean of 52 reported. Overall, there were 682 tornadoes for the nation for all of 1985, the fewest since 654 in 1970 (25% less than 1984).

4.2 Synoptic Situation

One of the purposes of this study is to show that a lid was involved in this outbreak of tornadic storms. To also illustrate that the lid can be followed over an extended period of time, the analysis begins 33 hours before the outbreak began (1200 GMT 30 May, 1985). Analysis shows that, as the lid evolved and moved eastward, severe convective storms occurred along its edges. A major outbreak did not occur, however, until a migrating

baroclinic zone and strong jet streak moved to a location near the lid edge and established an environment favorable for underrunning and lifting along that edge.

4.2.1 1200 GMT 30 May 1985

On the morning of 30 May 1985 there was a quasi-stationary frontal boundary positioned along the United States-Canadian border (Figure 4.2). A low pressure center was forming on the front in North Dakota and a thermal trough was situated along the eastern slopes of the Rockies, extending from the low to Kansas (Figure 4.2a). A short-wave trough with an associated upper-level jet streak was moving through the northern Rockies (Figure 4.2c). Strong gusting winds (gusts up to 26 ms^{-1} [51 kt]) were reported over Utah and Colorado as this jet streak moved eastward (Storm Data, May 1985).

Figure 4.2b shows very warm (Temperature (T) = 10°C) and dry (Dewpoint depression (Tdd) > 20°C) air over the south central United States at 700 mb. Note how closely the 10°C isotherm and 20°C isopleth of Tdd are associated and how weak the gradients of those two fields are. This supports the contention that this air is a relatively uniform (i.e. well mixed) warm, dry airmass.

Figure 4.3 was produced by using L.I.D. which is discussed in Section 3.2. The edge of the lid is depicted as a double solid line. The western edge coincides with the dryline. Recall from Section 2.1.3 that the dryline constitutes the boundary along which the surface mixed layer becomes elevated. Note that many of the Lid Strength Term isopleths tend to be coincident along the dryline. This emphasizes that the dryline is a very sharp transition zone between regions with and without a lid. The cold front is superimposed from Figure 4.2a for reference.

The numbered circles in Figure 4.3 show the location of severe weather events which developed within a time interval of three hours on either side of 1200 GMT. Table 4.4

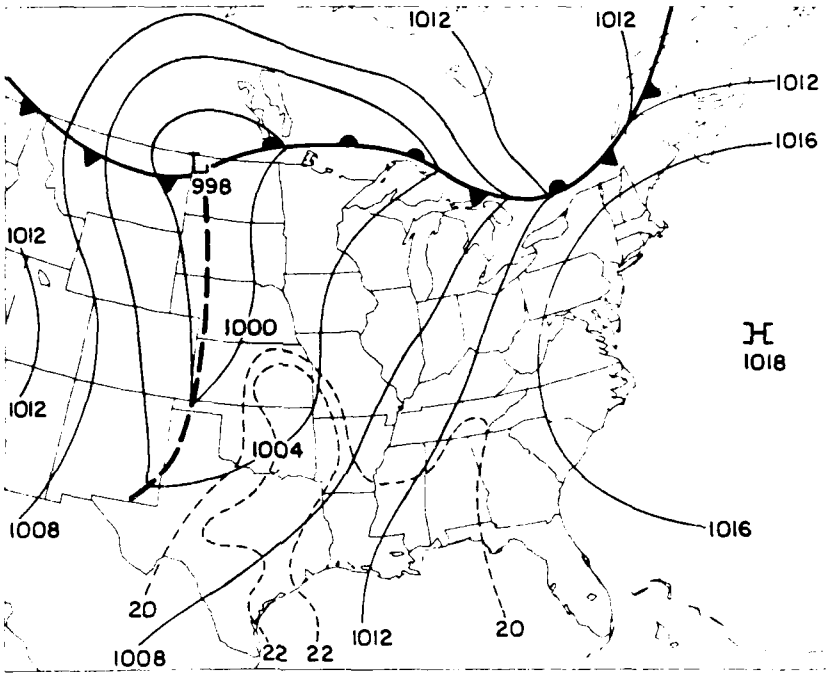

(a)

Figure 4.2: Synoptic situation for 1200 GMT 30 May 1985. (a) Surface: Fronts, troughs, and pressure centers are indicated with conventional symbolism; sea-level pressure in mb (thin solid lines); θ_{bw} in °C (short dashed lines). (b) 700 mb: Heights in meters (thin solid lines); 10°C isotherm (short dashed line); Dewpoint depression greater than 20°C is enclosed in scalloped line. (c) 500 mb: Heights in meters (thin solid lines); θ_{sw5} in °C (short dashed lines); winds greater than 25 ms^{-1} (50 kt) hatched.

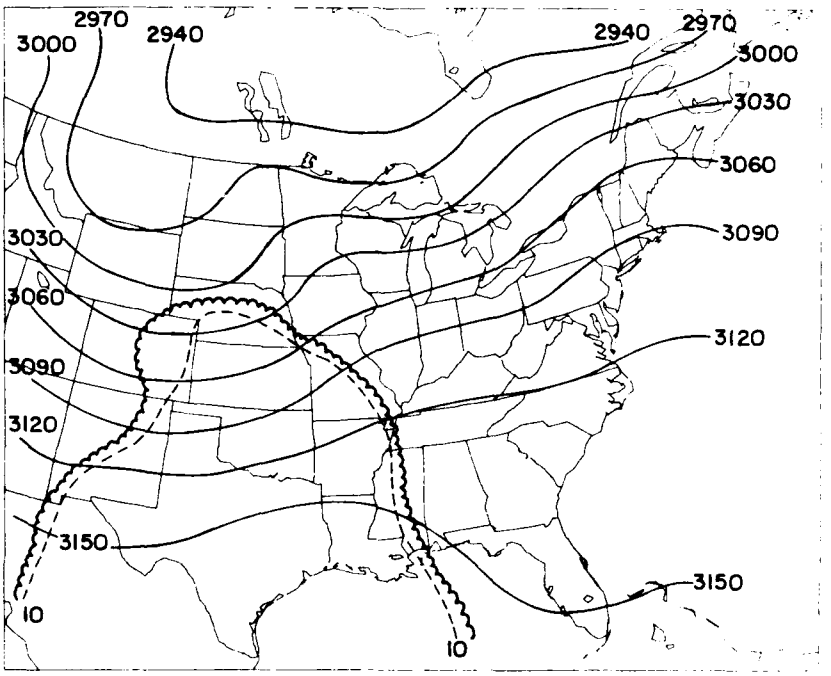

(b)

Figure 4.2 (continued)

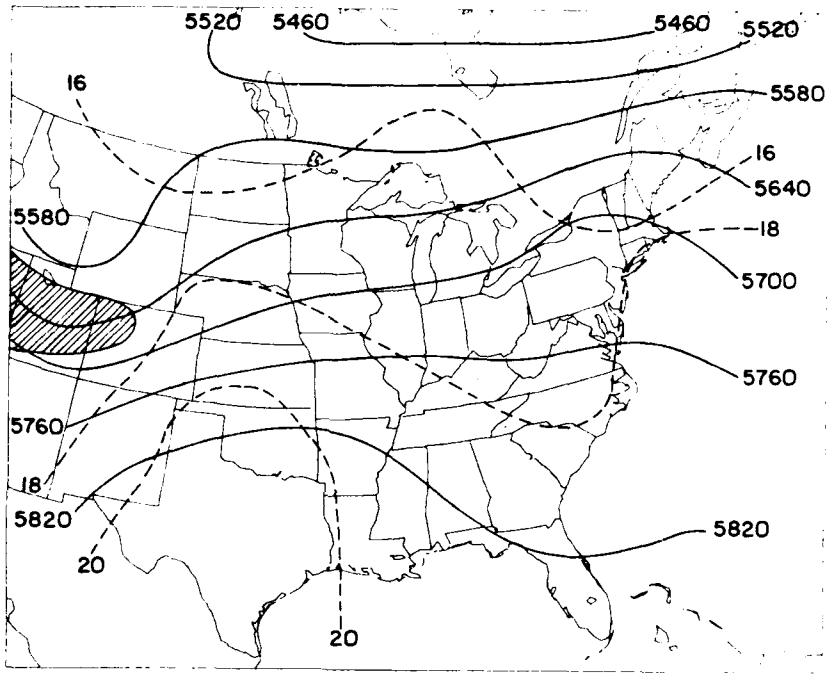

(c)

Figure 4.2 (continued)

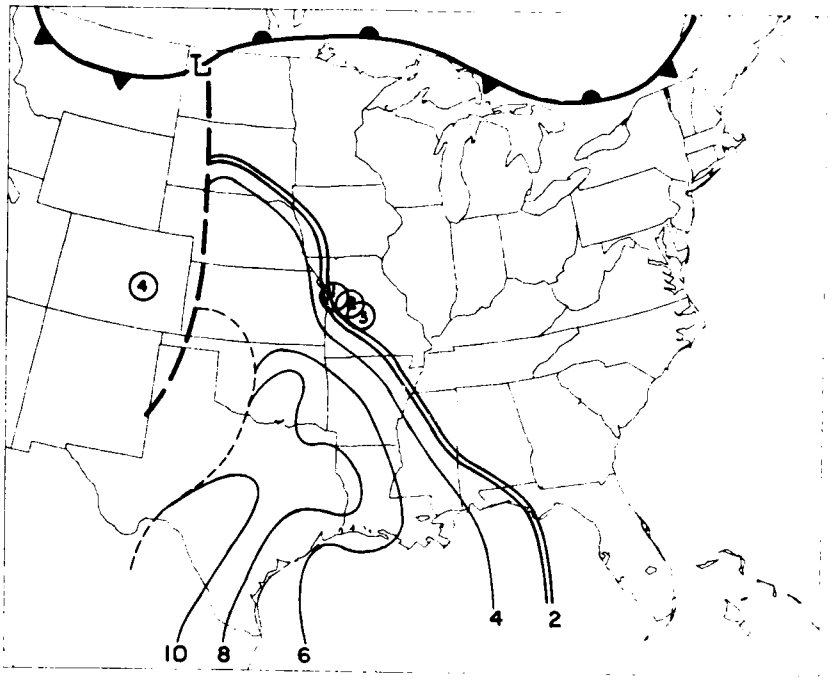

Figure 4.3: Lid Analysis for 1200 GMT 30 May 1985. Fronts, troughs, and pressure centers are indicated with convectional symbolism. Dryline (short dashed line); Lid Term of LSI [°C] (solid lines); Lid edge (solid double line, after Graziano and Carlson, 1987). Numbered circles indicate the location of severe weather events which occurred within a six hour window around the analysis time. Descriptions of these events are listed in Table 4.4.

lists the location, type of weather, and time of occurrence of each of the events (Storm Data, May 1985). The only severe convective weather reported in the nation during the six hour period was a series of hail storms in Missouri which began at 1020 GMT and persisted until 1530 GMT. The initial storm (circle #1 in Figure 4.3 on page 70) produced 7.5 cm (3") hail! This report was confirmed by the civil defense. All of these storms remained along the lid edge for their entire life cycle. A low-level jet formed beneath the lid and supplied a large flux of moisture to the storms.

Table 4.4: Storm Data: 0900-1500 GMT 30 May 1985

Numbers (#) refer to circles in Figure 4.3 on page 70. KEY: H=Hail [cm]; WG=Maximum wind gust [ms^{-1}]. (Storm Data, May 1985).

#	Weather	Location	Time (GMT)
1	H(7.6)	Jackson, Platte, & Clay Co., MO	1020-1100
2	H(2)	Saline, Pettis, & Copper Co., MO	1230-1430
3	H(2)	Cole Co., MO	1500-1530
4	WG(26)	El Paso Co., CO	1400-1600

Two soundings are shown in Figure 4.4. The first, Amarillo, Texas (72363), shows a very strong but shallow (16 mb deep) nocturnal inversion. Above this surface inversion there is a deep (293 mb deep) mixed layer with a relatively constant potential temperature (θ) (the static stability, $-T\theta^{-1}(\partial\theta/\partial p)$ [Gates, 1961], is only 1.5°C per 100 mb). The average θ in the layer is 42°C (315K). This value is referred to in later discussions.

The second sounding, Little Rock, Arkansas (72340), was within the region of the lid. It constitutes a typical lid sounding, such as that in Figure 1.1 on page 6. The Lid Strength Term was +4.9°C. The lid base over Little Rock is at 802 mb. The average θ above the lid base, in the EML, is 42°C (315K). This is identical to that in the surface

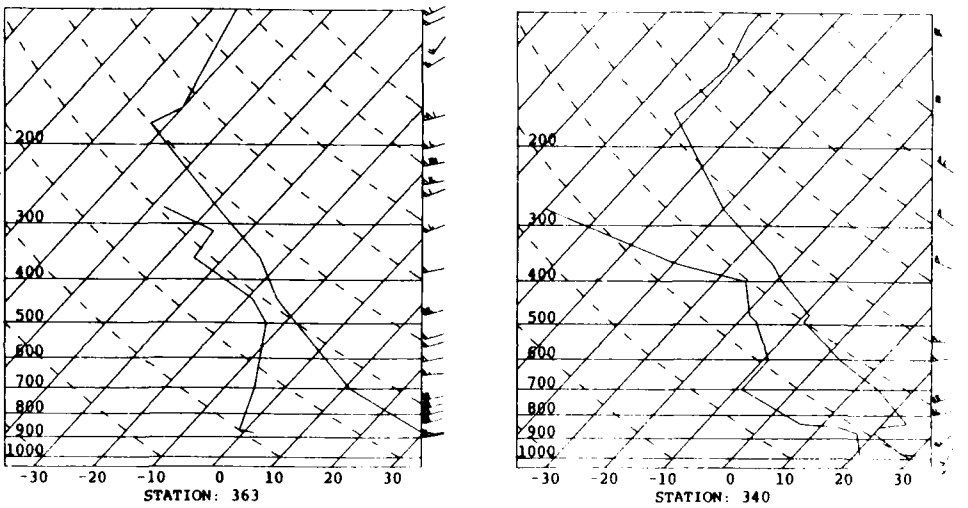

Figure 4.4: Upper air soundings for 1200 GMT 30 May: (a) Amarillo, TX (363) and (b) Little Rock, AR (340) on Skew-T Log-p diagrams. Horizontal lines are pressure levels labeled in mb. The solid lines slanting upward and toward the right are isotherms labeled in °C incremented every 10°C. The dashed lines slanting upward and toward the left are dry adiabates. The vertical temperature profile is indicated by the right most solid line; the dewpoint profile is indicated by the left most solid line. Wind direction and speed are depicted by wind barbs along the right of the diagrams (half barb: 2.5 ms^{-1} (5 kt), full barb: 5 ms^{-1} (10 kt), flag: 25 ms^{-1} (50 kt)).

mixed layer over Amarillo! This supports the contention that this air originated from within the deep surface mixed layer in the vicinity of Amarillo. θ_{bw} in the PBL is 22°C (295K) which gives a Buoyancy Term of -3.0°C. This value is also referred to in later discussions.

4.2.2 0000 GMT 31 May 1985

It is obvious from looking at Figure 4.5 that cyclogenesis had started over the last 12 hours. The surface low pressure center decreased by 2 mb and moved southeastward into Minnesota along the warm frontal boundary. The cold front intensified and moved out onto the Great Plains (Figure 4.5a), along with the upper-level short-wave trough (Figure 4.5b and Figure 4.5c). A cold pocket became evident at 500 mb over the surface low center. There were several reports of severe convective weather associated with this feature.

The jet streak was at the base of the trough and extended around and to the east of the trough. The maximum winds reported were 25 ms^{-1} (50 kt) over western Nebraska. This region reported severe dust storms throughout the afternoon. This supports the relationship between major dust storms and rapid cyclogenesis reported by Danielsen (1974a). Except for the position of the short-wave trough, there is not much of a difference at 700 mb from 12 hours earlier (Figure 4.5b compared to Figure 4.2b).

Figure 4.6 shows the position of the lid at this time. Symbol convections are the same as those in Figure 4.3 on page 70. In the 12 hours from the last chart (Figure 4.3 on page 70) the lid moved eastward approximately 750 km (466 n mi) at a speed of 17.4 ms^{-1} (33.7 kt), which is just a little slower than the short-wave trough. This allowed the baroclinic zone to move closer to the lid edge. Note that the lid strength decreased slightly; this is due to the slight diurnal increase of θ_{bw} in the PBL.

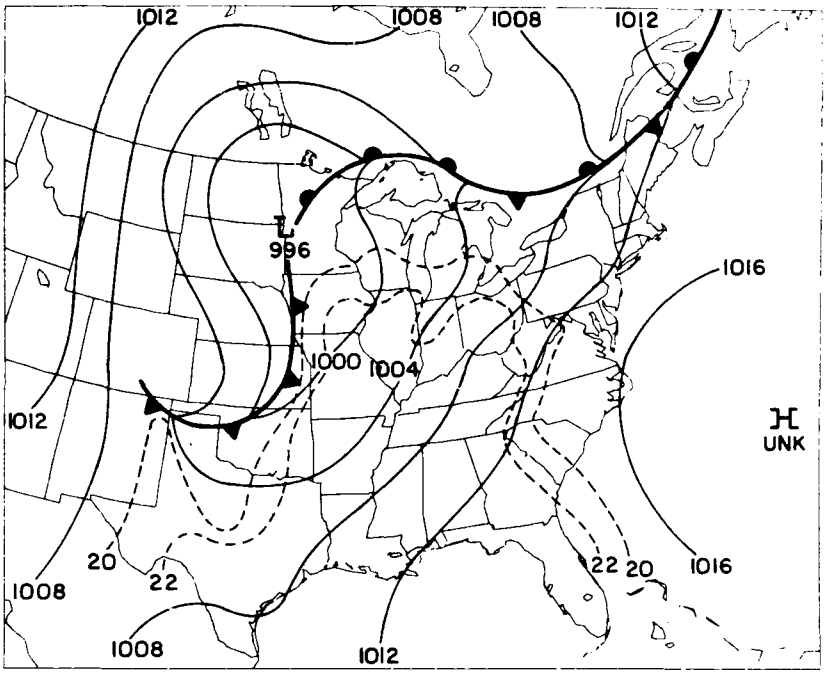

(a)

Figure 4.5: Synoptic situation for 0000 GMT 31 May 1985. (a) Surface (b) 700 mb (c) 500 mb. Conventions are the same as Figure 4.2 on page 67.

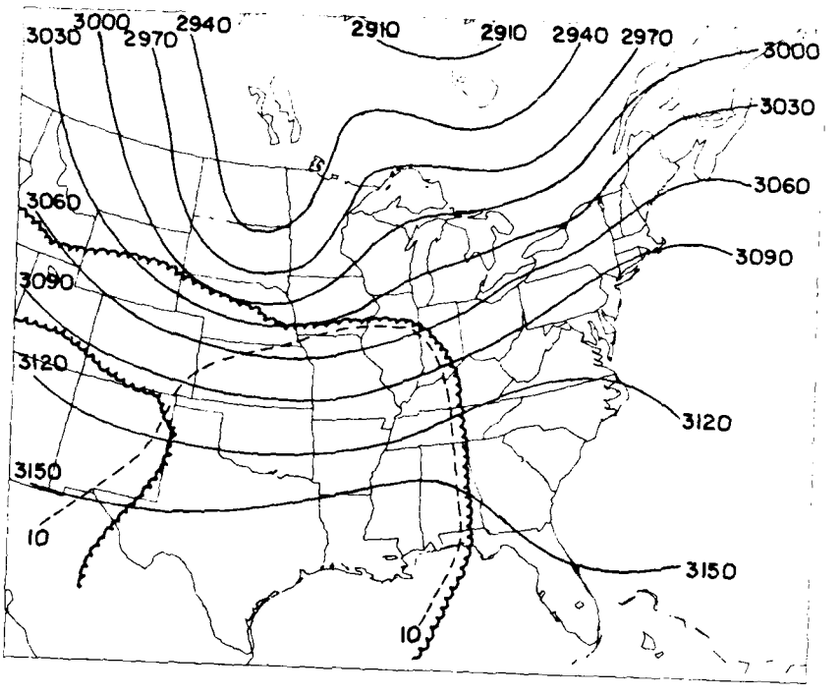

(b)

Figure 4.5 (continued)

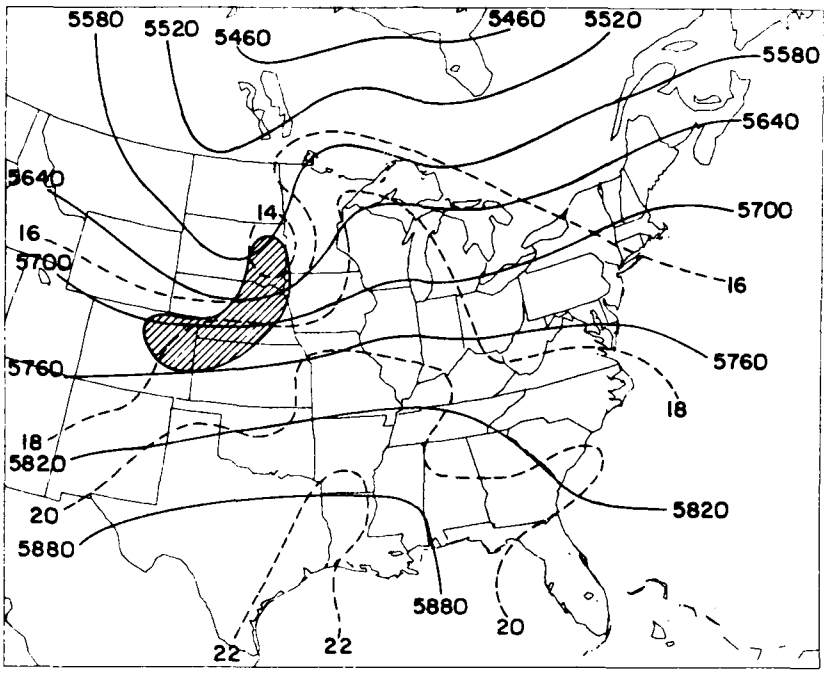

(c)

Figure 4.5 (continued)

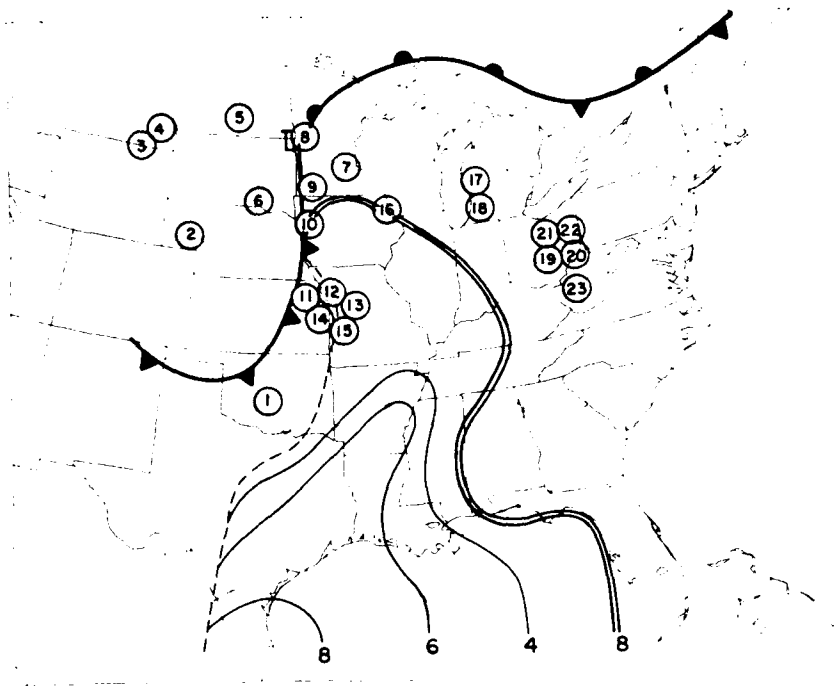

Figure 4.6: Lid Analysis for 0000 GMT 31 May 1985. Conventions are the same as Figure 4.3 on page 70. Descriptions of the numbered events are listed in Table 4.5.

There was quite a lot of severe weather during the afternoon and evening of the 30th. As in Figure 4.3 on page 70, the numbered circles indicate the location of severe weather events reported in the Storm Data (May 1985) within a time interval of six hours on either side of the time period. Table 4.5 lists the location, type of weather, and time of occurrence for each event depicted by the circles in Figure 4.6 on page 77. Some of this severe weather was tornado activity. Note that all of the activity in Missouri, Iowa, and Wisconsin was along the lid edge.

Much of Oklahoma was unseasonably dry and, consequently, surface sensible heating was able to increase surface temperatures dramatically (Wagner, 1986). (See Section 2.1.1 for a discussion on the relationship between sensible heating and soil moisture). Oklahoma had record-breaking high temperatures (exceeding 100°F [37.8°C]). Two women, 74 and 83 years old, died of heat stroke (Storm Data, May 1985). The large surface sensible heat flux also allowed a deep mixed layer to form (Section 2.1.1). It will be shown in Section 4.3 that this region was part of the lid's source region.

Finally, the heavy rain and hail activity in Michigan, Ohio, and West Virginia developed as a separate short-wave trough moved through that area (Figure 4.5c). This activity began about 0320 GMT and continued through the next morning. The activity in Ohio provided a very important contribution to the tornado outbreak 15 hours later (see Section 4.4)

As in Figure 4.4 on page 72, the two soundings shown in Figure 4.7 illustrate the lid structure and its source region. The first sounding is another sounding from Amarillo, Texas (72363). In this afternoon sounding, the nocturnal inversion had been replaced with a surface super-adiabatic layer. The average θ above this layer remained at 42°C (315K). The surface θ was almost 2°C higher than the layer average. This point is important in later discussions when determining a source region of the EML (Carlson and

Table 4.5: Storm Data: 1800 GMT 30 May - 0600 GMT 31 May 1985

Numbers (#) refer to circles in Figure 4.6 on page 77. KEY: H=Hail [cm]; WG=Maximum wind gust [ms^{-1}]; T: Tornado, catagorized by F-Scale (See Table 4.2 on page 63 for definition of F-Scale); TEMPS=Heat wave; DS=Dust storm. (Storm Data, May 1985).

#	Weather	Location	Time (GMT)
1	TEMPS	OK	Afternoon
2	DS	West NE	30/1500-31/0000
3	T(F0)	Powder River Co., WY	30/2000
4	T(F0)	Carter Co., MT	30/2315
5	T(F0)	Wells Co., ND	30/1955
	T(F2)	Burleigh Co., ND	30/1955
	T(F0)	Sheridan Co., ND	30/2012
	T(F0)	Burleigh Co., ND	30/2024
6	T(F0)	Gregory Co., MN	30/1937
	H(2) &		
	WG(31)	Charles Mix Co., MN	30/2010-2110
7	H(5)	Scott Co., MN	302135
8	T(F0)	Grant Co., MN	30/2228
	T(F1)	Jackson Co., MN	30/2250-2320
9	H(2)	Fairbault Co., MN	31/0000
10	T(F0)	Clay Co., IA	31/0038
11	H(2)	Brown Co., KS	30/2315
12	T(F1)	Buchanan & Platte Co., MO	30/2325-31/0030
13	T(F0)	Cliton, MO	31/0028
14	H(2)	Johnson Co., KS	31/0131
15	H(2)	Jackson Co., MO	31/0140
16	T(F3)	Clayton Co., IA	31/0322-0352
	T(F2)	Grant Co., WI [from IA]	31/0400-0445
	T(F2)	Grant Co. & Iowa Co., WI	31/0450-0530
	T(F2)	Pane Co., WI	31/0520-0555
	T(F1)	Barron & Chippena Co., WI	31/0530
17	H(4.5)	Nunica, Ottawa, & Kent Co., MI	31/0430-0600
18	H(5)	Barrion, Cass, Van Buren & Kalamazoo Co., MI	31/0500
19	H(2.5)	Franklin, OH	30/2225
20	H(2)	Perry & Muskingan, OH	31/0000-0105
21	WG(31)	Medina, OH	31/0323
22	H(5)	Portage, OH	31/0500
23	TSGR	West WV	Evening

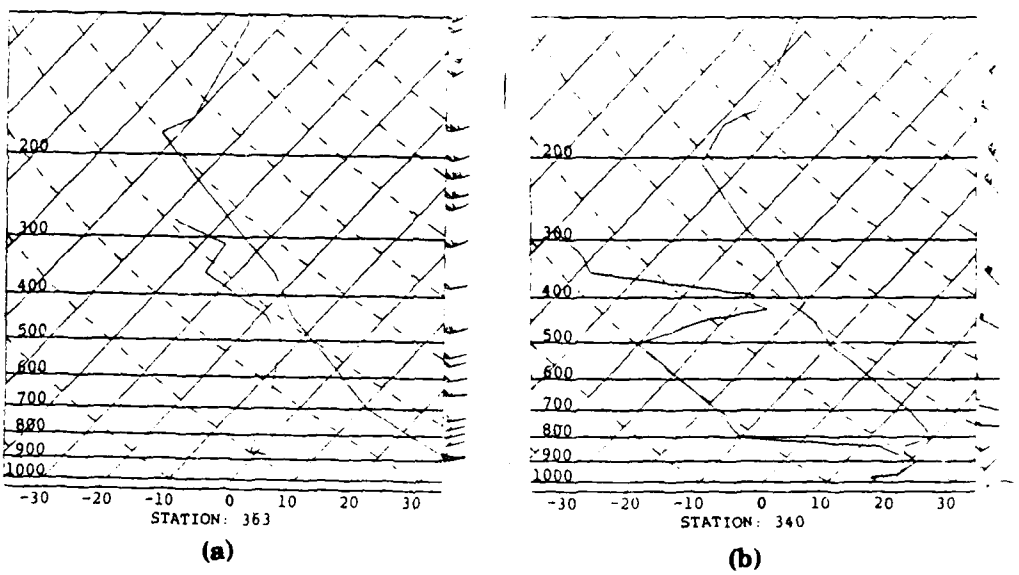

Figure 4.7: Upper air soundings for 0000 GMT 31 May: (a) Amarillo, TX (363) and (b) Little Rock, AR (340). Convections are the same as Figure 4.4 on page 72.

Ludlam, 1968). Note that the vertical wind shear was almost zero and that the relative humidity increases toward the top of the mixed layer (442mb). These observations conform with the definitions of a mixed layer presented in Sections 1.2 and 2.1.1.

Another sounding is that for Little Rock, Arkansas (72340), which remained within the region of the lid and continues to resemble Figure 1.1 on page 6. Here, the Lid Strength Term is +6.4°C, the Buoyancy Term is -2.8°C, the lid base is at 834 mb, the top of the EML is at 494 mb and the average θ in the EML was 44°C (317K), a little warmer than the average θ in the mixed layer over Amarillo. This difference in temperature is probably due to the fact that, although the mixed layer is relatively uniform in the vertical, there were some horizontal gradients of temperature, even over the source region. Note that the winds in the EML were relatively constant with height and in the same direction and speed as that in the Amarillo sounding.

4.2.3 1200 GMT 31 May 1985

By 1200 GMT on the 31st (Figure 4.8), the surface low had deepened by another 6 mb and moved northeastward to the tip of Lake Superior, continuing its propagation along the warm front (Figure 4.8a). The cold front intensified as it swept east and southward. The cyclone began to occlude at approximately 1000 GMT. The short-wave trough appeared to flatten out a little at 500 mb (Figure 4.8c). The cold pool evident at 0000 GMT was absent. The jet streak, however, continued to show some development. It remained at the base of the trough but it elongated along the eastern side of the trough. The maximum wind increased by 21 ms^{-1} (40 kt) to 49 ms^{-1} (95 kt) and was now over Wisconsin. The 700 mb trough deepened by over 60 meters and showed signs that it was about to cut off (Figure 4.8b). The 850 mb chart (not shown) also shows that there was strong low level cyclogenesis occurring at this time. The short-wave trough moved

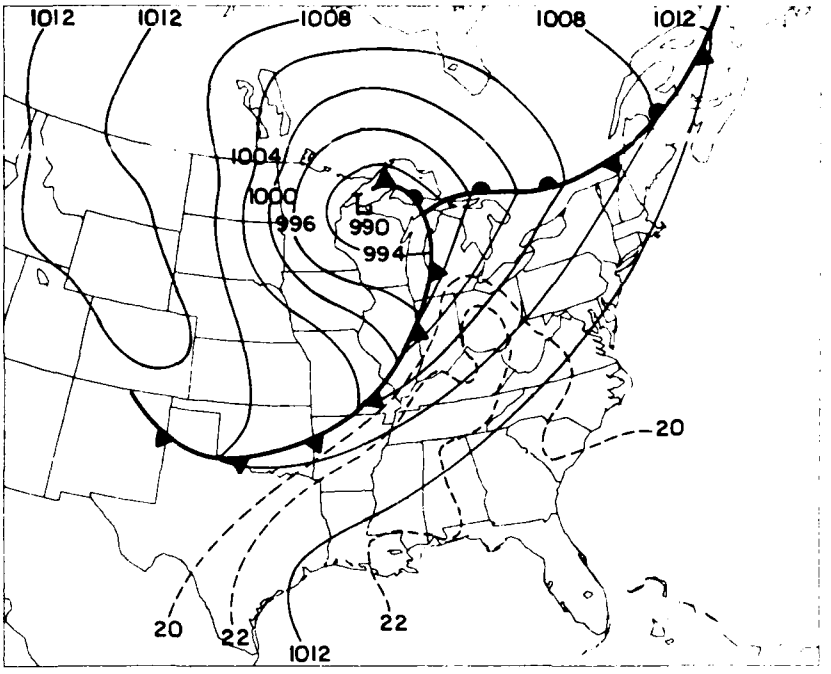

(a)

Figure 4.8: Synoptic situation for 1200 GMT 31 May 1985. (a) Surface (b) 700 mb (c) 500 mb. Conventions are the same as Figure 4.2 on page 67.

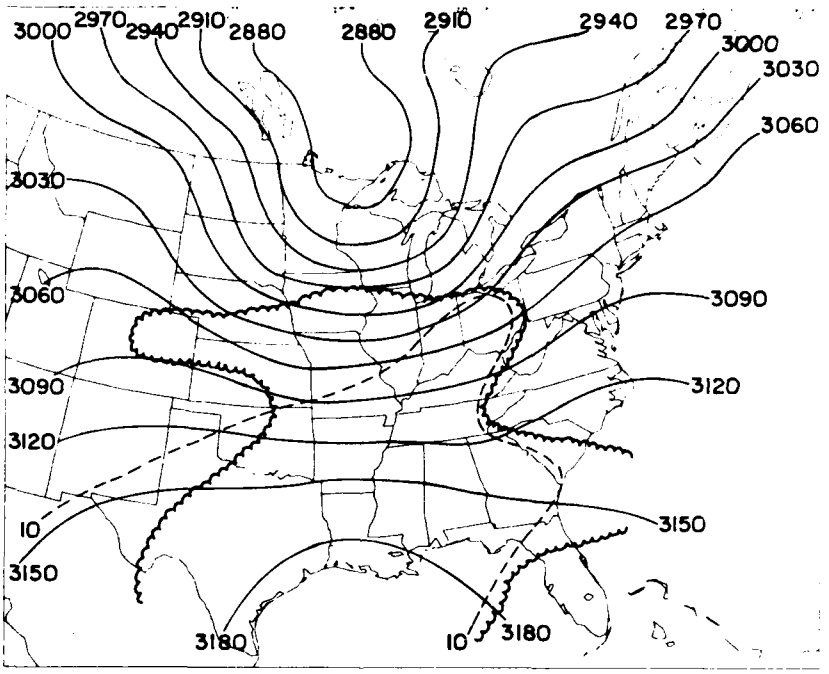

(b)

Figure 4.8 (continued)

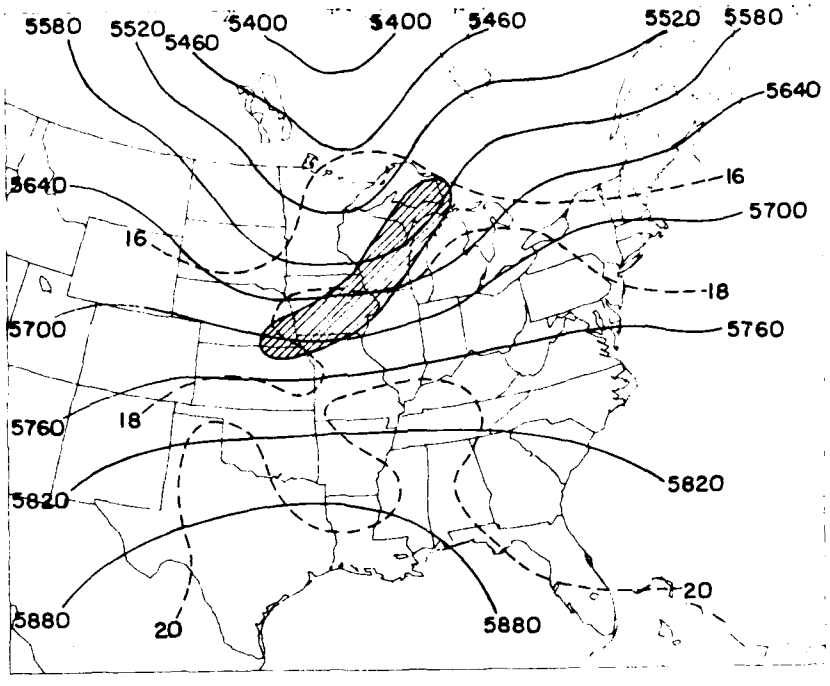

(c)

Figure 4.8 (continued)

eastward 500 km (311 n mi) over the 12 hours at a speed of 11.5 ms^{-1} (22 kt). The system slowed by 8.5 ms^{-1} (16.5 kt) as it intensified.

The very warm, dry air at 700 mb associated with the EML moved both east and north, and extended north of Dayton, Ohio. Note that the 10°C isotherm, over the central Great Plains, is no longer associated with the 20°C isopleth of Tdd as it was 12 hours earlier. This occurred for the following reason. Circulations within the approaching baroclinic zone lifted the EML, decreasing both the temperature and dewpoint depression (Tdd) in mid-levels via dry adiabatic ascent. The area encompassed by the 10°C isotherm decreased much more than the area encompassed by the 20°C isopleth of Tdd simply because several of the soundings included within the bounds of the 10°C isotherm had temperatures close to that value (11°C and 12°C) whereas most of those same soundings had Tdd's much greater than the 20°C isopleth of Tdd (26°C, 28°C, and 30°C+). Consequently, several of the soundings' 700 mb temperatures dropped below the 10°C value whereas most of the same soundings' 700 mb Tdd's remained above the 20°C value.

Figure 4.9 shows the position of the lid for this time. The most notable feature in this figure is the lack of reported severe weather within the six hour time period. A hail storm in Michigan was the only exception and it was a carry over from Figure 4.6 on page 77. Table 4.6 lists the location, type of weather, and time of occurrence, for each of these numbered events.

Table 4.6: Storm Data: 0600-1800 GMT 31 May 1985

Numbers (#) refer to circles in Figure 4.9. KEY: H=Hail [cm]. (Storm Data, May 1985).

#	Weather	Location	Time (GMT)
1	H(4.5)	Leslie & Ingham Co., MI	31/0705
2	H(2)	Leslie & Ingham Co., MI	31/1130-1230

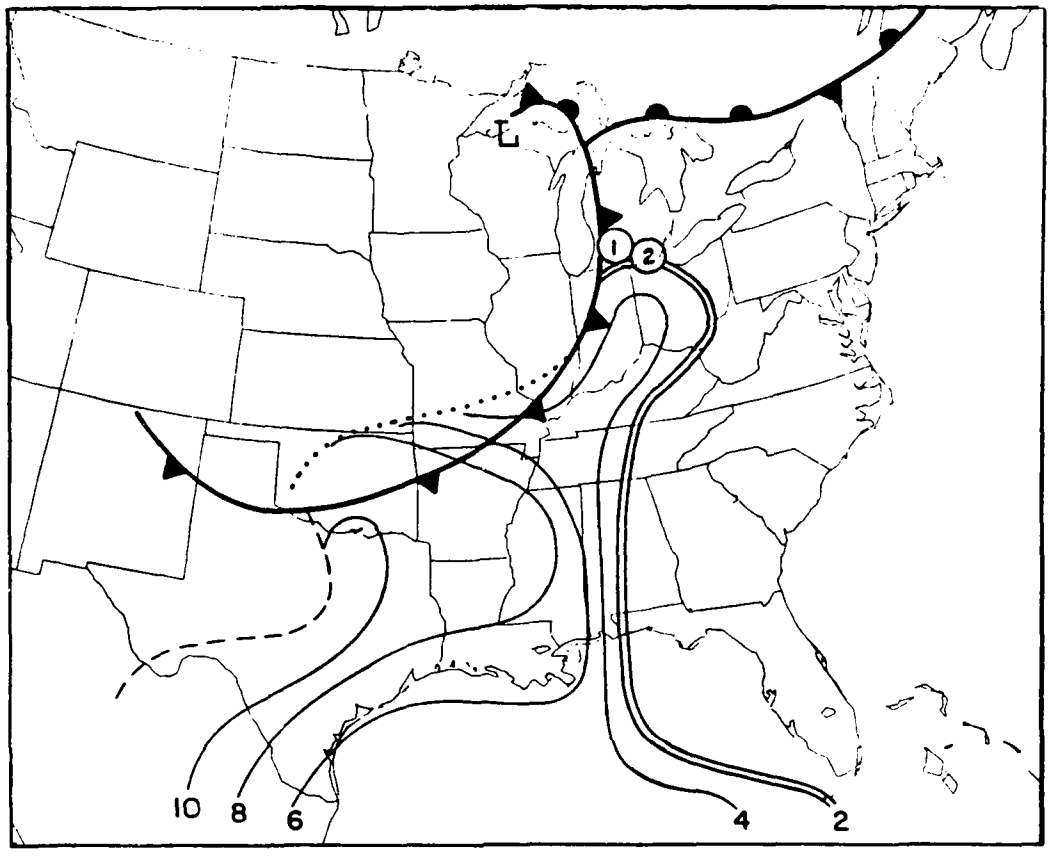

Figure 4.9: Lid Analysis for 1200 GMT 31 May 1985. Conventions are the same as Figure 4.3 on page 70 with the addition of a dotted line denoting an elevation of the mixed layer by the advancing cold front. Descriptions of the numbered events are listed in Table 4.6 on page 85.

The most important feature in this figure is that the lid extends up into Ohio. The western edge of the lid moved eastward 600 km (373 n mi) in 12 hours at a speed of 14 ms^{-1} (27 kt), which is slightly faster than the speed of the short-wave trough. Hence, the gap between the baroclinic zone and the lid edge widened a little. As a side note, the dryline had indeed returned westward during the night, in agreement with the discussion of Section 2.1.2.

One sounding shown in Figure 4.10, Dayton, Ohio (72429), is indicative of an EML that has been gradually lifted. The transition from the moist PBL air to the very dry EML was not as sharp as that in the Little Rock, Arkansas sounding in Figure 4.7 on page 80; however, it still meets the lid sounding criteria determined in Section 3.2. This diffusion of the lid boundary is probably the result of several days of turbulent mixing as discussed in Section 2.2. The Lid Strength Term was +2.9°C. The lid base was at 752 mb and the top of the EML was at 551 mb giving an EML depth of 201mb. This is shallower than that found over Little Rock 12 hours earlier (Figure 4.7 on page 80). Clearly, the EML was rising in height and shrinking in depth as it flowed northward and eastward. The average θ in the EML was 41°C (314K), which also supports the contention that this air originated from within a mixed layer west of the dryline.

The other sounding shown in Figure 4.10 is from Huntington, West Virginia. This sounding shows a weak lid (Lid Strength Term was +1.6°C) with a base at 679mb. This sounding is indicative of soundings near the downstream edge of the lid. Note that the average θ in the EML was 42°C (315K); the wind direction was a uniform 265° with a speed of about 21 ms^{-1} (40 kt). This is further evidence that the inversion in this area of the nation was produced by differential advection and not by subsidence. For, in a subsidence inversion the winds back with height.

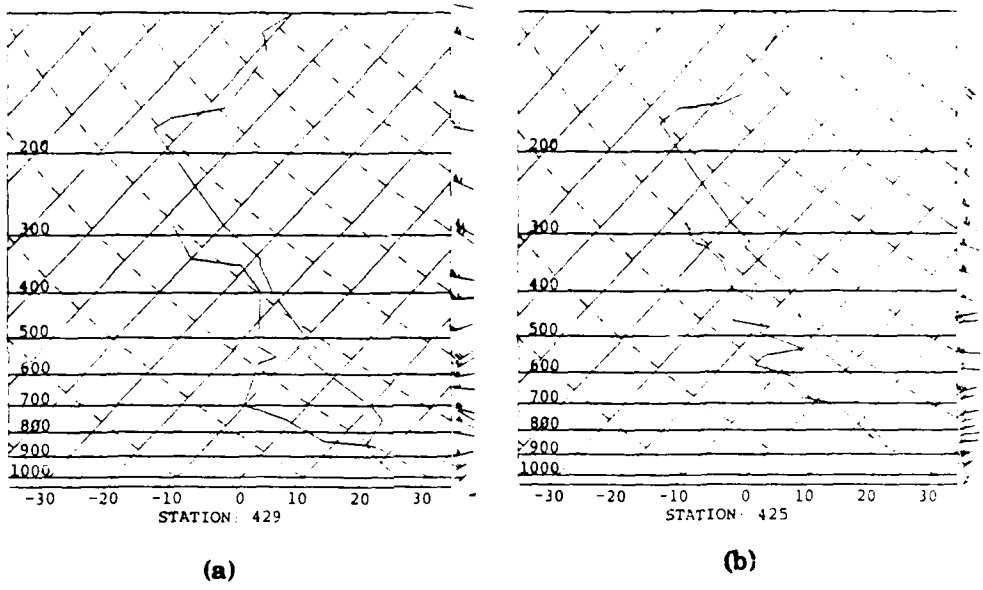

Figure 4.10: Upper air soundings for 1200 GMT 31 May: (a) Dayton, OH (429) and (b) Huntington, WV (425). Convections are the same as Figure 4.4 on page 72.

Note the dotted line west of the cold front in Oklahoma and Missouri in Figure 4.9 on page 86. The soundings in Oklahoma City, Oklahoma and Monett, Missouri (not shown) show that there was a very strong lid in this area (lid strength term of +10.5°C for Oklahoma City) at the time. This situation occurred because the cold front moved underneath the mixed layer and lifted it. Because the air being lifted was very dry, there was no cloud or precipitation associated with the frontal passage. Also, since the lapse rate of mixed layers is necessarily near dry adiabatic, the θ in the layer was not modified by the ascent. Thus, the low-level cold air became "capped" by the elevated mixed layer; however, because the low-level air was cold and dry, there was no latent instability (the Buoyancy Term was positive +2.7°C for Oklahoma City). Hence, the criteria outlined in Section 3.2 does not mark Oklahoma City and Monett as lid soundings, although one is clearly present on the soundings. Consequently, the edge of the lid in this area is denoted by a dotted line instead of the solid double line.

4.2.3.1 Cross-sectional Analysis

A cross-section is presented in Figure 4.11 to illustrate the structure of the lid. The cross-section is orientated along a path (shown in the inset) from Victoria, Texas (255) to Buffalo, New York (528) through the center of the lid region, parallel to the mid-level (700 mb) flow. The isentropes (solid lines) show that there was indeed a very strong lid extending from Victoria to Little Rock, Arkansas (340) just above the 900 mb level (tight vertical gradient in potential temperature). The isentropes then flared out gradually, along the cross-section, to Dayton, Ohio (429). Further downwind, the vertical gradient of potential temperature is so weak that there was no longer an effective lid; this point is reached near Dayton. A notable feature is that the lid base gradually rises from 888 mb at Victoria to 752 mb at Dayton. This observation is discussed in Section 2.2.

Figure 4.11: Vertical cross-section for 1200 GMT 31 May 1985. Small map on bottom shows the line along which the cross-section was taken. Fronts and pressure center are indicated with conventional symbolism; dryline is indicated by short dashed line; lid edge is depicted as a thin solid line. Asterisks show locations of stations which reported upper air soundings for this data collection time. Vertical coordinate of cross-section is ln p and is labeled along the right margin; potential temperature in K (solid line) is labeled along the left margin; relative humidity in percent (short dashed lines). Location of stations used to calculate section is indicated on the bottom margin. The lid edge is denoted by an "E"; the moist tropical layer (M in Figure 2.1 on page 11) and the EML (CD in Figure 2.1 on page 11) are depicted to the left.

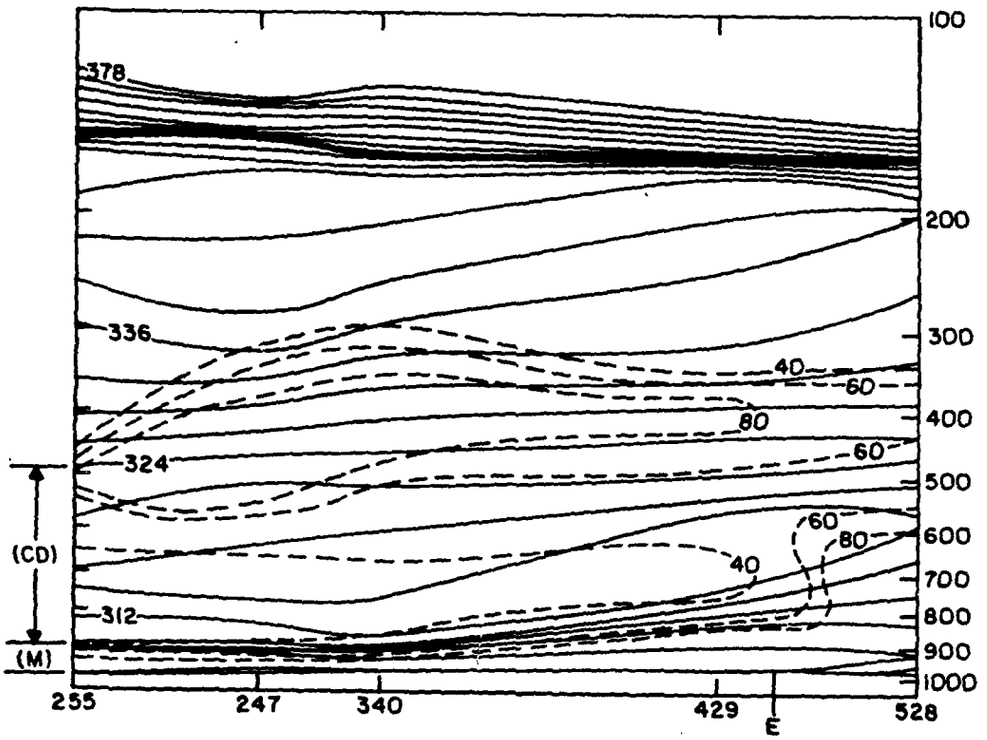
100
200
300
400
500
600
700
800
900
1000
378
336
324
312
40
60
80
60
60
80
40
(CD)
(M)
255
247
340
429
E
528

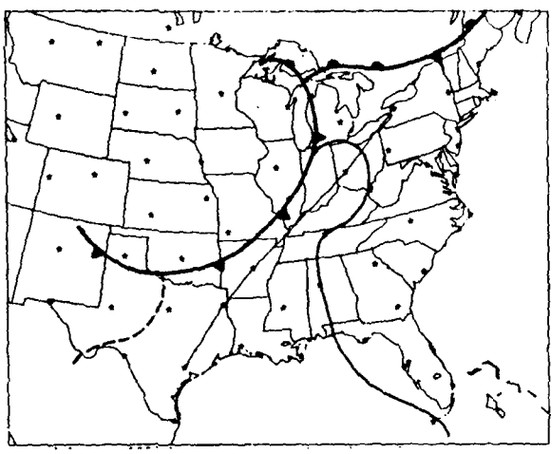

There was also a very sharp vertical gradient in relative humidity associated with the inversion (80% below the lid base and less than 40% above it). Downstream, however, this gradient decreases and quickly disappears. Also note that there is a relatively sharp horizontal gradient in the 700 mb relative humidity, from less than 40% at Dayton (429) to over 70 % at Buffalo (528). This sharp horizontal transition coincides with the disappearance of the vertical gradient of both relative humidity and θ. This point marks the lid's downstream edge. This supports the placement of the lid edge in Figure 4.9 on page 86.

Another notable feature is an increase in the vertical gradient of θ above 500 mb accompanied by a vertical maximum in relative humidity. This is the signature of the mixing inversion at the top of the EML, as discussed in Sections 1.2 and 2.1.1.

4.2.4 0000 GMT 01 June, 1985

As mentioned in Section 4.1, the severe convection started at 2059 GMT 31 May and persisted through 0000 GMT. The low pressure center deepened by 2 more millibars in 12 hours (Figure 4.12a). The 700 mb trough cut off and deepened by 40 meters (Figure 4.12b). The 500 mb trough also cut off and deepened by 100 meters (Figure 4.12c).

A pronounced thermal trough was evident at 500 mb over New York State, Pennsylvania, and West Virginia. This trough developed despite strong warm advection at that level. This reveals that there was strong ascent reversing the warming by advection in this area at the time. The presence of this thermal trough was a contributor to the severity of the outbreak and will be discussed in Section 4.5. The jet streak remained anchored to the base of the trough but it branched into two forks, one flowing northward with the trough and one cutting across it, flowing eastward (Figure 4.12c). This created a diffluent zone which was also a contributing factor to the severity of the outbreak.

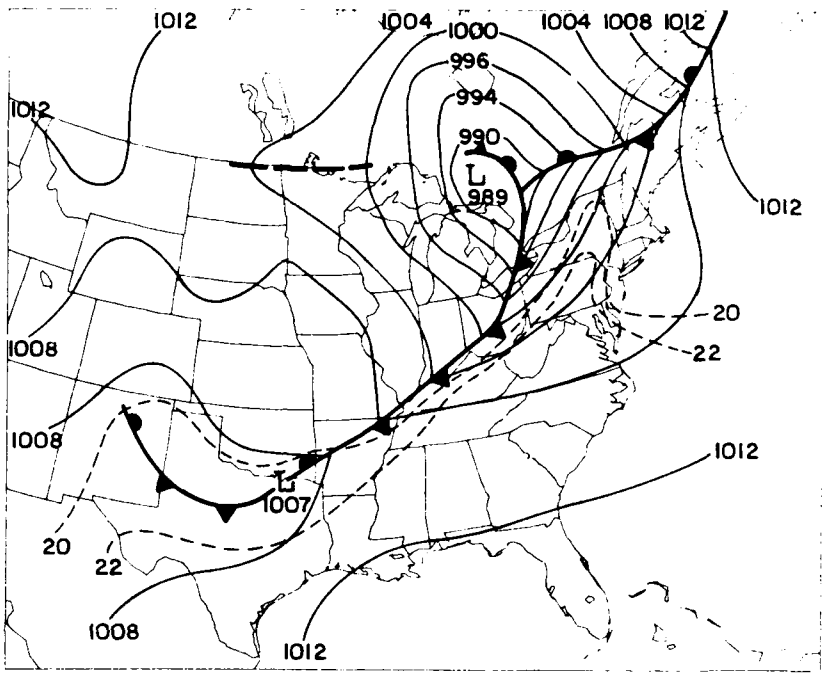

(a)

Figure 4.12: Synoptic situation for 0000 GMT 01 June 1985. (a) Surface (b) 700 mb (c) 500 mb. Conventions are the same as Figure 4.2 on page 67.

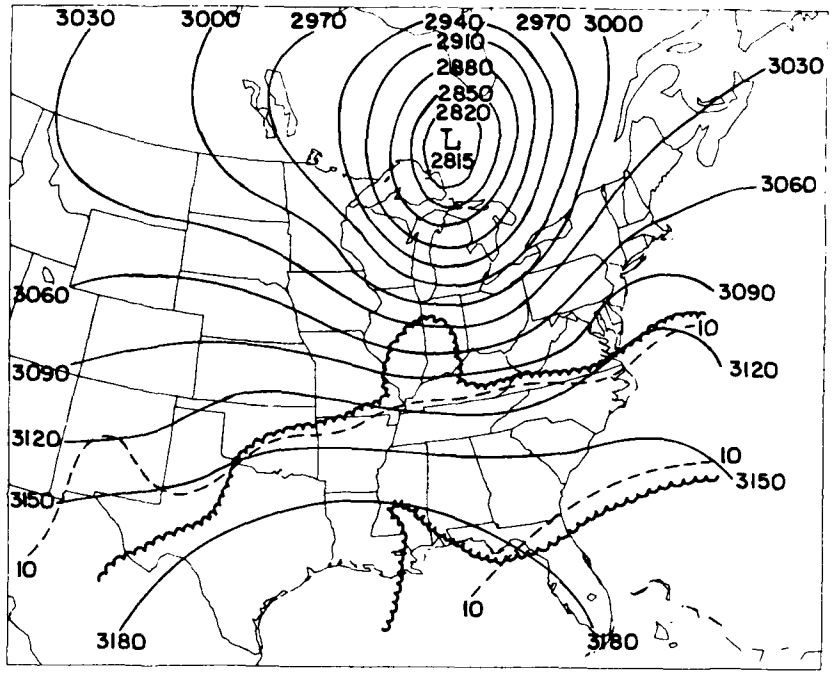

(b)

Figure 4.12 (continued)

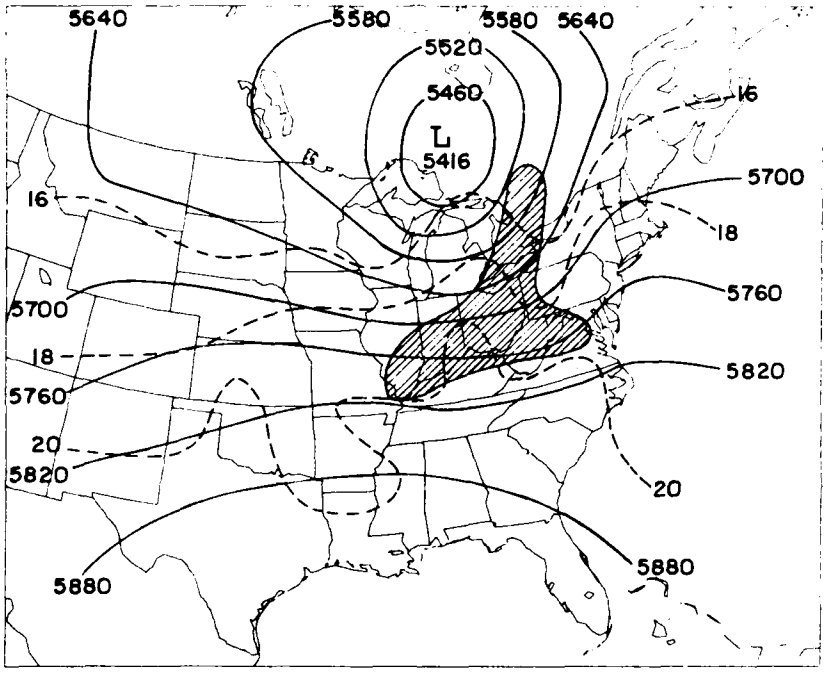

(c)

Figure 4.12 (continued)

A severe dust storm, which had earlier moved through Nebraska, was occurring in Illinois, Indiana, Wisconsin, and Michigan. Winds gusted up to 31 ms^{-1} (61 kt) causing visibilities to drop below 6 meters (20 feet), which resulted in numerous traffic accidents and power outages. There was one traffic related death in Illinois (Storm Data, May 1985). This storm occurred behind the cold front in the deep mixed layer which was being advected in behind it. As a result, efficient vertical mixing of the momentum from the strong upper-level jet streak was allowed to occur there. See the discussion in Section 2.1.1.

The abnormally warm, dry air at 700 mb moved further east (Figure 4.12b). The 10°C isotherm remains associated with the 20°C isopleth of Tdd except for a small area in southern Illinois and Indiana. The EML in this area has been destroyed in the same manner as that in the Nebraska area 12 hours earlier (see Section 4.2.3)

Figure 4.13 shows the position of the lid for this time. The lid was evident as far north as Portland, Maine! It's leading edge had moved off the coast. With no sounding data east of the coastline, there is no way to determine the position of this edge. For this reason, a squiggled line is used to depict the downstream data cutoff. The soundings along the coast, as is often the case, are complicated by the superpostion of a sea-breeze circulation. The western edge of the lid moved 750 km (466 n mi) in 12 hours at a speed of 17.4 ms^{-1} (34 kt). This is 4.4 ms^{-1} (8.5 kt) faster than the baroclinic zone! As a result, the gap between the cold front and the western edge of the lid increased, in part due to intensifying ascent along the cold front which was destroying the EML.

Severe weather not directly associated with the tornado outbreak is depicted in Figure 4.13 as numbered circles (Table 4.7), while the location of the tornado family inception-points are depicted as dots (from Figure 4.1b).

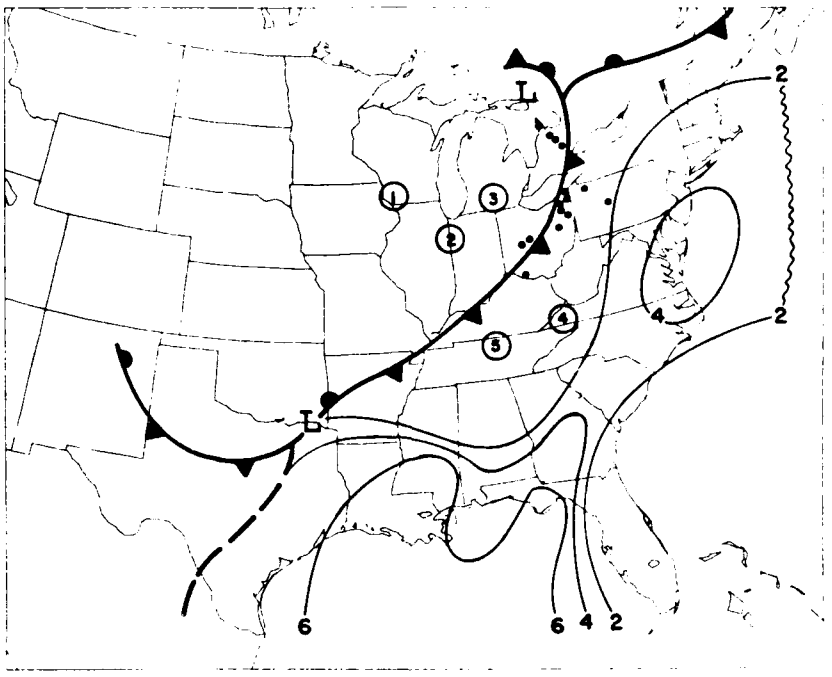

Figure 4.13: Lid Analysis for 0000 GMT 01 June 1985. Conventions are the same as Figure 4.3 on page 70 with the addition of a squiggled line indicating a cutoff in the data. Descriptions of the numbered events are listed in Table 4.7. Dots are inception points of tornado families (Figure 4.1b and Table 4.1).

Table 4.7: Storm Data: 1500 GMT 31 May - 0600 GMT June 1985

Numbers (#) refer to circles in Figure 4.13 on page 97. KEY: DS=Dust Storm [wind Gusts ms^{-1}]; H=Hail [cm]. (Storm Data, May and June 1985).

#	Weather	Location	Time (GMT)
1	DS(G32.5)	South WI	31/1500-2000
2	DS(G31)	North IL & North IN	31/1500-2200
3	DS(G30)	South MI	31/1500-2300
4	H(4.5)	Lee & Scott Co., VA	31/2205-2215
5	Svr Tstms	Goodlettsville & Davidson Co., TN	01/0000

Two soundings are shown in Figure 4.14. Portland, Maine (72606) was chosen to provide evidence that a lid is indeed that far north. The Lid Strength Term was +1.0°C, the Buoyancy Term was 0°C. The lid base was at 543 mb, the average θ in the layer above the base was 42°C (315K), and the winds averaged 240° at 20 ms^{-1}. (40 kt). The geostrophic winds veered with height in response to the warm air advection and the general ascending motion in the area.

The Pittsburgh, Pennsylvania (72520) sounding was a special taken at 2300 GMT. Although there was an equipment failure just above 500 mb this sounding shows an inversion at 785 mb above which there is an average θ of 41°C. Thus, the EML was indeed over Pittsburgh, although, with the approach of the baroclinic zone, it was lifted to the extent where it was no longer an effective cap to convection. The Lid Strength Term was only +0.8°C; however, the Bucyancy Term was - 5.4°C, which equates to a Lifted Index value of -10.0°C. Needless to say, the environment was quite convectively unstable.

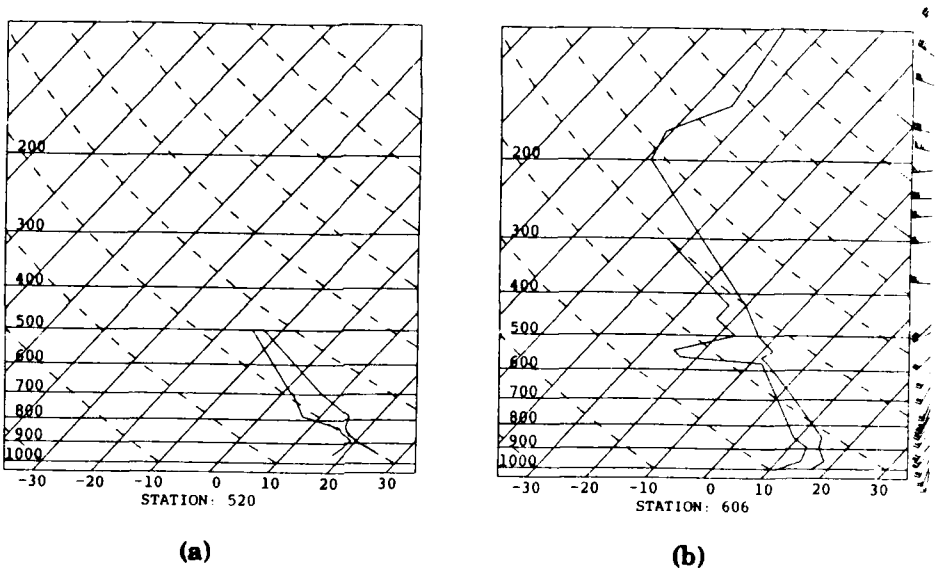

Figure 4.14: Upper air soundings for 0000 GMT 01 June: (a) Pittsburgh, PA (520) and (b) Portland, ME (606). Convections are the same as Figure 4.4 on page 72. Note that Pittsburgh is missing some data. The sonde malfunctioned above 500 mb and winds were unattainable.

4.3 Source Region Determination

As further support to the hypothesis that the capping inversion in the severe storm environment was the result of advection of an elevated mixed layer (EML) from a mixed layer source and not the result of subsidence, an isentropic trajectory analysis was preformed. Using the objective routine developed by Forbes et al. (1984), it was possible to track the course of the air in the EML through time by calculating backward trajectories in 2 hour time-steps starting in the morning before the outbreak and back-tracking for 24 hours. A phase speed of some translating system is required to calculate Eulerian trajectories. Their trajectory analysis operates under the restrictive assumption that the system remains isentropic and steady state over a given time period so that the phase speed remains a constant.

To remain as close as possible to this steady state requirement, the 1200 GMT 31 May data was used to calculate the trajectories backwards only 12 hours and then the earlier data set (0000 GMT 31 May) was used to calculate the trajectories backwards for the last 12 hours, picking up where the previous calculations left off. The phase speed used was the speed of the western edge of the lid. The lid edge speed used from 1200 GMT 31 May to 0000 GMT 31 May was 14 ms^{-1} (Section 4.2.3). The speed used from 0000 GMT 31 May to 1200 GMT 30 May was 17.4 ms˙ 1. (Section 4.2.2).

Figure 4.15 shows the trajectories of two parcels found over Dayton Ohio. One trajectory is of a parcel within the EML. This air is far from saturation so an isentropic surface was used to calculate the trajectories. The potential temperature, θ, chosen is the average value of θ in the EML over Dayton (41°C (314K); see the Dayton sounding in Figure 4.10 on page 88 and Figure 4.11 on page 91). The backward trajectory of this

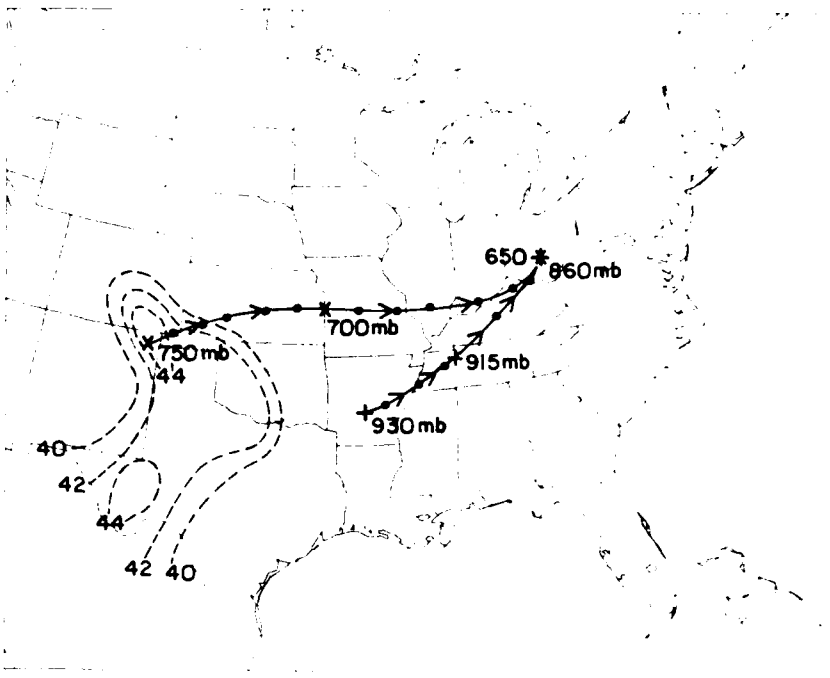

Figure 4.15: Isentropic Trajectory Analysis from 1200 GMT 30 May 1985 to 1200 GMT 31 May 1985. Northern trajectory: $\theta = 314K$ surface; southern trajectory: $\theta_w = 294K$ surface. Dots are placed every two hours; arrowheads every four hours; and X's at data collection times (i.e. every twelve hours). Pressure level of trajectories are denoted in millibars near respective X's. Surface potential temperature over the source region at 0000 GMT 30 May 1985 is depicted as thin dashed lines [°C]).

parcel shows that it was over the northeastern corner of New Mexico only 24 hours earlier! It originated approximately 100 mb above the surface (at 750 mb) in the deep mixed layer region (see the Amarillo sounding in Figure 4.4 on page 72).

In the discussion of Figure 4.4 on page 72 it was noted that the average θ in the mixed layer was 42°C (315K). Isentropes of surface θ at 0000 GMT 31 May were placed in Figure 4.15 on page 101 to show the areal extent of the 42°C (315K) value. The values at 0000 GMT 31 May were used instead of the values at 1200 GMT 30 May because the afternoon surface values are more representative of the average potential temperatures in the mixed layer than are the values in the morning. Recall from an earlier discussion (Section 4.2.2), however, that the surface values are usually a little higher (2°C) than the layer average. This is the case in this analysis. The source point of the air parcel is situated over an area that has a surface θ of 44°C (317K).

As the air parcels flowed eastward and northward from New Mexico, they gradually rose, from 750 mb to 650 mb in 24 hours giving a vertical velocity of 1.16 μbs^{-1}. This shows that there was general rising in the inversion layer and not subsidence. Therefore, it can be concluded that the capping inversion present over Dayton, Ohio the morning before the storm was an EML which originated over the Desert Southwest 24 hours earlier (i.e. the morning before).

As a side note, the Lid Strength Term analysis for 1200 GMT 31 May 1985 (Figure 4.9 on page 86) reveals that there were two bubbles of maximum lid strength; one over Ohio, and one over Texas. It is suggested that these two maxima resulted from a diurnal, inertial oscillation of the advective winds in the mixed layer in the manor discussed in Section 2.2. In that discussion, it is noted that the air in the EML associated with maxima in lid strength leaves the source region during the morning hours. This isentropic analysis supports this.

The second trajectory depicted in Figure 4.15 on page 101 is a parcel within the planetary boundary layer (PBL) over Dayton. Because this air is very moist and the parcels are very close to saturation, a θ_w surface was used. The highest 50mb-layer-averaged θ_w (θ_{bw}, see Section 3.1) over Dayton was 21°C (294K) so it was this value that was used to trace the air in the PBL. The isentropic motion is more difficult to follow in the surface mixing layer but the trajectory is representative of the air at the base of the lid because it is not far from the level at which the vertical divergence of sensible heat flux (and therefore the diabatic heating) is zero. Section 4.4 discusses the impact of the diabatic affects on the air at the surface.

Following the 294K θ_w trajectory 24 hours backward in time shows that the air originated over Arkansas. From a previous discussion (Section 4.2.1) it was shown that θ_{bw} in this region was 22°C (295K). As this air flowed from Arkansas to Ohio in 24 hours, it rose from 930 mb to 860 mb giving a vertical velocity of only 0.8 μbs^{-1}. Of course, once the baroclinic zone and the strong upper-level jet streak reached Ohio, the vertical velocities increased dramatically.

4.4 Surface Diabatic Contribution

As the low-level air flowed northward, sensible and latent heat fluxes from the surface, resulting from solar heating at the ground, increased θ_w in the surface layer. Therefore, it was obviously not isentropic. To get a general idea of how insolation and its resulting diabatic effects affected parcels as they flowed into the tornado inception area, some "quasi-trajectories" were determined for two separate parcels. These trajectories were determined by picking two points (one from behind the line of thunderstorms and one at the location where the first tornado initiated) and tracking them backwards in time, in

one hour increments, using surface and 850 mb winds as a guide in determining a general direction and distance (speed × 1 hr) to move the parcels each hour. The backward trajectories are plotted in Figure 4.16 in three hour increments from 2100 to 1200 GMT. Note that, as might be expected, the parcels accelerated as they approached the intensifying low pressure system. The parcels' temperature, mixing ratio, θ_w, and LCL are depicted in a station model format centered around the location markers, as defined in the key which is positioned in the bottom right corner of the figure.

Following the parcels from their starting positions in the morning, it is clearly seen that θ_w increases for both parcels; however, recalling that θ_w is proportional to both temperature and mixing ratio, and upon further inspection of the parcels' temperatures and mixing ratios, it becomes clear that the reasons behind the increases are different. Table 4.8 shows the percent change of θ_w, temperature, and mixing ratio for the two parcels in the total nine hour period. Parcel A's θ_w increased by 2.7% and Parcel B's θ_w increased by 21.2%; however, Parcel A's temperature increased by 32% whereas Parcel B's temperature increased by only 17.4%! On the other hand, Parcel B's mixing ratio increased by 43.5% whereas Parcel A's decreased by 21.5%. Therefore, it can be concluded that Parcel A's θ_w increased because of the large increase in temperature while Parcel B's θ_w increased because of the large increase in mixing ratio. This difference resulted for two reasons.

The first reason is that there was a significant difference in the environments of the two parcels. Parcel A flowed just ahead of the cold front staying just west of the lid edge, whereas Parcel B flowed ahead of the cold front beneath the lid. Consequently, vertical mixing for Parcel A was dramatically greater than that for Parcel B. Notice in Figure 4.16 that for the first six hours, Parcel A's temperature and mixing ratio slightly increased and then in the last three hours, the temperature rose 6°C and the mixing ratio

Table 4.8: Parcel Changes

P	θ_{w12}	θ_{w21}	$\Delta\theta_w$	Δ%
A	22.0	22.6	0.6	2.7
B	19.8	24.0	4.2	21.2

P	T_{b12}	T_{b21}	ΔT_b	Δ%
A	25	33	8	32.0
B	23	27	4	17.4

P	w_{b12}	w_{b21}	Δw_b	Δ%
A	15.8	12.4	-3.4	-21.5
B	12.4	17.8	5.4	43.5

KEY: P: Parcel in Figure 4.16
θ_w: Surface Wet-bulb potential temperature [°C]
T_b: Boundary layer Temperature [°C]
w_b: Boundary layer Mixing ratio [gkg^{-1}]
12: Value at 1200 GMT 31 May 1985
21: Value at 2100 GMT 31 May 1985
D:X: Difference between the 1200 GMT and 2100 GMT values of the variable X (were X = θ_w, T, or w)
D%: Percent difference: $[(X_{24}-X_{12})/X_{12}]\times 100$

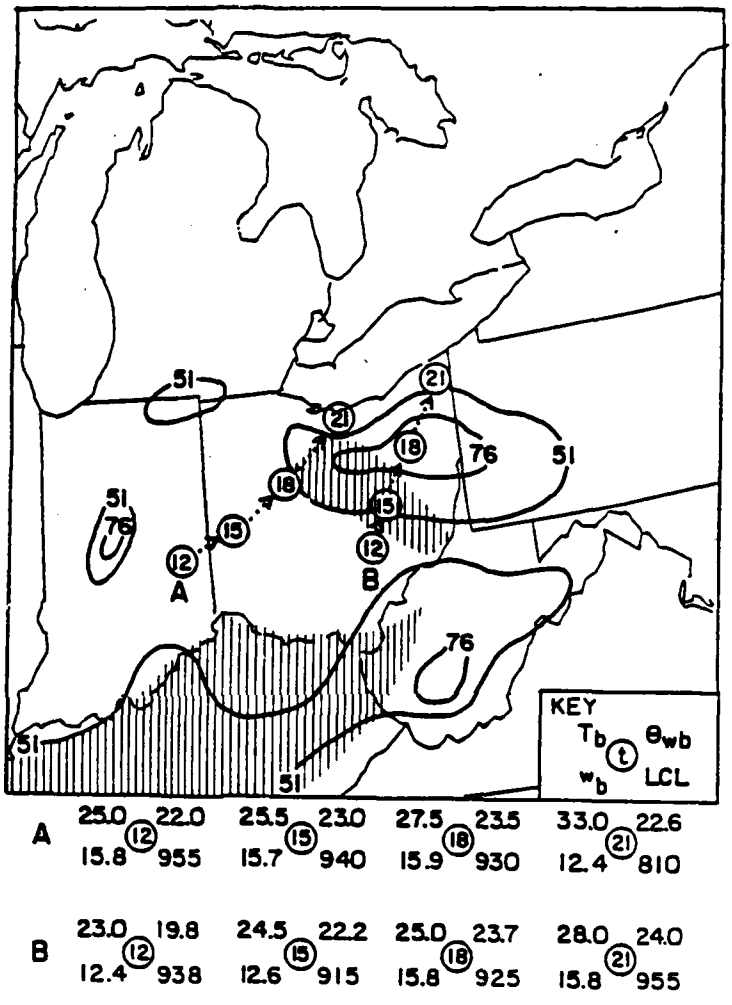

Figure 4.16: PBL Trajectory Analysis from 1200 GMT to 2100 GMT 31 May 1985. Dotted arrows show motion of two parcels, A and B, along the ground. The locations of parcels are indicated with a circle enclosing the respective GMT times at three hour intervals. Antecedent Precipitation Index (API; defined in the text and calculated by Mr. Barry Lynn) is depicted with thin solid lines [mm]. Hatching outlines the areas in which w exceeds 15.5 gkg^{-1} at 1800 GMT. The T=Dry-bulb temperature [°F], w=mixing ratio [gkg^{-1}], θ_w=surface wet-bulb potential temperature [°C], and LCL=lifted condensation level [mb] are shown below the map for both trajectories in a station model format as defined in the key (bottom right corner of map) for 1200, 1500, 1800, and 2100 GMT 31 May 1985 (t in center of circle).

dropped 3 gkg^{-1}. The early increase of mixing ratio occurred because the vertical mixing was restricted by a nocturnal inversion which covered a large area just ahead of and behind the cold front at that time. The sharp change occurred when the nocturnal inversion broke allowing dry air to mix down to the surface. This abrupt change also coincided with the start of the severe dust storm in Wisconsin and Michigan (see Section 4.2.3). Parcel B never had this change because the dry air could not penetrate the lid.

The second reason is that there was a marked difference in the Bowen ratio for the surfaces over which the parcels were moving (see Section 2.1.1). Inferring from Table 4.8 on page 105, because the temperature of Parcel A increased more than the temperature of Parcel B, the sensible heat flux affecting Parcel A over time was greater than that of Parcel B. On the other hand, because the mixing ratio of Parcel B increased more than the mixing ratio of Parcel A, the latent heat flux affecting Parcel B over time was greater than that of Parcel A. Consequently, the average Bowen ratio (over time) for Parcel A is larger than that for Parcel B. As mentioned in Section 2.1.1, the Bowen ratio is dependent on the soil moisture. The drier the soil, the larger the Bowen ratio. To determine whether soil moisture did indeed influence the two parcels, an analysis of soil moisture amounts is needed.

A parameter, called the antecedent precipitation index (API), has been used in assessing soil moisture amounts (Harlan, 1980; Blanchard et al., 1981; Wetzel and Atlas, 1981) and is defined as:

$$API_i = kAPI_{i-1} + R_i \tag{3}$$

where R_i is the amount of precipitation on Day i and k is a weighting coefficient that determines the substrate memory for drying out of the ground. For $k = 0$, antecedent precipitation is determined solely from the day's rainfall whereas a large value for k such

as 1.0 indicates a long response time for soil drying. A value of 0.92 was adopted for this study. This is justified on the basis of a study by Wetzel and Atlas (1981) who found that this value, similar to that of Saxton and Lenz (1967), yeilded the the optimum correlation between API and moisture availability.

API was calculated from data obtained from the National Climate Center of NOAA. Altogether, data for 90 rainfall stations were analyzed over the area of tornado inception. Initial API values (for i=0) were assumed to be the mean precipitation for the month of April; the first day of calculation (i=1) was 1 May 1985. By the end of the month, the memory of the April rainfalls would have exerted minimal impact on the API values.

The API analysis for 31 May 1985 is included in Figure 4.16 on page 106. Note the API maximum in east central Ohio (API > 108mm). The bulk of this soil moisture resulted from thunderstorm activity the previous evening (noted in Section 4.2.2). This analysis shows that for most of the nine hours, Parcel A flowed over relatively dry ground (API < 38mm) and Parcel B flowed over moist ground (API > 51mm and for awhile > 76mm). This is what was expected!

The fact that the flux of moisture from the surface increased the θ_w in Parcel B as opposed to the temperature proves to be significant. Although the θ_w's of the two parcels are relatively close (1.4°C), the LCLs are much different. At 2100 GMT, Parcel A's LCL is 810 mb whereas Parcel B's LCL is 955 mb (see Figure 4.16 on page 106). This results because Parcel B has much more moisture associated with it than does Parcel A so it reaches saturation more quickly. Recall from a discussion in Section 2.4 that the lower the LCL is, the more buoyant energy is available. Therefore, it can be concluded from this discussion that soil moisture availability exerts some impact on the buoyant energy available to developing convection and added to the severity of this particular tornado outbreak. Maddox et al. (1981, p. 72) have also determined that evaportransporation plays a major role in severe convection in Colorado.

4.5 Inception Area Analysis

This section focuses in on the area within which the tornado outbreak began. For three times, 1200 GMT, 1800 GMT, and 2100 GMT, an analysis of the latent instability and underrunning are presented. Their purpose is to help show how secondary (ageostrophic) circulations associated with the baroclinic zone and the strong jet streak interacted with the high θ_w in the PBL under the lid.

An important element in the inception area is the location of the lid edge. Since the movement of the lid is tied to the advective winds in the EML, it is possible to interpolate the position of the lid edge through time. Using a combination of the known positions of the lid edge, the 0000 GMT 01 June speed of the lid edge (14 ms^{-1}), and forward and backward trajectories, the lid edge was determined at three hour intervals, between 1200 GMT 31 May and 0000 GMT 01 June. The results are depicted in Figure 4.17. These positions are used as overlays on the remaining figures in this chapter. As to not disrupt the flow of the text, those figures are grouped at the end of the chapter.

The L.I.D. program revealed that θ_{bw} was close to the surface at both 1200 GMT 31 May and 0000 GMT 01 June. Therefore, the surface θ_w is representative of θ_{bw}. Hence, the surface θ_w and interpolated values (Appleby, 1954) of saturation wet-bulb potential temperature at 500 mb (θ_{sw5}) were used to produce detailed analyses of the buoyancy for the intermediate times. This procedure is similar to the procedure recommended by the Air Weather Service (Gesser and Wallace, 1985). This new surface buoyancy term (defined as: θ_{sw5}-θ_{wsfc}) is abbreviated SBT in this chapter.

At 1200 GMT 31 May, there was a minimum in the SBT of less than - 4.0°C in Indiana and southern Michigan (Figure 4.18). The lid edge at this time is superimposed from Figure 4.17 and is depicted as hatching. As in Figure 4.9 on page 86, the lid

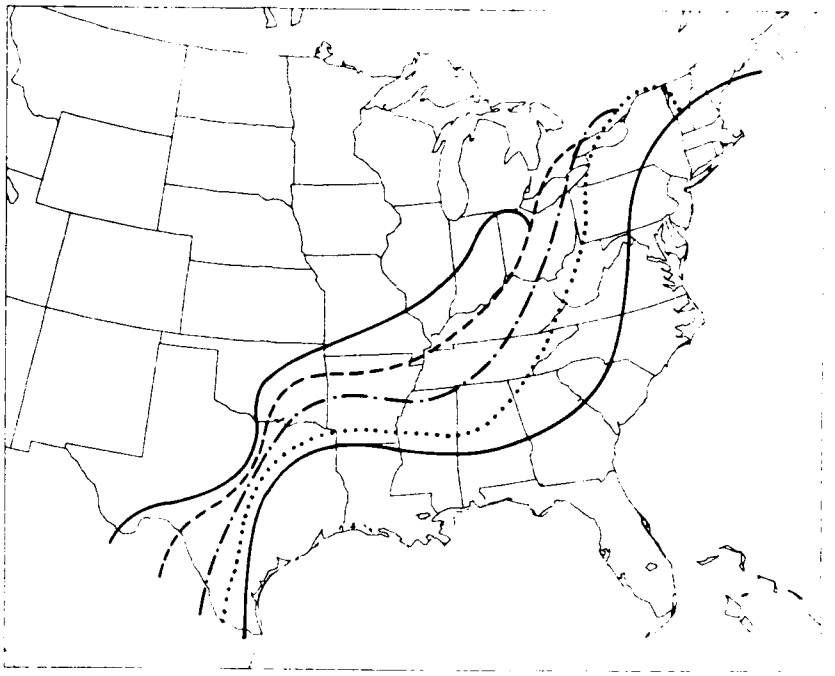

Figure 4.17: Lid Edge Interpolation. Lines depict western edge of the lid on 31 May 1985 at 1200 GMT (solid), 1500 GMT (short dashed line), 1800 GMT (dot dashed line), 2100 GMT (dotted line), and on 01 June 1985 at 0000 GMT (easternmost solid line).

extended through Illinois, northern Indiana, and into Ohio. Most of the region with negative SBT values was capped by the lid. The exception, however, was a small area in southern Michigan which was the only area experiencing severe convective weather at the time! (See Figure 4.9 on page 86 and Table 4.6 on page 85). Note that the high θ_{bw} was not near the surface over Canada (it was elevated over the warm front). Therefore, the SBT analysis does not reflect the true latent instability present there. That is why the gradient of SBT is so sharp along the warm front.

As mentioned in Section 2.5, underrunning is essentially an ageostrophic process. A good measure of the low-level ageostrophic response to the forcing by a baroclinic zone and an upper-level jet streak is the isallobaric wind (Section 2.5). Since the forcings involved in this process are on the mesoscale, one hour pressure tendencies are used. They are calculated using the changes in reported altimeter settings and converted to millibars (Fujita et al., 1970).

This was done for two reasons. First, it eliminates the influence of inferred temperature change in the column beneath the ground included in reducing station pressure readings to sea level. Second, since many stations report altimeter setting but not sea level pressure, this technique provides a higher spatial data density. From these analyses, a sense of the surface ageostrophic motion (i.e. underrunning) can be obtained.

Figure 4.19 shows that the isallobaric wind (ageostrophic) at 1200 GMT was flowing out from under the lid toward the minimum in pressure tendency (denoted with an asterisk in the figure), which was centered under the left exit region of the jet streak over eastern Lake Superior. Hence, underrunning of high θ_w air was indeed occurring in response to the ageostrophic forcing associated with the jet streak. This lateral flux of moisture from underneath the lid provided the buoyant energy for the hailstorms over their nine hour life cycles! Figure 4.19 shows the position of both the 500 mb jet streak (cross-hatching; from

Figure 4.8c) and the frontal boundaries (from Figure 4.8a). This configuration is similar to that shown in Figure 2.5 on page 44 except that the baroclinic zone and the jet streak are not yet coincident with the lid edge.

Six hours later, at 1800 GMT 31 May, the area of latent instability had moved eastward and northward (Figure 4.20). The minimum in SBT was positioned over the area of maximum API (see Section 4.4) and under the lid. As previously mentioned, the SBT was decreasing both as a result of increasing surface θ_w and decreasing 500 mb θ_{sw5}. The decreasing θ_{sw5} was due to the development of the very pronounced thermal trough (see Figure 4.12c). The minimum SBT was -5.0°C (Lifted Index of -10°C) and the -4.0°C isopleth extended into Ontario, where the first tornadoes developed. The production of those thunderstorms were aided by the ascent over the warm front.

By 1800 GMT, the minimum in pressure tendency had moved eastward and a trough of pressure falls extended southward through Ohio (Figure 4.21). As a result, the isallobaric winds backed to the southeast and began flowing out from under the lid in eastern Ohio. The baroclinic zone and the lid edge were much closer together than three hours earlier.

By the start of the tornadoes in Ohio (31/2059 GMT), the SBT had decreased to below -6.0°C (Lifted Index of -12.0°C)! (Figure 4.22). This is a reflection of both the lid's ability to concentrate high θ_w in the PBL and the relative coldness of the upper-level thermal trough. Note that the gradient of SBT along the cold front increased as the front intensified. The lid edge is estimated to have moved as far north as northern New York State by 2100 GMT while it continued to cap most of the negative SBT region. Also, the baroclinic zone and lid edge were now sufficiently close to interact in a manner suggested by Figure 2.5 on page 44, in which underrunning and forced ascent occur together along the lid edge. The initial convection began where air, with high θ_w concentrated beneath

the lid, was advected into a region of strong ascent just beyond the lid edge (Figure 4.23). Hence, by 2100 GMT there was strong underrunning of high θ_w air into the region under the upper-level thermal trough where there was also favorable large-scale forcing.

Eventually, the cold front increased its speed and moved through the lid, destroying the lid's features. During this process, a squall line associated with the cold front formed and fed off of the moisture that had been trapped beneath the lid. As a result, northeastern Ohio and northwestern Pennsylvania, which experienced the first convective storms resulting from the initial underrunning, later received 2 cm (3/4") hail as the squall line passed.

4.6 Summation

In this case, the critical factors were: (1) the presence of the lid and resulting build-up of high θ_w in the PBL, (2) readily available soil moisture, (3) underrunning, and (4) forced ascent associated with baroclinic forcing resulting from a migrating short wave. This progression of events illustrates that the Carlson-Ludlam Conceptual Model is an invaluable tool for understanding the interaction of the physical processes responsible for the severity of this outbreak.

Vigorous short-wave troughs move across that part of the nation several times each Spring. Severe convective outbreaks of this magnitude, however, are very rare events indeed. Therefore, the most critical factor must have been the presence of the lid. For without it, the huge latent instability which was present would never have developed. This fact suggests that the frequency of severe weather in the northeastern United States is correlated to the frequency of lid occurrences. The rare occurrence of lids over this part of the nation is substantiated by climatological analysis, the results of which follow.

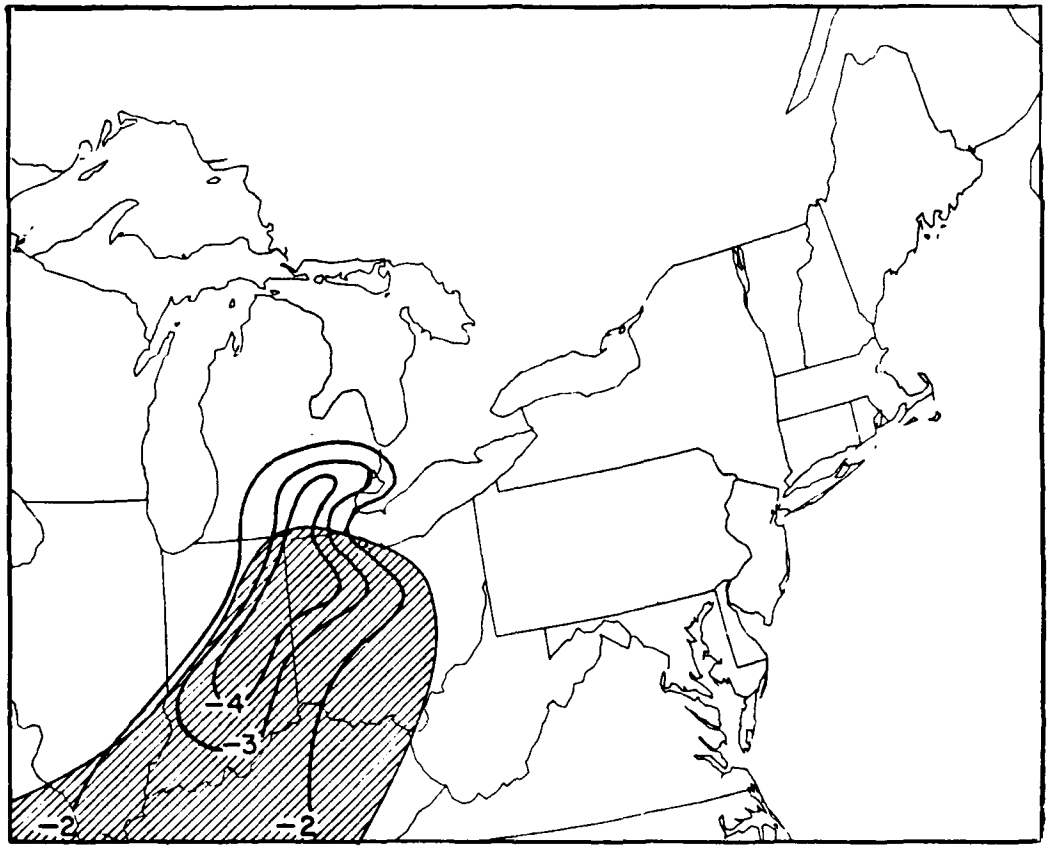

Figure 4.18: Buoyancy Analysis for 1200 GMT 31 May 1985. Surface Buoyancy Term (SBT) [°C] (solid lines); The lid from Figure 4.17 on page 110 is included (hatched area).

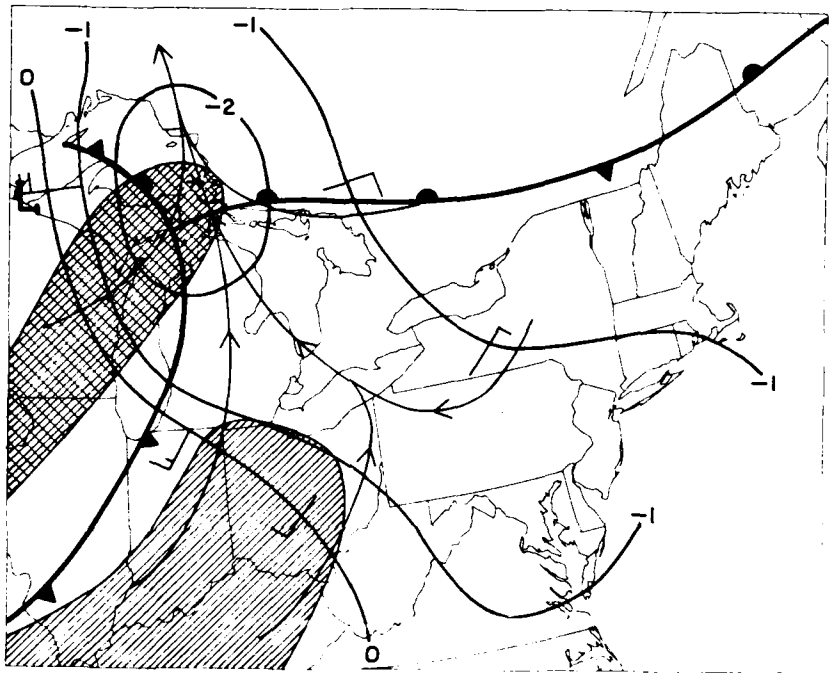

Figure 4.19: Underrunning Analysis for 1200 GMT 31 May 1985. Fronts are indicated with conventional symbolism; one hour pressure tendency is shown in mb hr^{-1} (solid lines); pressure tendency minimum is denoted with an asterisk. Wind barbs depict isallobaric winds (half barb: 2.5 ms^{-1} (5 kt), full barb: 5 ms^{-1} (10 kt), flag: 25 ms^{-1} (50 kt)); isallobaric streamlines are indicated with thin solid lines. The 500 mb wind maximum from Figure 4.8c is indicated with cross-hatching. The lid from Figure 4.17 on page 110 is included (hatched area).

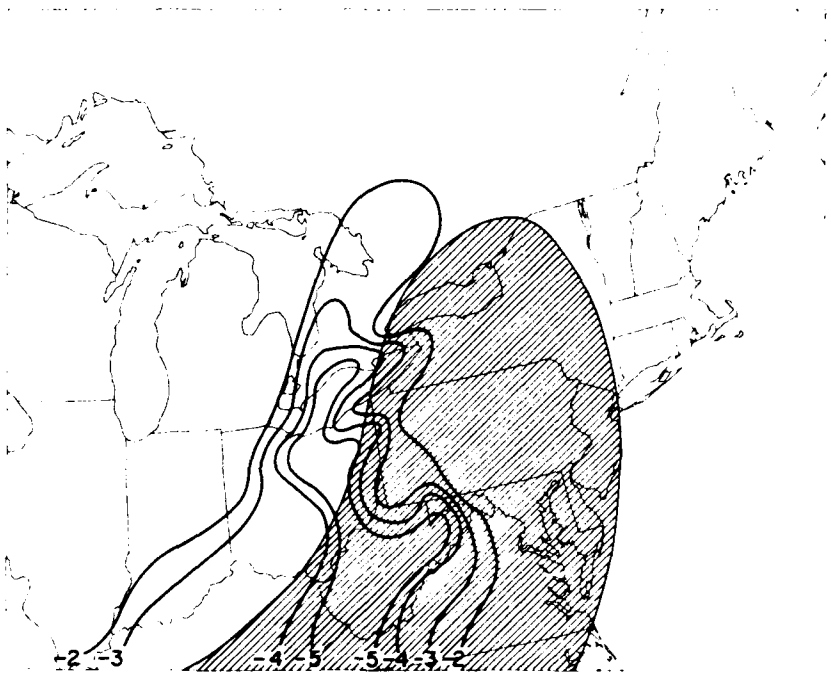

Figure 4.20: Buoyancy Analysis for 1800 GMT 31 May 1985. SBT [°C] (solid lines); the lid from Figure 4.17 on page 110 is included (hatched area).

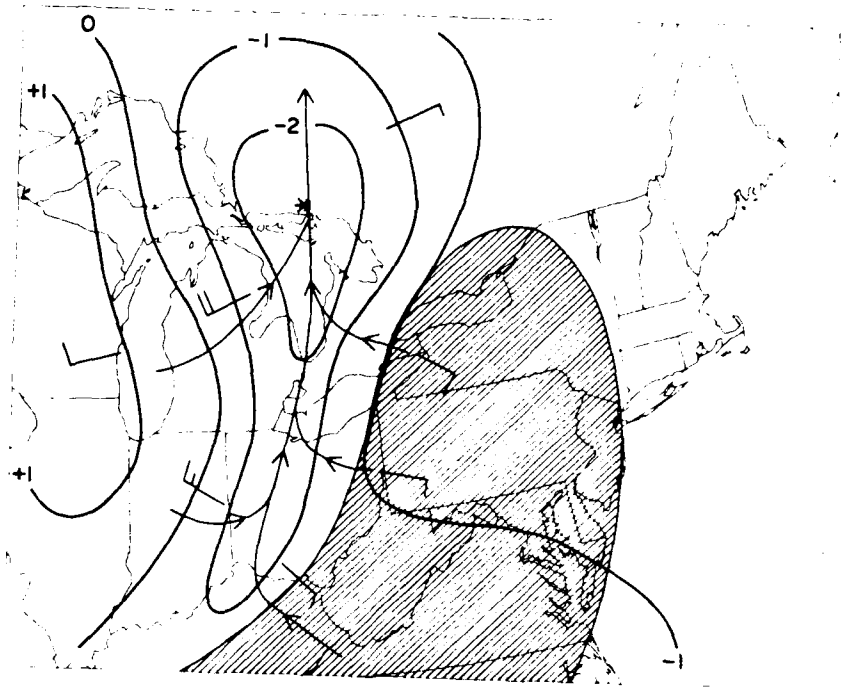

Figure 4.21: Underrunning Analysis for 1800 GMT 31 May 1985. Conventions are the same as Figure 4.19 on page 115.

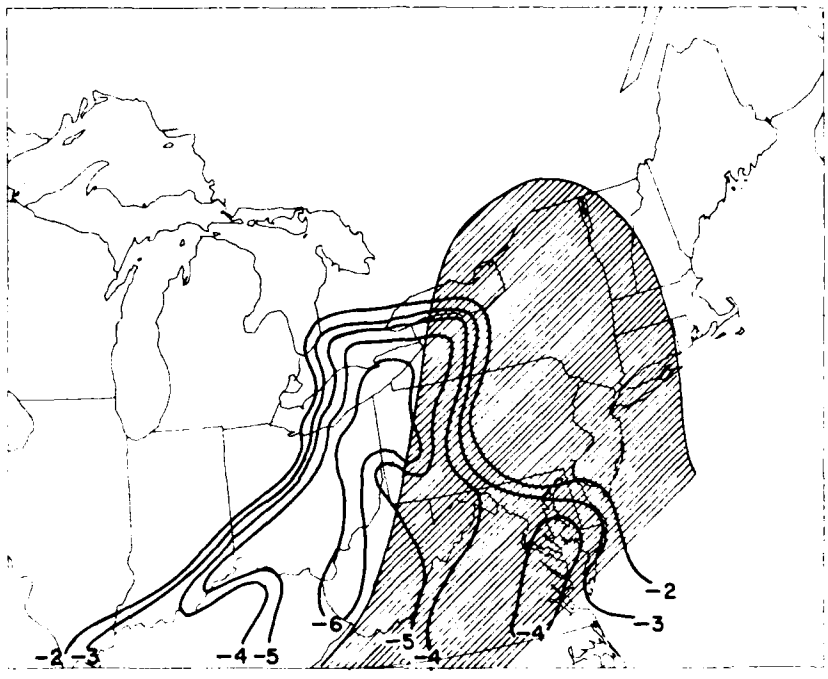

Figure 4.22: P oyancy Analysis for 2100 GMT 31 May 1985. SBT [°C] (solid lines); The lid from Figure 4.17 on page 110 is included (hatched area).

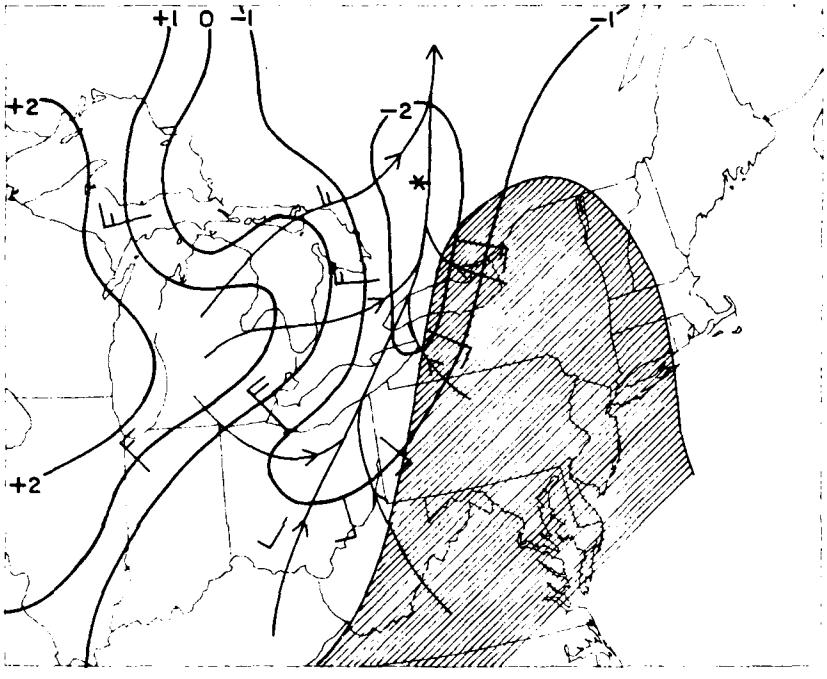

Figure 4.23: Underrunning Analysis for 2100 GMT 31 May 1985. Convections are the same as Figure 4.19 on page 115.

Chapter 5

LID CLIMATOLOGY

The purpose of this chapter is to present the results of a preliminary climatology of the lid and a few related parameters. This climatological study was conducted to ascertain whether the occurrence of the lid and the values of those parameters in the 31 May 1985 Tornado Outbreak were unusual for that part of the nation (eastern Ohio and western Pennsylvania) at that time.

The computer application, L.I.D., which is discussed in Section 3.2, was used in a batch mode to compile the necessary statistics. The period of record (POR) was four years (1983-1986) of a six month block (April to September). The following discussion is limited to this six month block because it was found that the frequencies of lid occurrences in the other six months were insignificant. The data used is from archives being collected at the Penn State Department of Meteorology. This data base has small gaps in it and is not quality controlled; however, these problems were partially overcome by averaging over the four year POR and using L.I.D.'s validators (Section 3.2).

Monthly means of many parameters were calculated; however only four are presented: (1) lid days, (2) θ_{bw}, (3) a difference field of θ_{bw} without conditions from θ_{bw} when a lid is present (henceforth denoted as $\Delta\theta_{bw}$), and (4) θ_{sw5}. The analysis found that all these parameters have an insignificant difference between their means at 1200 GMT from those at 0000 GMT. This conservatism supports using the lid parameters when forecasting severe convection as suggested in Section 3.1. Also, since these parameters are conservative and brevity is desirable, only the 0000 GMT values are presented in this chapter.

5.1 Lid Days

Figure 5.1 shows the number of days each month (a-f) in which sounding stations were under the influence of a lid (lid days). The means were rounded to the nearest whole day. Consequently, stations showing zero lid days for a given month might have had a few lid days in that month over the four years but not enough for the mean to round up to one day. Inspection of these figures reveal some interesting facts. First, in answer to the question posed in Chapter 4: Lids are indeed a rare occurrence over the northeastern United States in May (Figure 5.1b). In fact, the 31 May 1985 Tornado Outbreak proved to be the only lid day in May over that part of the country for the entire four years! Note, however, that the one-day-per-month isopleth does progress northward with time, reaching the northern Great Lakes by August. It then begins to retrogress in September.

Although lids are such rare events in the northeastern United States, they have been documented as far north as Portland, Maine (Section 4.2.4). Penn et al. (1955) reported that a "capping inversion" in the warm sector of a cyclone (i.e. lid) was present over Massachusetts in June during a tornado outbreak. This same cyclone produced tornadic storms two days earlier in Michigan. Whitney and Miller (1956) reported that the same stratification was an integral part of that outbreak. Therefore, the stratification must have moved along with the cyclone. Neither study discusses the origin of the "capping inversion"; however, inspection of the data presented in both articles lends support that the inversion was produced by an EML advected along ahead of the cyclone. It is the same scenario as the tornado outbreak presented in Chapter 4!

Second, there is a definite translation of the maximum in lid days. In April (Figure 5.1a), the maximum is in extreme southern Texas. By July (Figure 5.1d), it is centered in Iowa and extends as far north as Minnesota. In September (Figure 5.1f), however, the

Figure 5.1: Mean Lid Days. The mean number of days each month a lid occurs over the four year POR (solid lines). (a) April (b) May (c) June (d) July (e) August (f) September.

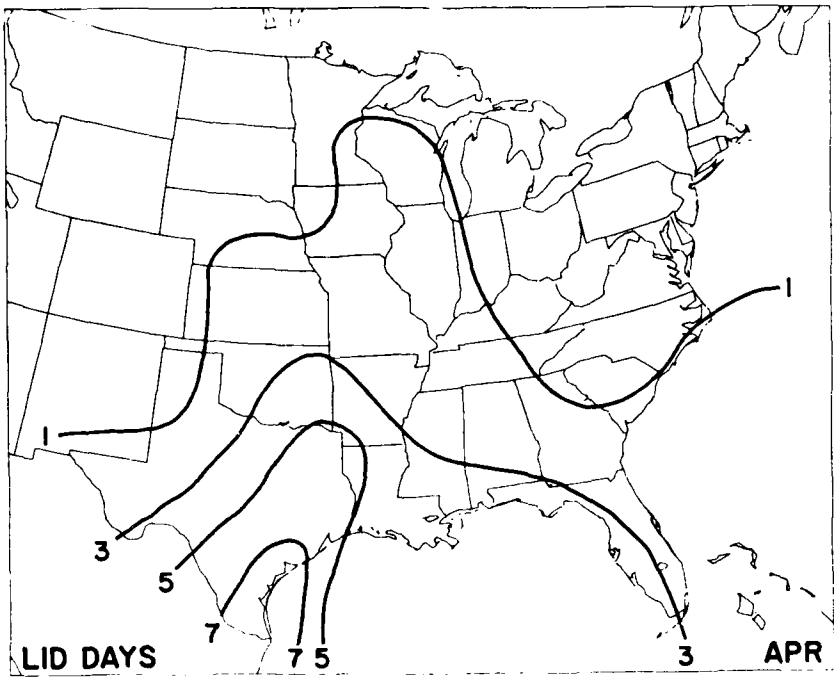

(a)

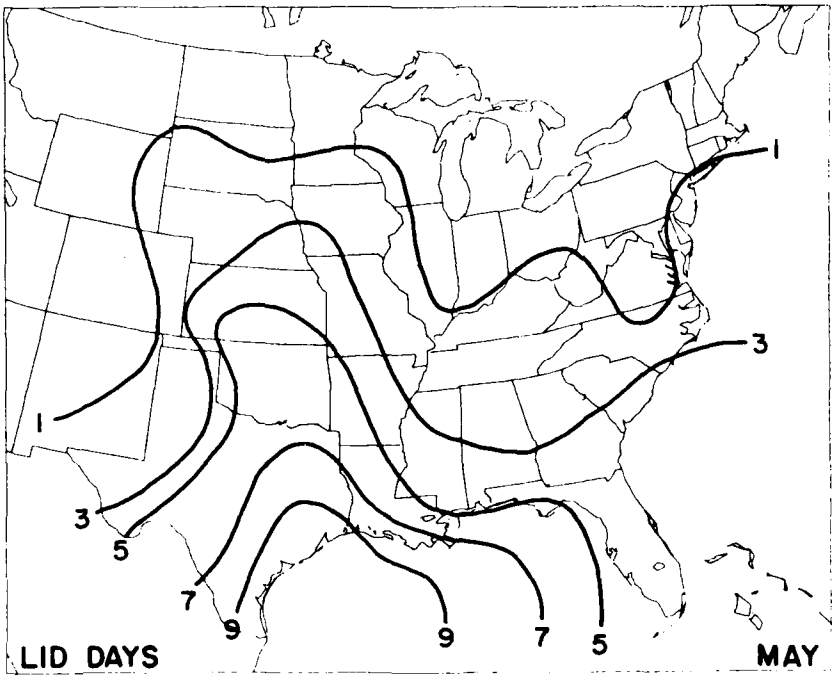

(b)

Figure 5.1 (continued)

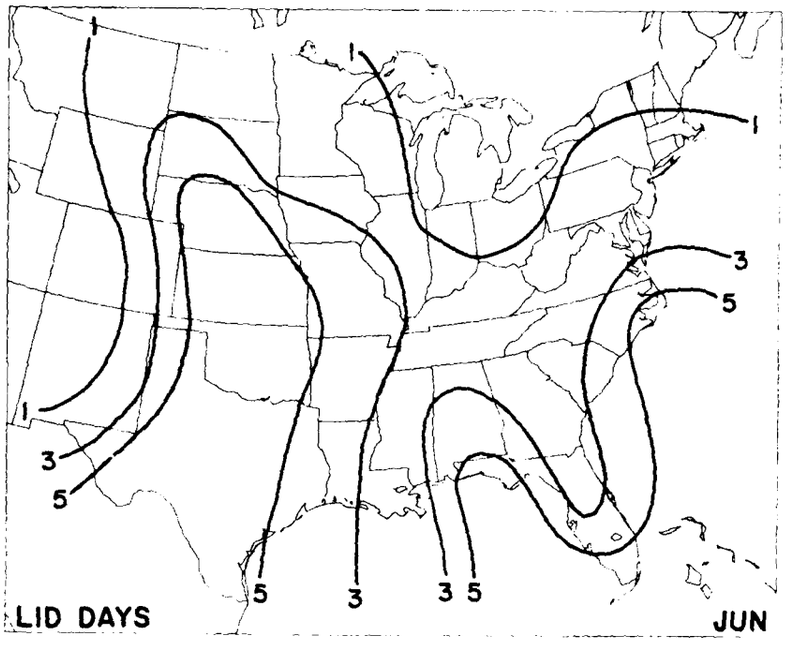

(c)

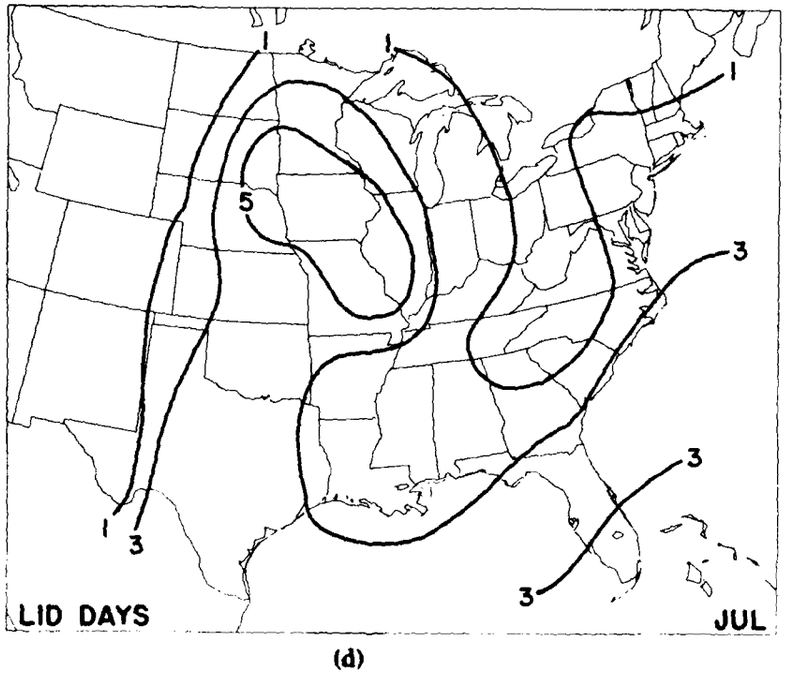

(d)

Figure 5.1 (continued)

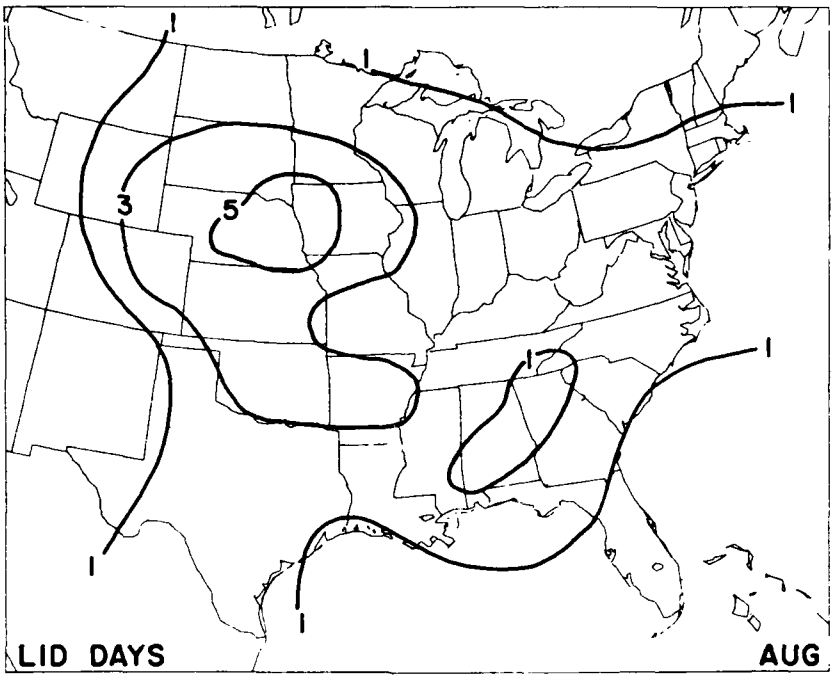

(e)

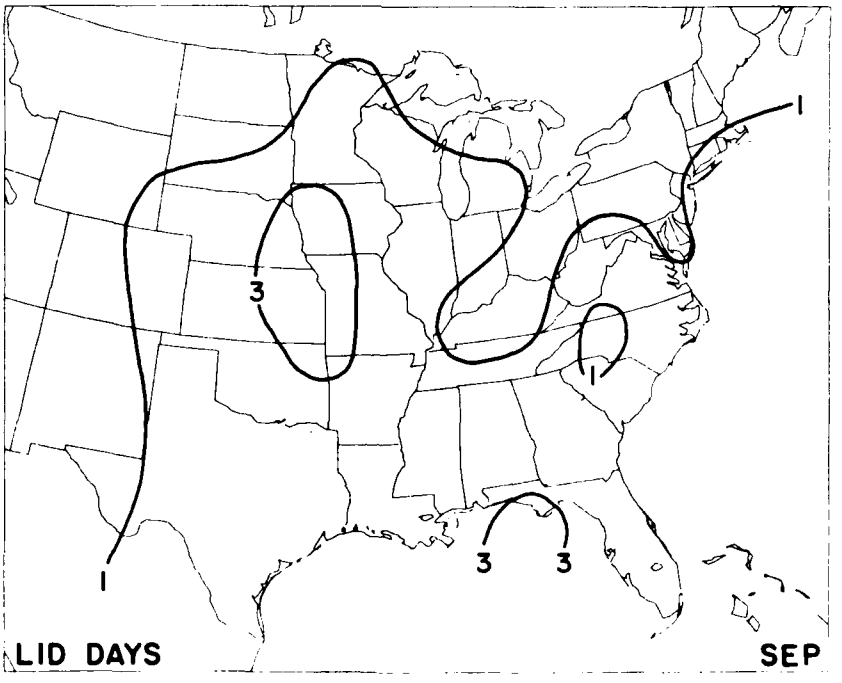

(f)

Figure 5.1 (continued)

maximum moves a little southward, centering more in Kansas and Missouri. Figure 5.1 a and b suggest that the source region in April and May is northern Mexico. Figure 5.1c suggests that the source region in June is sometimes northern Mexico and some times the Desert SW. Figure 5.1 d and e suggest that the source region in July and August is predominately the central Rocky Mountains. Figure 5.1f, however, suggests that the source region begins to move southward by September. As discussed in Section 2.1.3, this translation is most probably a consequence of the seasonal, meridional oscillation of the arid source regions of the EML.

Several studies have shown a similar oscillation in the frequency of tornadoes (Fawbush et al., 1951) and thunderstorms in general (Long, 1966; Changery, 1981). Fawbush et al. (1951) analyzed storm data from the U.S. National Weather Bureau to calculate their tornado frequencies; Long (1966) analyzed radar reports to calculate the frequencies of thunderstorms penetrating the tropopause; and Changery (1981) analyzed surface reports to calculate thunderstorm frequencies. All three studies show that the maxima progress northward during the Spring and Summer and retrogress during the fall. Figure 5.2 shows the results of Fawbush et al. (1951). Comparing this figure with Figure 5.1 on page 123, there is a general agreement between frequencies of lid days with those of tornadoes.

Fawbush and Miller (1952) noted that the "typical" tornado proximity sounding shows no great variation with the seasons (see Section 1.2). Furthermore, they note:

> Tornadoes occur less frequently during the fall and winter periods only because the required airmass structure [lids] occurs less often during these seasons. (p. 306)

This statement is supported by the results shown in Figure 5.1 on page 123. These observations suggest a connection between lids and tornadoes, but obviously, further research is needed to substantiate this.

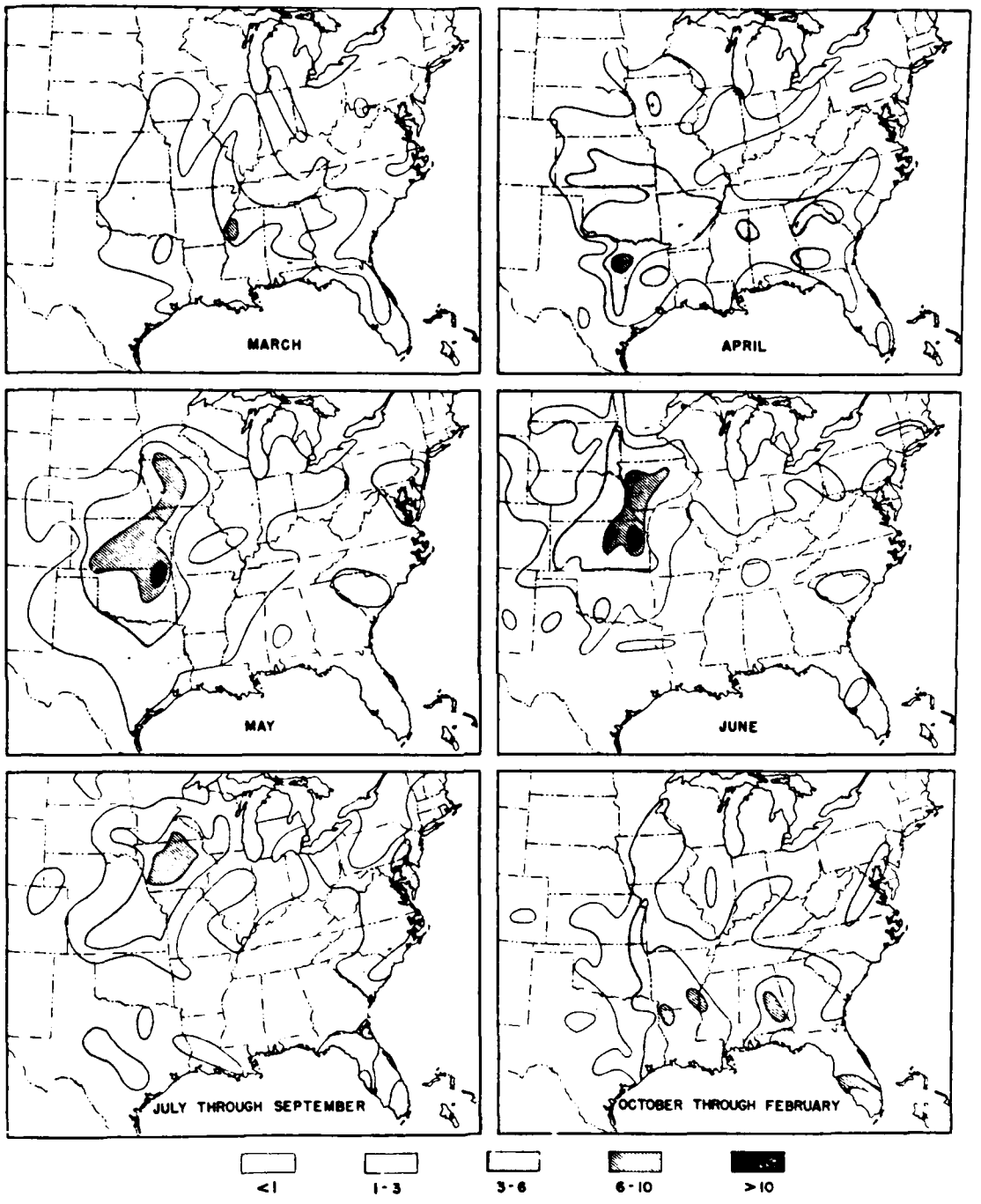

Figure 5.2: Tornado Frequency. Total number of tornadoes per 50 mile square reported in the period 1920-1949, by months. (From Fawbush et al., 1951).

A third, and surprising, finding is the presence of a secondary maximum in lid days located along the southern Atlantic coast. This feature begins to show up in May (Figure 5.1b), is most prevalent in June (Figure 5.1c), persists through July (Figure 5.1d), and disappears by August (Figure 5.1e). It is not immediately obvious what produces this feature. It seems clear that it is not simply an EML advected from the west. If this was the case, there should be a uniform progression in the number of lid days from Texas to the Carolinas, but there isn't. A large effort was made to differentiate these soundings from the typical lid sounding, but no difference could be found.

One plausible explanation is that this feature is truly an EML but the source region is the Saharan Desert. Several investigators have shown that Saharan Air does reach the United States (Carlson and Prospero, 1973; Caracena and Fritsch, 1983). This advection of Saharan air is made possible by the intensification of the Bermuda High during the early summer; however if this were the reason, the feature would be strongest in the Fall. Another explanation is that L.I.D. is actually picking up inversions produced by the sea breeze. This would explain the maxima along the coast, but it is questionable whether a sea breeze circulation can produce such uniform layers above the inversion. This is an item for further research.

5.2 Mean θ_{bw}

The mean of the "maximum (best) 50 mb-layer-averaged planetary boundary layer wet-bulb potential temperature," θ_{bw}, is presented in Figure 5.3 for each of the six months (a-f). The pattern starts out relatively flat (Figure 5.3a), develops a ridge over the Great Plains during the Summer (Figure 5.3b-e), and flattens out again by September (Figure 5.3f). The meridional gradient is uniform in April; however a slight maximum in

Figure 5.3: Mean θ_{bw}. The mean of the maximum (best) 50-mb layer-averaged wet-bulb potential temperature in the PBL [°C]. (a) April (b) May (c) June (d) July (e) August (f) September.

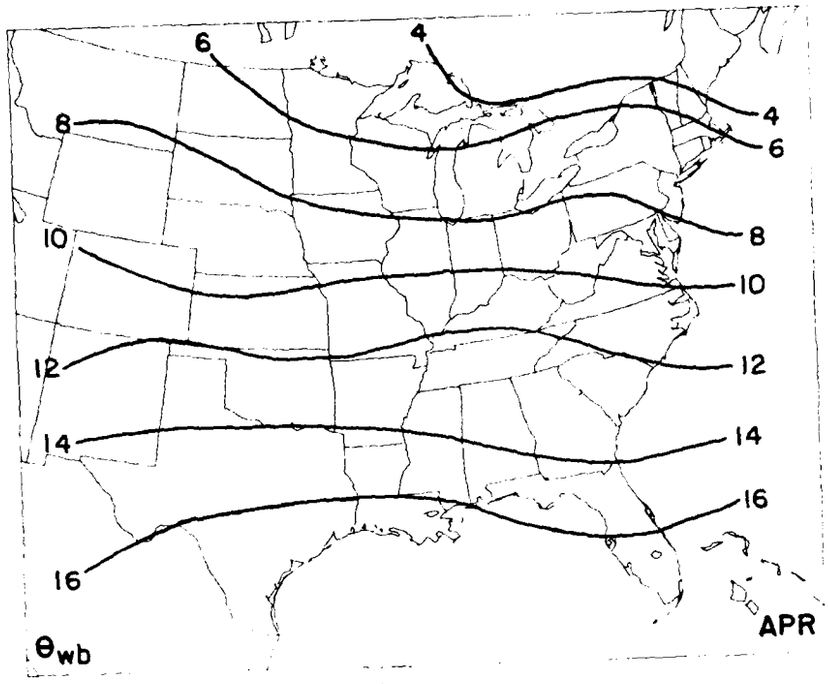

(a)

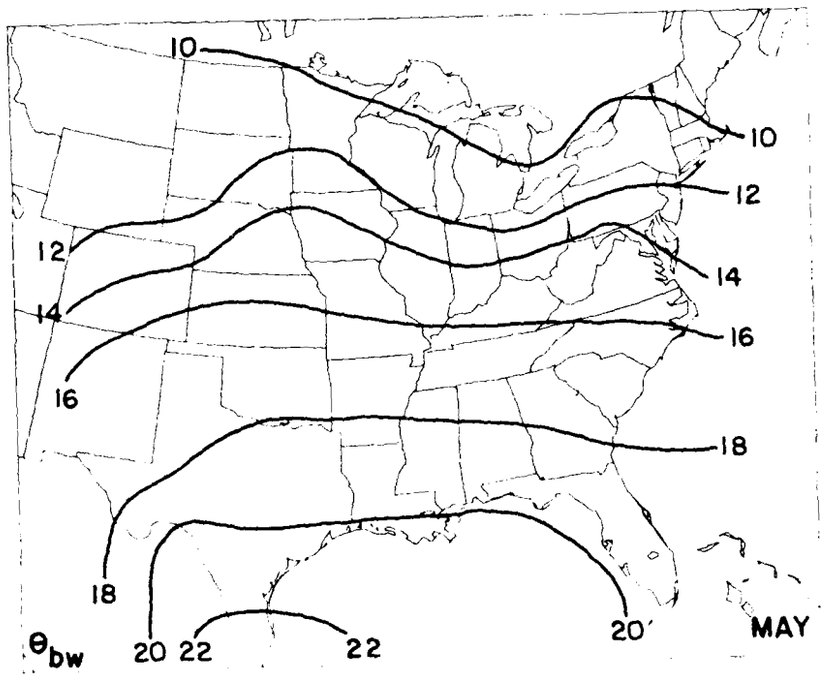

(b)

Figure 5.3 (continued)

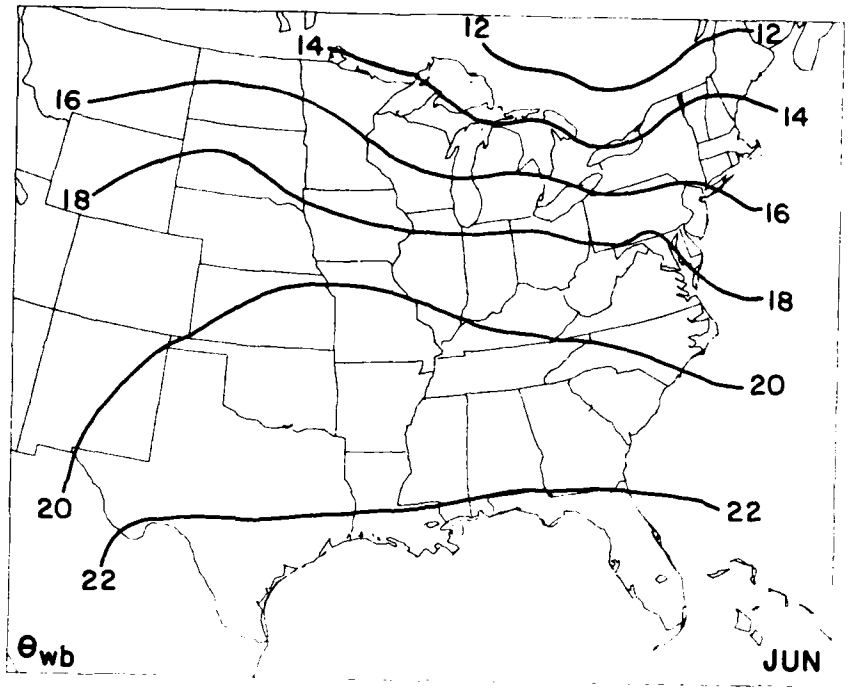

(c)

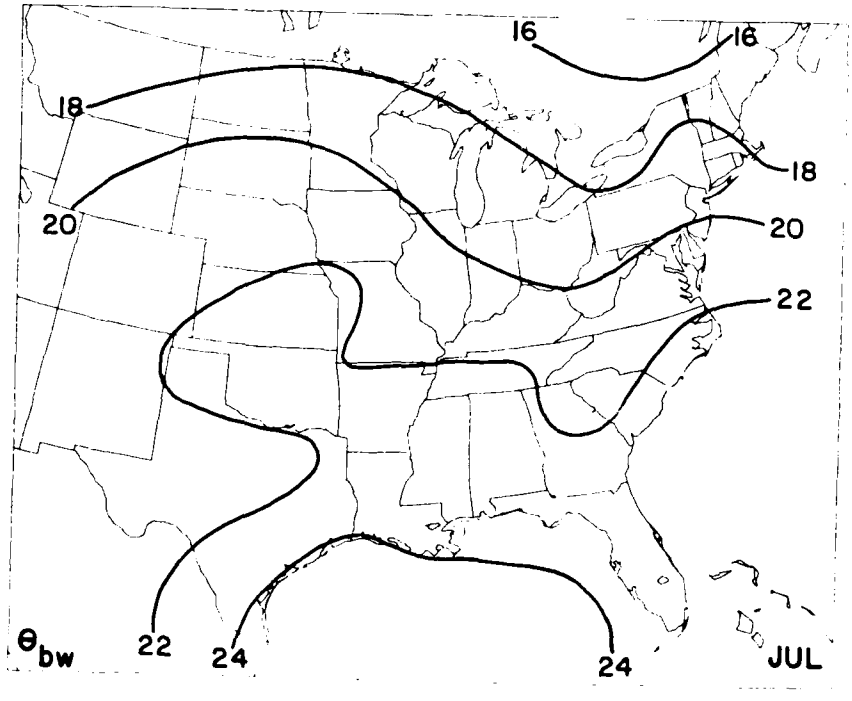

(d)

Figure 5.3 (continued)

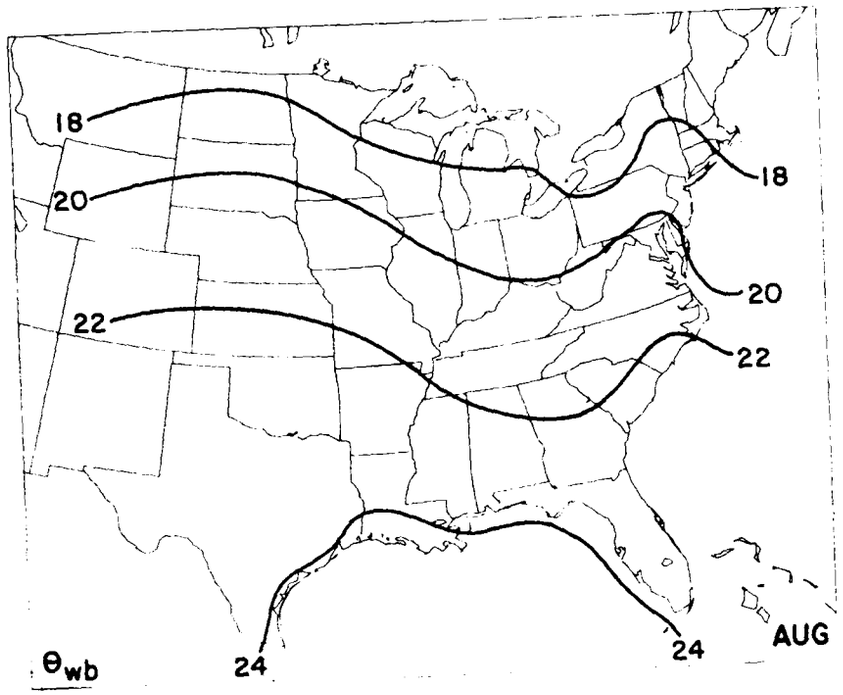

(e)

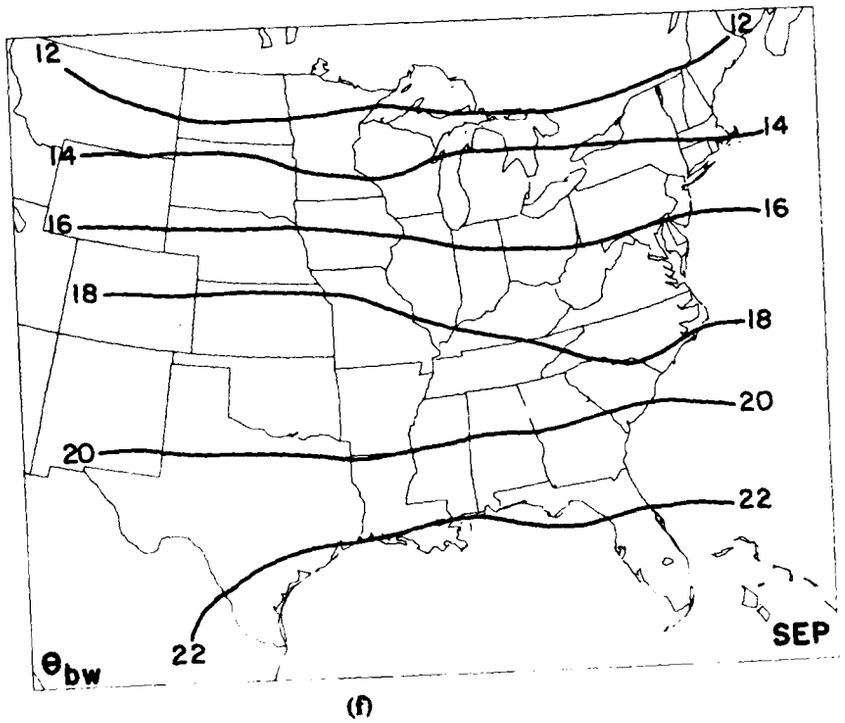

(f)

Figure 5.3 (continued)

the gradient develops and moves northward during the Summer. These two features are consistent with the northward migration of the polar jet and the influx of warm, moist air over the Great Plains. There is also a hint of a zonal oscillation in the gradient over Texas. This feature supports Dodd's investigation (1965) which shows a similar seasonal dependence of dewpoint gradient in that part of the country (see Section 2.1.2). In April, θ_{bw} along the Gulf coast is 16°C; by July, it is 24°C. These values are comparable to Carlson and Ludlam's (1968) values even though their definition of θ_w differs (see Table 5.1).

Table 5.1: Comparison of Average θ_w Results

Investigator	Early April	Late April	Early May	Late May	Early June
C and L	18.2	21.6	22.0	23.1	22.0
This study	16.3		22.0		22.0

NOTES: (1) C and L: Carlson and Ludlam (1968).
(2) Units are °C.
(3) Vaules for this study are for the full month.

An analysis of the difference field of the mean θ_{bw} with no condition- (Figure 5.3 on page 130) from the mean θ_{bw} when a lid is present (not shown) found a dependence on both season and latitude ($\Delta\theta_{bw}$, Figure 5.4). At any given latitude, $\Delta\theta_{bw}$ is a maximum in April (Figure 5.4a) and a minimum in July (Figure 5.4d). By July, the difference is near zero for much of the south. This pattern shifts southward in September paralleling the shift in lid days. In any given month, $\Delta\theta_{bw}$ is greatest in the north. When lids occur in April north of 40°N latitude, the difference is more than 7°C (as much as 11°C!), whereas south of 30°N latitude, the difference is less than 4°C. The θ_{bw} value associated

Figure 5.4: Mean $\Delta\theta_{bw}$. A difference field of the mean θ_{bw} when a lid is present from the mean θ_{bw} with no conditions [°C]. Areas which did not have lid days during the month, are not analyzed. (a) April (b) May (c) June (d) July (e) August (f) September.

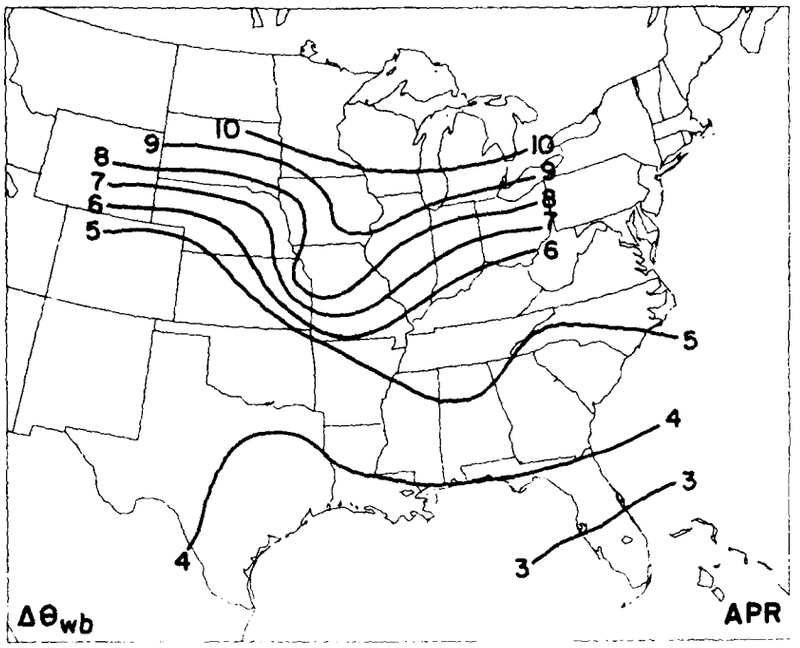

(a)

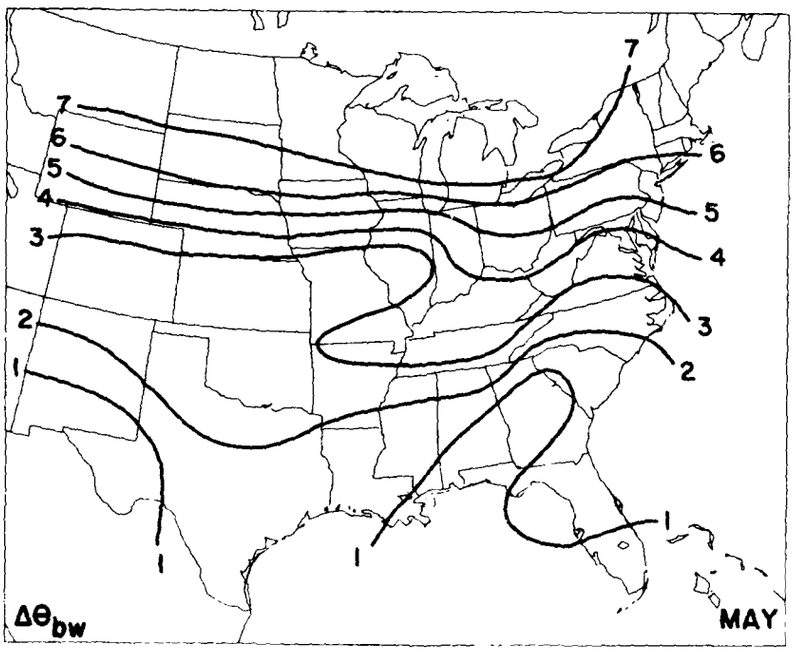

(b)

Figure 5.4 (continued)

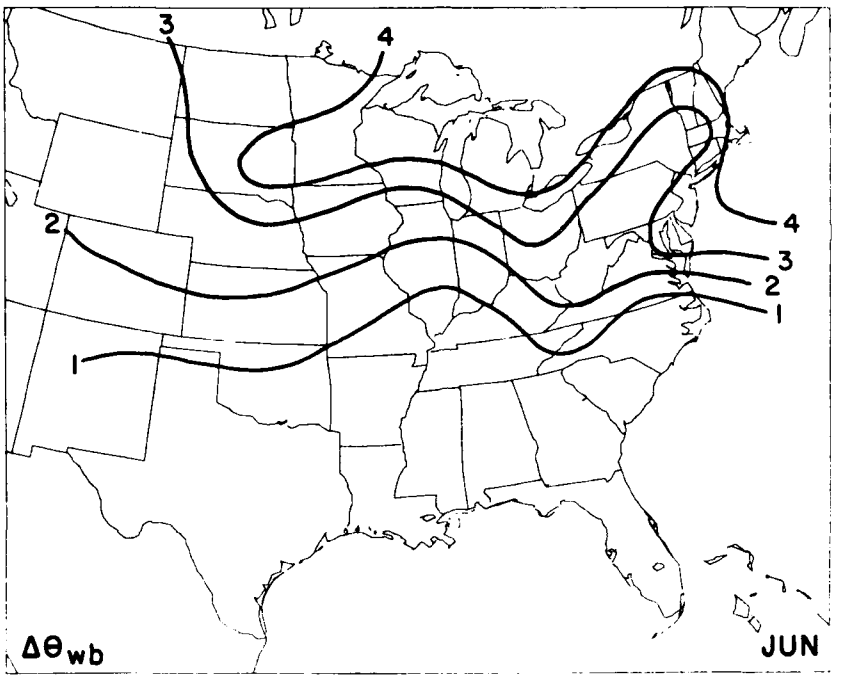

(c)

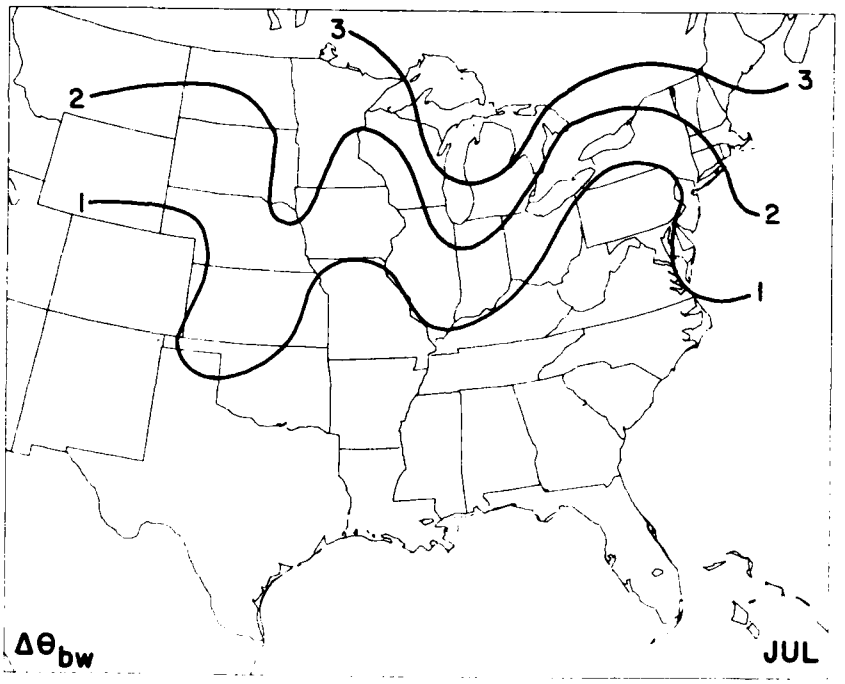

(d)

Figure 5.4 (continued)

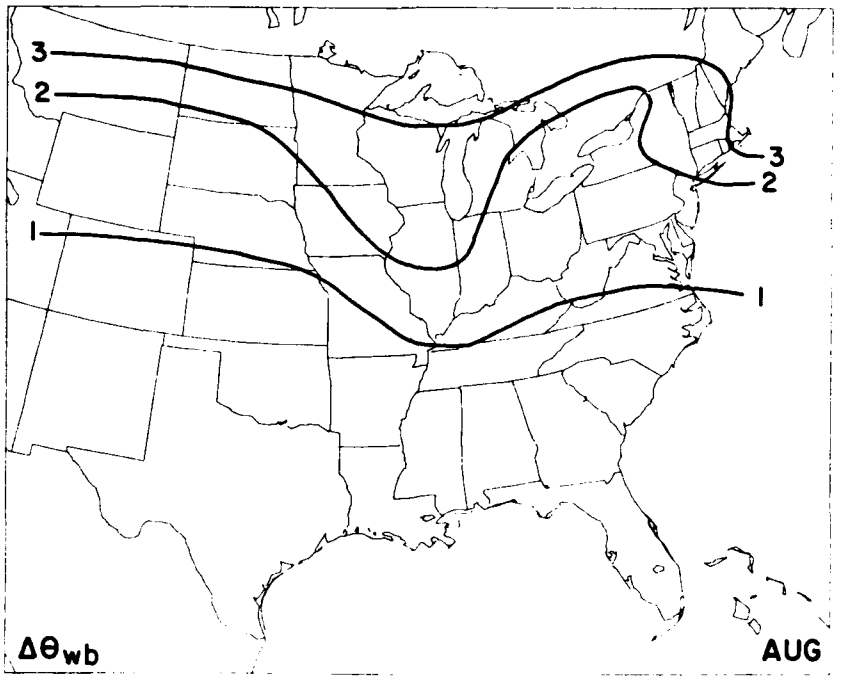

(e)

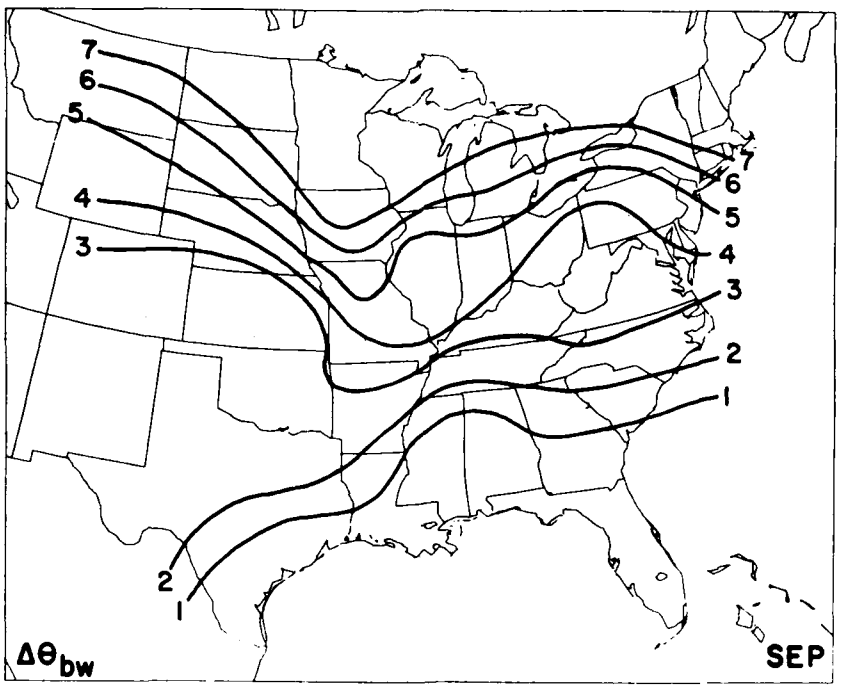

(f)

Figure 5.4 (continued)

with the lid involved in the 31 May 1985 Tornado Outbreak (Chapter 4) is 11.1°C from the climatological mean (24.3°C - 13.2°C)! (These values were taken from Table 4.8 on page 105 and Figure 5.3b respectively).

From this analysis, it can be concluded that lids have a different impact on the synoptic environment depending on the season and the latitude. Lids have a larger impact in the Spring than in the Summer, and a larger impact in the north than in the south. In fact, lids have a huge impact in the north during the Spring, and hardly any at all in the south during the Summer. This may partially explain why the frequency of tornadoes drops dramatically in July, from a maximum of more than ten in June (Figure 5.2c) to less than ten for the entire July through September period (Figure 5.2d), even though lid days remain relatively the same, from a maximum of more than five in June to three in September.

5.3 Mean θ_{sw5}

The intent of this section is to offer support for the contention, made in Sections 3.1, 4.4, and 4.6, that most severe storms have been found to be associated, not with abnormally low θ_{sw} aloft, but with abnormally high θ_w in the PBL. Figure 5.5 presents the mean θ_{sw5} for each of the six months (a-f). The θ_{sw5} values associated with the lid involved in the 31 May 1985 Tornado Outbreak were only 1.1°C from the climatological mean (16.5°C-15.4°C)! (These values were taken from Figure 4.12c and Figure 5.5b respectively). This small difference occurred even though an intense thermal trough existed in the inception area at the time. Hence, during the tornado outbreak, the PBL θ_w was at an extreme while the mid-level θ_{sw} was near the norm (even despite the thermal trough).

Figure 5.5: Mean θ_{sw5}. The mean saturation wet-bulb potential temperature at 500 mb. (a) April (b) May (c) June (d) July (e) August (f) September.

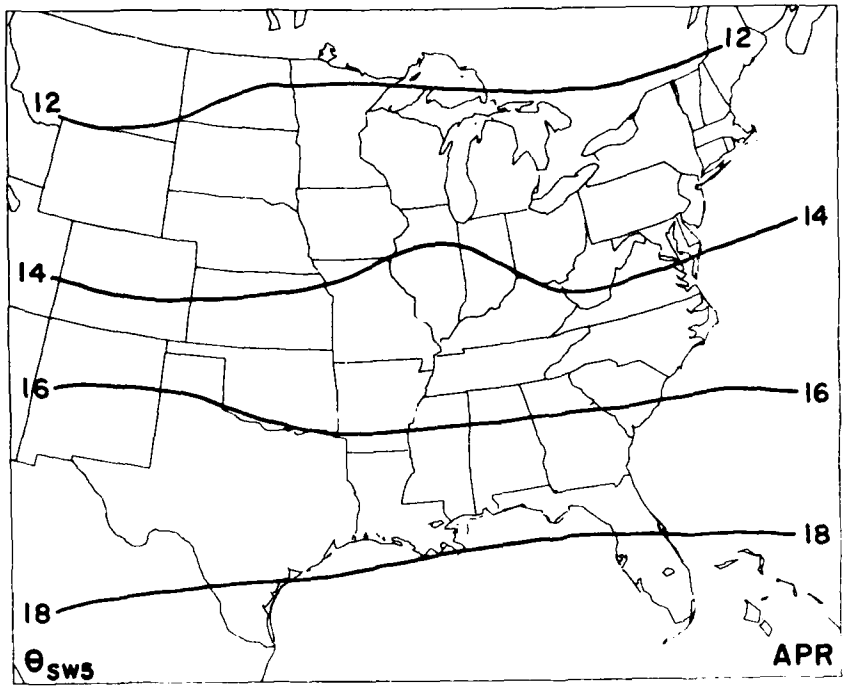

(a)

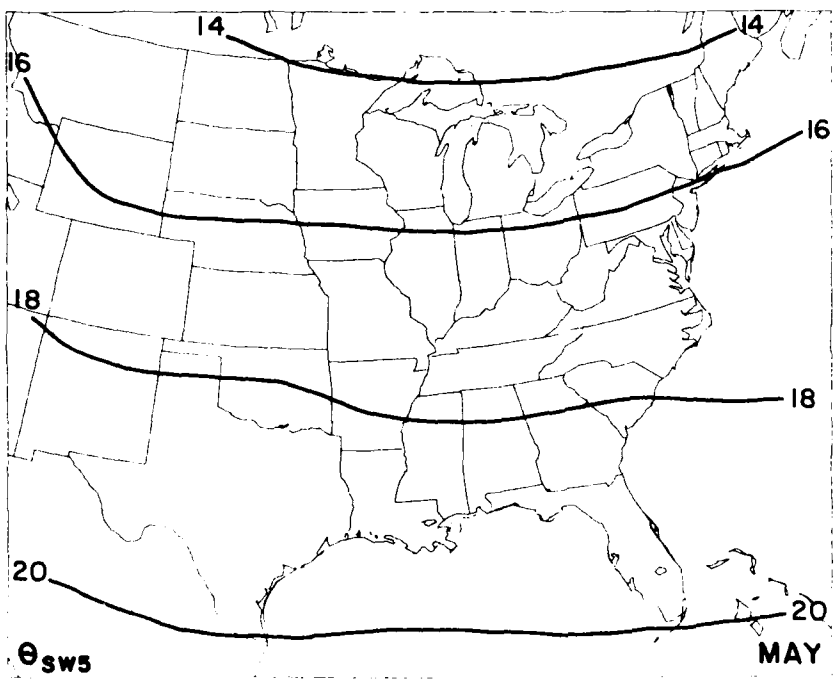

(b)

Figure 5.5 (continued)

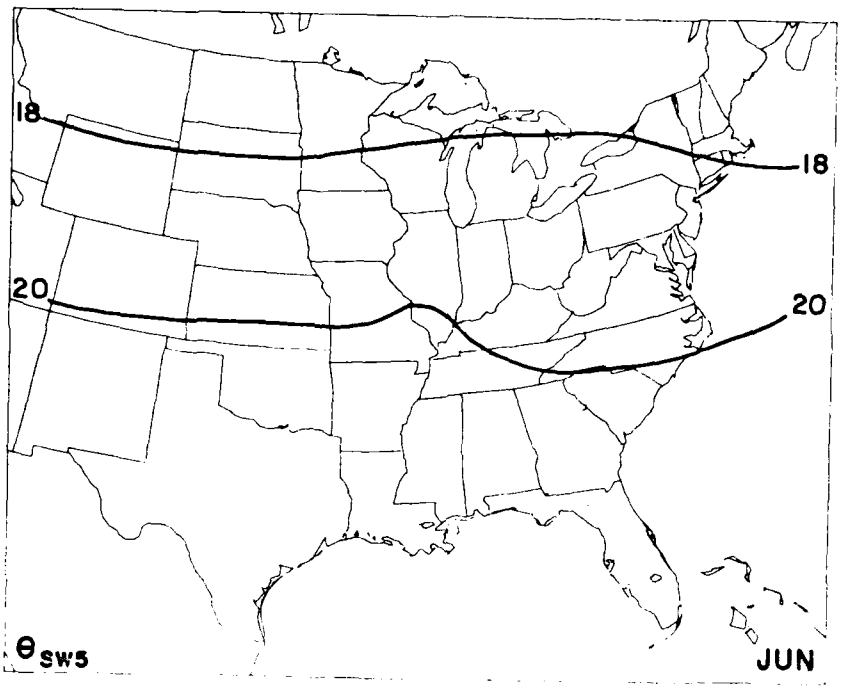

(c)

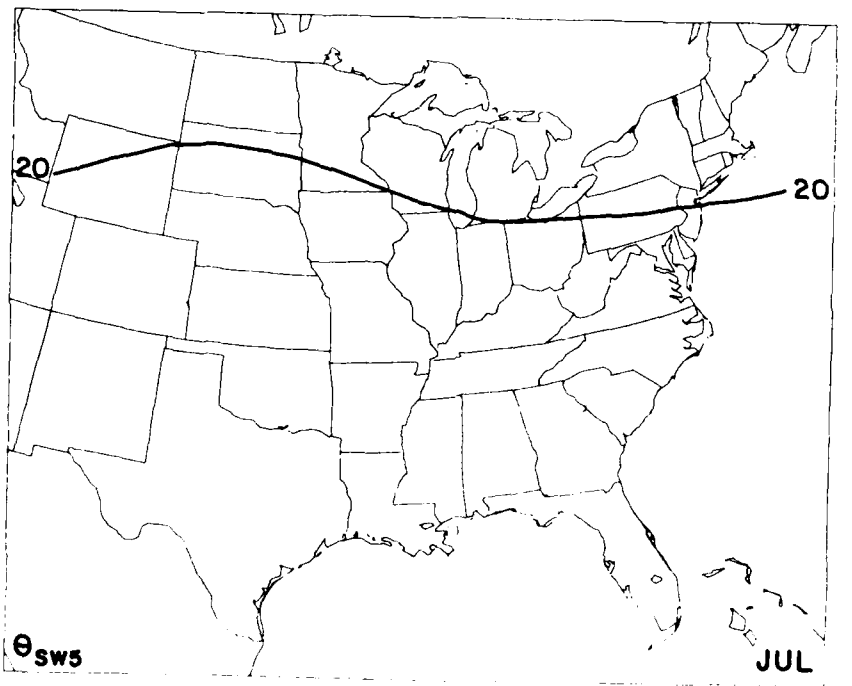

(d)

Figure 5.5 (continued)

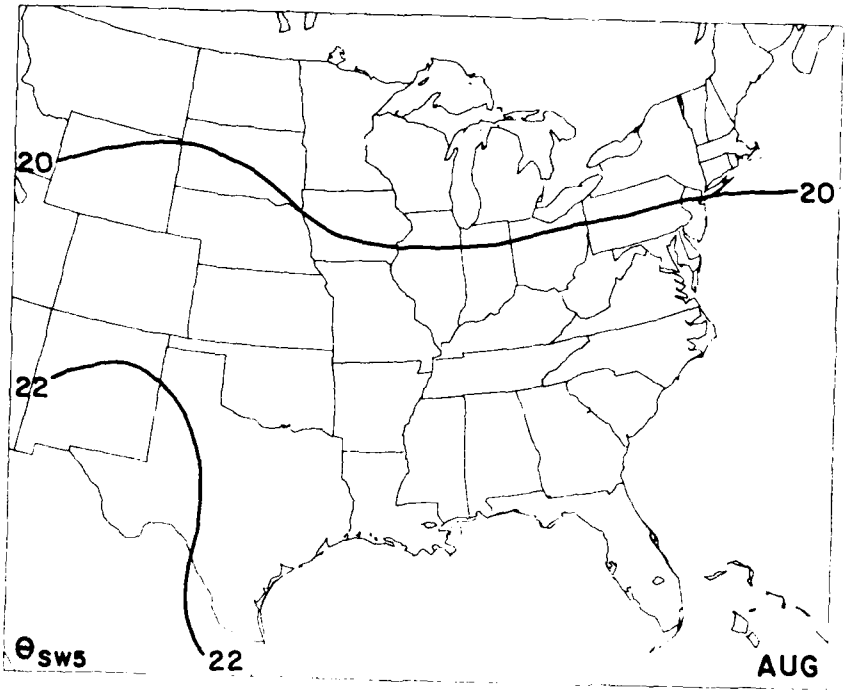

(e)

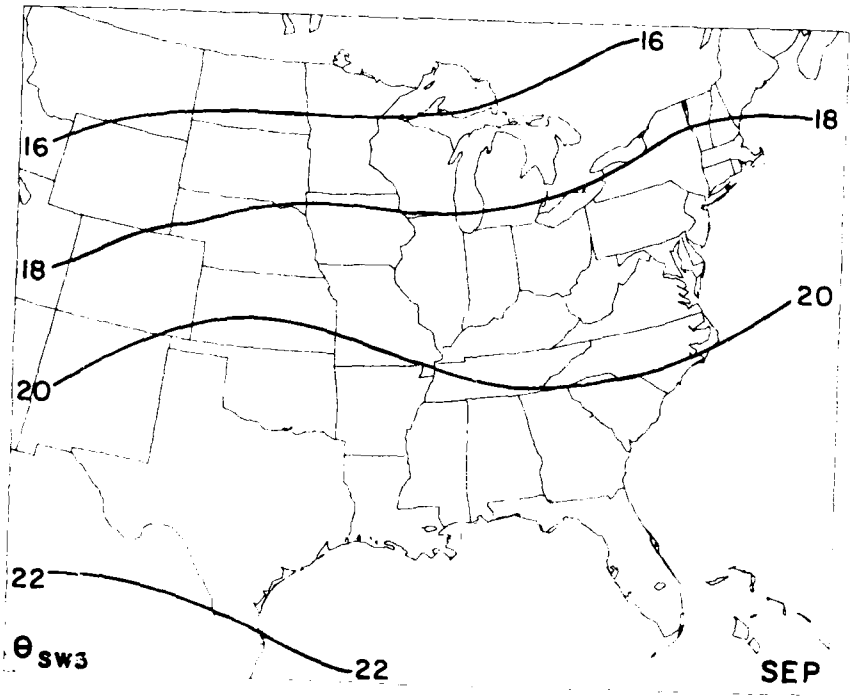

(f)

Figure 5.5 (continued)

One other feature to note from these figures is that the average meridional gradient of θ_{sw5} is surprisingly weak. It only changes 6°C from southern Texas to the northern Great Lakes for April and September, and is even weaker in the intervening months. In July, θ_{sw5} only changes 1°C over that distance! Clearly, the θ_{sw5} pattern is not as important as the θ_{bw} pattern.

5.4 Summation

This climatological analysis establishes the occurrence of lids in eastern Ohio and western Pennsylvania during May as very rare events. The analysis also reveals that when lids do occur in that part of the nation during that time of year, they have a very large impact on the synoptic environment. The fact that the resulting θ_{bw} in the pre-severe storm environment during the 31 May 1985 tornado outbreak was 11.1°C above the mean lends credence to the lid's capabilities. For a lid to have reached that far north that early in the year, there must have been an anomalous pattern in the mid-level flow preceding the tornado outbreak. Wagner (1986) reports that this was indeed the case.

The mean circulation pattern at 700 mb in Spring of 1985 was characterized by below normal geopotential heights at higher latitudes and above normal heights at low latitudes which led to faster than normal westerlies at mid latitudes (Wagner, 1986). There was also a strong trough centered over the Rocky Mountains creating a flow directed from the desert SW northeastward toward the Great Lakes. This overall pattern persisted with minor variations throughout the entire season.

Much of the nation had an abnormally dry Spring, particularly in the Southeast and southern Great Plains. The dryness was related to the above normal 700 mb heights and westerlies north of their normal spring position (i.e. much of the storm activity was farther

north over Canada). This fostered the growth of a deep, well mixed layer over a large area of the southwest and southcentral United States earlier in the spring than is usually the case. The abnormal flow at 700 mb created a relatively barotropic environment in mid-latitudes. Consequently, EML's originating over the desert southwest could move farther eastward and poleward without distruction, while troughs at higher latitudes remained vigorous.

Chapter 6

CONCLUSIONS

The purpose of this chapter is twofold: 1) to summarize the conclusions of this study; and 2) recommend areas for future research.

6.1 Summary

The analysis of the 31 May 1985 Tornado Outbreak presented in Chapter 4 reveals that there were four critical factors responsible for the severity of the outbreak: (1) the presence of a lid and a resultant build-up of high θ_w in the PBL, (2) readily available soil moisture, (3) underrunning, and (4) forced ascent associated with baroclinic forcing resulting from a migrating short wave. Because vigorous short-wave troughs move across the northeastern United States several times each Spring and outbreaks of that magnitude rarely occur, it is concluded that the presence of the lid was the most critical factor. The huge latent instability which was present would never have developed without it.

This conclusion is supported by the climatological analysis presented in Chapter 5. First, this analysis determined that lids are in fact very rare events in the northeastern United States. Second, the analysis found two important relationships: (1) the frequency of lid days highly parallels the frequency of tornado occurrences; and (2) lids have a significant impact on the value of θ_w in the PBL, particularly in the north during the Spring. A climatological analysis of θ_{sw5} shows that the relatively intense thermal trough associated with the outbreak was of secondary importance.

These results show that the Carlson-Ludlam Conceptual Model is very useful for understanding the complex interactions among the physical processes which are

responsible for the production of severe weather, and is consequently very successful at determining the location of severe weather inception areas. This model has been proven useful time and time again but the meteorological society at large is still very reluctant to accept and use this model; however, because of its successes, if research on this topic is kept alive, the concept will inevitably be accepted.

6.2 Recommendations For Future Research

- The most obvious and most needed research is to model the case study numerically to determine:
  - The impact of both the lid and the soil moisture in Ohio and New Mexico
  - The true cause of the lid day maximum on the east coast.
- The encouraging results of the preliminary climatological analysis suggest that more in-depth studies would be beneficial. The following list is a few suggestions to pursue:
  - Produce a climatology with a larger period of record (POR) to see if it agrees with the analysis using only the four year POR;
  - Verify if there is a correlation between the fluctuation in lid days and the fluctuation in the frequency of severe weather occurrences;
  - Relate lid *edge* occurrences to the frequency of severe convection;
  - Relate soil moisture climatology (API?) to the location of source regions and the frequency of lid days. Does the severity of droughts in northern Mexico and the Desert Southwest of the United States influence the frequency of severe convection in the Great Plains?
- Determine if vertical refractivity gradients can be used to objectively find lids.
- Relate lid occurrences to significant anomolous propogation events.

REFERENCES

Aleman, Pedro A. Mosino and Enriqueta Garcia, 1974: The Climate of Mexico. World Survey of Climatology, Vol. 11, Climates of North America, Reid A. Bryson and F. Kenneth Hore, eds., H.E. Landsberg ed. in Chief. Elsevier Scientific Publishing Co., New York, 345-391.

Appleby, J.F., 1954: Trajectory method of making short range forecasts of differential temperature advection, instability and moisture. Mon. Wea. Rev., 82, 320-334.

Anthes, R.A., Y.H. Kuo, S.G. Benjamin, and Y.F. Li, 1982: The evolution of the mesoscale environment of severe local storms: Preliminary modeling results. Mon. Wea. Rev., 110, 1187-1213.

Balachandran, N.K., 1980: Gravity waves from thunderstorms. Mon. Wea. Rev., 108, 804-816.

Ball, F.K. 1960: Control of inversion height by surface heating. Quart. Jour. Roy. Meteor. Soc., 86, 483-494.

Beebe, R.G., and F.C. Bates, 1955: A mechanism for assisting in the release of convective instability. Mon. Wea. Rev., 83, 1-10.

Beebe, R.G., 1958: An instability line development as observed by the tornado research airplane. Jour. Meteor., 15, 278-282.

Benjamin, S.G., 1983: Some effects of heating and topography on the regional severe storm environment. Ph.D. thesis, The Dept. of Meteor., The Pennsylvania State University, University Park, PA 16802, 265pp.

Benjamin, S.G., and T.N. Carlson, 1982: Numerical simulations of the severe storm environment for the 10-11 April 1979 (SESAME I) case. Preprints Ninth Conf. on Severe Local Storms, San Antonio, Amer. Meteor. Soc., 201-204.

Benjamin, S.G., and T.N. Carlson, 1986: Some effects of surface heating and topography on the regional severe storm environment, Part I: Three-dimensional simulations. Mon. Wea. Rev., 114, 307-329

Berry F.A. Jr., E. Ballay and N.R. Beers, eds. 1945: Handbook of Meteorology, McGraw-Hill, New York, 1068pp.

Betts, A.K., 1974: Further comments on "A comparison of the equivalent potential temperature and the static energy." Jour. Atmos. Sci., 31, 1713-1715.

Bidner, A., 1970: The AFGWC Severe Weather Threat Index, A Preliminary Report., AWS TR 242, (AD 724093), 229-231.

Bjerknes, J., 1919: On the structure of moving cyclones. Geofysiske Publikasjoner, 1(1), 8pp.; reprinted in J.A.B Bjerknes, Selected Papers (Western Periodicals Company, 1975).

Bjerknes, J. and Solberg H., 1922: Life cycle of cyclones and the polar front theory of atmospheric circulation. Geofysiske Publikasjoner, Norske Bidenskaps-Akod, Oslo, 3(1), 1-18.

Blackadar, A.K., 1957: Boundary-layer wind maxima and their significance for the growth of nocturnal inversions. Bul. Amer. Meteor. Soc., 38, 283-290.

Blanchard, B., M.T. McFarland, T.J. Schmugge, and E. Rhodes, 1981: Estimation of soil moisture with API algorithm and microwave emission. Water Resources Bul., 17, 769-774.

Bluestein, H., and K. Thomas, 1984: Diagnosis of a jet streak in the vicinity of a severe weather outbreak in the Texas Panhandle. Mon. Wea. Rev., 112, 2499-2520.

Bonner, W.D., and J. Paegle, 1970: Diurnal variations in the boundary layer winds over the south-central United States in summer. Mon. Wea. Rev., 98, 735-743.

Brill, K.F., L.W. Uccellini, R.P. Burkhart, T.T. Warner and R.A. Anthes, 1985: Numerical simulations of a transverse indirect circulation and low-level jet in the exit region of an upper-level jet. Jour. Atmos. Sci., 42, 1306-1320.

Brooks, F.A., W.O. Pruitt, D.R. Nielsen and others, 1963: Investigations of energy and mass transfer near the ground including influences of the soil-plant-atmosphere system. Final report, Task 3A99-27-005-08, (15 Dec 1961 to 30 Jun 1963). *Departments of* Agricultural Engineering and Irrigation, University of California, Davis CA. Under contract number DA-36-039-SC-80334. 285pp. (AD410263).

Burkhart, R.P., 1980: Subsynoptic scale processes leading to the development of severe weather in the vicinity of an upper level jet streak. M.S. thesis, The Dept. of Meteor., The Pennsylvania State University, University Park, PA 16802, 101pp.

Caracena, F. and J.M. Fritsch, 1983: Focusing mechanisms in the Texas Hill Country flash floods of 1978. Mon. Wea. Rev., 111, 2319-2332.

Cahir, J.J., 1971: Implications of circulations in the vicinity of jet streaks at subsynoptic scales. Ph.D. thesis, The Dept. of Meteor., The Pennsylvania State University, University Park, PA 16802, 170pp.

Carlson, T.N. and F.H. Ludlam, 1965: Research on characteristics and effects of severe storms, Part I: Large scale conditions for the occurrence of severe local storms. Annual Summary Report Number 1, Grant AF EOAR 64-60, 146pp.

Carlson, T.N. and F.H. Ludlam, 1968: Conditions for the occurrence of severe local storms. Tellus, 20, 203-226.

Carlson, T.N. and J.M. Prospero, 1972: The large-scale movement of Saharan air outbreaks over the Northern Equatorial Atlantic. Jour. Appl. Meteor., 11, 283-297.

Carlson, T.N. and J.M. Prospero, 1973: An aircraft investigation of the Saharan air layer and the Saharan air front. Project Stormfury Annual Report 1972, National Hurricane Research Laboratory, Coral Gables, FL; NOAA- 74071702, [NTIS COM-74-11431/5], 131-147.

Carlson, T.N., R.A. Anthes, M. Schwartz, S.G. Benjamin and D.G. Baldwin, 1980: Analysis and prediction of severe storms environment. Bul. Amer. Meteor. Soc., 61, 1018-1032.

Carlson, T.N. and S.G. Benjamin, 1980: Radiative heating rates for Saharan dust. Jour. Atmos. Sci., 37, No. 1, 193-213.

Carlson, Toby N. and Robert J. Farrell, 1983: The lid strength index as an aid in predicting severe local storms. National Weather Digest, 8, 27-39.

Carlson, T.N., S.G. Benjamin, G.S. Forbes and Y.F. Li, 1983: Elevated mixed layers in the regional severe storm environment: Conceptual model and case studies. Mon. Wea. Rev., 111, 1453-1473.

Carson, D.J., 1973: The Development of a dry inversion-capped unstable boundary layer. Quart. Jour. Roy. Meteor. Soc., 99, 450-467.

Changery, M.J., 1981: National Thunderstorm Frequencies for the Contiguous United States. U.S. Nuclear Regulatory Commission/CR2252.

Colon, J., 1964: On interrelations between the southwest monsoon current and the sea surface over the Arabian Sea. Indian Jour. of Meteor. Geophys., 15, 183-198.

Court, Arnold, 1974: The Climate of the Conterminous United States. World Survey of Climatology, Vol. 11, Climates of North America, Reid A. Bryson and F. Kenneth Hare., eds., H.E. Landsberg, ed. in Chief. Elsevier Scientific Publishing Co., New York, p. 223.

Crumrine, H.A., 1965: The use of the horizontal temperature advection, the 850-500mb shear wind in severe local storms forecasting. Paper presented at 244th National meeting of Amer. Meteor. Soc. on Cloud Physics and Severe Local Storms, October 18-22, 1965, Reno, Nev.

Danielsen, E.F., 1974a: The relationship between severe weather, major dust storms and rapid cyclogenesis. Part I. Synoptic Extratropical Weather Systems: Observations, Analysis, Modeling, and Prediction. Notes from a colloquim Summer, 1974, Vol. II, M. Shapiro Ed., NCAR, 215-241.

Danielsen, E.F., 1974b: A conceptual theory of tornadogenesis: Part I. Large scale generation of severe storm potentials. Synoptic Extratropical Weather Systems: Observations, Analysis, Modeling, and Prediction. Notes from a colloquim Summer, 1974, Vol. II, M. Shapiro Ed., NSF, 247-286.

Darkow, G.L., 1968: The total energy environment of severe storms. Jour. Applied Meteor., 7, 199-205.

David, C.L. and J.S. Smith, 1971: An evaluation of seven stability indices as predictors of severe thunderstorms and tornadoes. Preprints Seventh Conference on Severe Local Storms, Kansas City, MO, Amer. Meteor. Soc., 105-109.

Diaz, H.F., Toby N. Carlson and Joseph M. Prospero, 1976: A Study of the Structure and Dynamics of the Saharan Air Layer Over the Northern Equatorial Atlantic During BOMEX, NOAA Tech. Memo. ERL WMPO-32, 61pp.

Dodd, A., 1965: Dewpoint distribution in the contiguous U.S. Mon. Wea. Rev., 93, 113-122.

Doswell, C.A. III, 1982: The Operational Meteorology of Convective Weather. Vol. 1: Operational Mesoanalysis. [NOAA Tech. Memo NWS NSSFC-5] Air Weather Service Tech. Note 83/001, Air Weather Service, 172pp.

Doviak, Richard J., and Dusan S. Zrnić, 1984: Doppler Radar and Weather Observations, Academic Press Inc., Orlando FL, 458pp.

Dutton, John A., 1976: The Ceaseless Wind. An Introduction to the Theory of Atmospheric Motion, McGraw-Hill, New York, 579 pp.

Dyer. A.J., 1961: Measurements of evaporation and heat transfer in the lower atmosphere by an automatic eddy-correlation technique. Quart. Jour. Roy. Meteor. Soc., 87, 401-412.

Dyer, A.J., 1967: The turbulent transport of heat and water vapour in an unstable atmosphere. Quart. Jour. Roy. Meteor. Soc., 93, 501-508.

Eliassen, A., 1951: Slow thermally or frictionally controlled peridional circulation in circulations in a circular vortex. Astrophys. Norv., 5, 19-66.

Eliassen, A., 1962: On the vertical circulations in frontal zones. Geofysiske Publikasjoner, 24 (4), 147-160.

ESSA (Environmental Science Services Administration), 1981: Radiosonde Observations. Federal Meteorological Handbook No. 3, Silver Spring, MD.

Estoque, M.A., 1968: Vertical mixing due to penetrative convection. Jour. Atmos. Sci., 25, 1046-1051.

Farrell, Robert J. and Toby N. Carlson, 1988: The role of the lid in the May 31, 1985 tornado outbreak Preprints Fifteenth Conference on Severe Local Storms. Baltimore MD, Amer. Meteor. Soc., 257-262.

Fawbush, E.J., R.C. Miller, and L.G. Starrett, 1951: An empirical method of forecasting tornado development. Bul. Amer. Meteor. Soc., 32, 1-9.

Fawbush, E.J. and R.C. Miller, 1952: A mean sounding of the tornado airmass environment. Bul. Amer. Meteor. Soc., 33(7), 303-307.

Fawbush, E.J. and R.C. Miller, 1954: The types of air masses in which North American tornadoes form. Bul. Amer. Meteor. Soc., 35(4), 154-165.

Ferguson, E.W., F.P. Ostby and P.W. Leftwich, Jr., 1986: 1985 - An average year for tornadoes. Weatherwise, 39, 33-39.

Ferguson, Edward W., Frederick P. Ostby, and Preston W. Leftwich Jr., 1987: The tornado season of 1985. Mon. Wea. Rev., 115, 1437-1445.

Ferrel, W., 1895: Recent advances in meteorology. Report of the Chief Signal Officer for 1885, Appendix 71, 324-325, 327.

Feteris, P.J., 1978: Interaction between mesoscale flow and cumulus convective systems - A forecast problem. Preprints Seventh Conference on Weather Analysis and Forecasting, Silver Spring, MD, Amer. Meteor. Soc., 102-105.

Finley, J.P., 1885: Tornado studies for 1884. U.S. Signal Corps Professional Paper No. 16, Washington D.C.

Finley, J.P., 1890: Tornadoes. Am. Meteor. Jour., 7, 165-179.

Forbes, G.S., P.O.G. Heppner, J.J. Cahir, and W.D. Lottes, 1984: Prediction of delayed-onset nocturnal convection based on air trajectories. Preprints Tenth Conference on Weather Forecasting and Analysis, Clearwater Beach, FL, Amer. Meteor. Soc., 474-479.

Forbes, G.S., 1985: Preliminary tornado statistics - - May 31, 1985 outbreak. Weatherwise, 38, 194-195.

Fujita, T.T., 1958: Structure and movement of a dry front. Bul. Amer. Meteor. Soc., 39(11), 574-582.

Fujita, T.T., D.L. Bradbury and C.F. VanThullenar, 1970: Palm Sunday tornadoes of April 11, 1965. Mon. Wea. Rev., 98, 29-69.

Fujita, T.T., 1971: Proposed Characterization of Tornadoes and Hurricanes by Area and Intensity. SMRP Research Paper No. 91, University of Chicago, 42pp.

Fulks, J.R., 1951: The instability line. Compendium of Meteorology, Amer. Meteor. Soc., 647-652.

Galway, J.G., 1956: The lifted index as a predictor of latent instability. Bul. Amer. Meteor. Soc., 37(10), 528-529.

Gates, W.L., 1961: Static stability measures in the atmosphere. Jour. of Meteor., 18, 526-533.

George, J.J., 1960: Weather Forecasting for Aeronautics, Academic Press, New York, 673pp.

Gesser, F. and D. Wallace, 1985: The Forecast Sounding. AWS/FM-85-001, Air Weather Service, Scott AFB, IL 62225, 13pp.

Goldman, J.D., 1981: A conceptual model and its application in the analysis of severe convective storm simulations. M.S. thesis, The Dept. of Meteor., The Pennsylvania State University, University Park, PA 16802, 98pp.

Graziano, Thomas M. and Toby N. Carlson, 1987: A statistical evaluation of lid strength on deep convection. Weather and Forecasting, 2, 127-139.

Graziano, Thomas M., 1985: A statistical determination of the critical Lid strength and its implications to severe weather forecasting. M.S. Thesis., The Dept. of Meteor., The Pennsylvania State University, University Park, PA 16802, 191pp.

Green, J.S.A., F.H. Ludlam and J.F.R. McIlveen, 1965: Research on characteristics and effects of severe storms, Part II: The Analysis of Atmospheric Motion Systems, Annual Summary Report Number 1. Grant AF EOAR 64-60, 75-88.

Green, J.S.A., F.H. Ludlam and J.F.R. McIlveen, 1966: Isentropic relative-flow analysis and the parcel theory. Quart. Jour. Roy. Meteor. Soc., 92, 210-219.

Halstead, M.H., 1954: Publications in Climatology, John Hopkins University, 7, 353pp.

Harlan, J.C., 1980: Dryland pasture and crop conditions as seen by HCMM. Report to HCMM investigators meeting, 24-26 November, NASA/GSFC, Greenbelt, MD. Unpublished manuscript.

Harley, William S., 1971: Convective storm diagnosis and prediction using two layer combined indices of potential and latent instability in combination with other special and standard significators. Preprints Seventh Conference on Severe Local Storms, Boston MA, Amer. Meteor. Soc., 23-30.

Heppner, P.O.G., 1984: Application of an Air Trajectory Model to Test a Theory Concerning Nocturnal Thunderstorm Development. M.S. Thesis, Dept. of Meteor., The Pennsylvania State University, University Park, PA 16802.

House, D.C., 1959: The mechanics of instability-line formation. Jour. Meteor., 16, 108-124.

Hoxit, L.R. and C.F. Chappell, 1975: Tornado outbreak of April 3-4, 1974, Synoptic Analysis, NOAA Technical report, NOAA TR ERL 338-APCL 37, U.S. Dept. of Commerce, 48pp.

Humphreys, W.J., 1926: The Tornado. Mon. Wea. Rev., 54, 501-503.

Humphreys, W.J., 1940: Physics of the Air, 3rd ed., McGraw-Hill, New York, 676 pp.

Hung, R.J., T. Phan, D.C. Lin, R.E. Smith, R.R. Jayroe and G.S. West, 1980: Gravity waves and GOES IR data study of an isolated tornadic storm on 29 May 1977. Mon. Wea. Rev., 108, 456-464.

Huschke, R.E. ed., 1959: Glossary of Meteorology, Amer. Meteor. Soc., Boston MA, 3rd printing, 1980, 638pp.

Jakl, V.J., 1944: Pressure gradient wind and tornadoes. Jour. Aeronautical Meteor., 1(1), 16-22.

James, R.W., 1951: The structure of mean circulation. Tellus, 3(4), 258-267.

Karyampudi, V.M., 1979: A detailed synoptic-scale study of the structure, dynamics and radiative effects of the Saharan air layer of the Eastern Tropical Atlantic during the GARP Atlantic Tropical Experiment. M.S. Thesis, Dept. of Meteor., The Pennsylvania State University, University Park, PA 16802, 136pp.

Karyampudi, V.M., 1986: A numerical study of the evolution, structure and energetics of the Saharan air layer. Ph.D. Thesis, The Dept. of Meteor., The Pennsylvania State University, University Park, PA 16802, 287.

Keyser, Daniel, and Toby N. Carlson, 1984: Transverse ageostrophic circulations associated with elevated mixed layers. Mon. Wea. Rev., 112, 2465-2478.

Koch, S.E., 1979: Mesoscale gravity waves as a possible trigger of severe convection along a dryline. Ph.D. Thesis, The Dept. of Meteor., University of Oklahoma OK, 195pp.

Koch, S.E. and J. McCarthy, 1982: The evolution of an Oklahoma dryline. Part II: Boundary-layer forcing of mesoconvective systems. Jour. Atmos. Sci., 39, 237-257.

Lakhtakia, M.N., 1985: A real-data numerical simulation of a severe local-storm environment: The SESAME IV Case. M.S. Thesis, Dept. of Meteor., The Pennsylvania State University, University Park, PA 16802, 81pp.

Lakhtakia, M.N. and T.T. Warner, 1987: A real-data numerical study of the development of precipitation along the edge of an elevated mixed layer. Mon. Wea. Rev., 115, 156-168.

Lanicci, J.M., 1984a: The influence of soil moisture distribution on the severe-storm environment of the southern great plains: A numerical study of the SESAME IV Case. M.S. Thesis, The Dept. of Meteor., The Pennsylvania State University, University Park, PA 16802, 237pp.

Lanicci, J.M., 1984b: A Conceptual Model of the Severe-Storm Environment for Inclusion into Air Weather Service Severe-Storm Analysis and Forecast Procedures. AFGL-TR-84-0311, Air Force Geophysics Laboratory, Hansom AFB, MA, 84pp.

Lemons, H., 1939: Temperature and vapor pressure as factors in tornadic inception in Nebraska. Bul. Amer. Meteor. Soc., 20 (2), 49-50.

Levine, J., 1972: Comments on "A comparison of the equivalent potential temperature and the static energy". Jour. Atmos. Sci., 29, 201-202.

Lilly, D.K., 1968: Models of cloud-topped mixed layers under a strong inversion. Quart. Jour. Roy. Meteor. Soc., 94, 292-309.

Lloyd, J.R., 1942: The development and trajectories of tornadoes. Mon. Wea. Rev., 70, 65-75.

Long, M.J., 1966: A preliminary climatology of thunderstorm penetrations of the tropopause in the United States. Jour. Appl. Meteor., 5, 467-473.

Ludlam, F.H., 1963: Severe local storms, a review. Meteor. Monographs. No. 27, 5, Amer. Meteor. Soc..

Madden, R.A., and F.G. Robitaille, 1970: A comparison of the equivalent potential temperature and the static energy. Jour. Atmos. Sci., 27, 327-329.

Maddox, R.A., D.M. Rodgers, W. Deitrich, and D.L. Bartels, 1981: Meteorological Settings Associated with Significant Convective Storms in Colorado. NOAA Tech. Memo. ERL OWRM-4, Office of Weather Research and Modification, Boulder, CO, 75pp.

Malkus, J., 1958: On the structure of the trade wind moist layer. Papers Phys. Oceanogr. Meteor., 13(2), 75pp.

Marht, L., 1976: Mixed layer moisture structure. Mon. Wea. Rev., 104, 1403-1407.

Matsumoto, S. and T. Akiyama, 1970: Mesoscale disturbances and related rainfall cells embedded in the "Baiu Front" with a proposal on the role of convective momentum transfer. Jour. Meteor. Soc., Japan, 48, 91-102.

McCarthy J. and S.E. Koch, 1982: The evolution of an Oklahoma dryline. Part I: Meso- and subsynoptic-scale analysis. Jour. Atmos. Sci., 39, 225-236.

McGuire, E.L., 1962: The Vertical Structure of Three Drylines as Revealed By Aircraft Traverses, NSSP Staff Report No. 7, U.S. Weather Bureau, 10pp.

McNider, R.T. and R.A. Pielke, 1981: Diurnal boundary-layer development over sloping terrain. Jour. Atmos. Sci., 38, 2198-2212.

McNulty, R.P., 1980: Differential advection of wet-bulb potential temperature and convective development: An evaluation. Preprints Eighth Conference on Weather Analysis and Forecasting. Denver, Amer. Meteor. Soc., 286-291.

Means, L.L., 1944: The nocturnal maximum occurrence of thunderstorms in the Mid-western States. Misc. Report No. 16, Dept. of Meteor., University of Chicago, Chicago, IL, 38pp.

Means, L.L., 1952: On thunderstorm forecasting in the central United States. Mon. Wea. Rev., 80, 165-189.

Miller, G.K., W.B. Moreland, and L.N. Ortenburger, 1979: Radiosonde Data Analysis III, World Contour Maps, Elevated Duct Percent Occurrence, Elevated, Superrefracting Layer Percent Occurrence, Elevated Duct Coverage Height. Contract: MDA-904-78- C-0511, GTE Sylvania Inc., Electronic Systems Group, Western Division, Mountain View, CA, 94042, 39pp.

Miller, James E., 1955: Intensification of precipitation by differential advection. Jour. Meteor., 12, 472-477.

Miller, R.C., 1959: Tornado-producing synoptic patterns. Bul. Amer. Meteor. Soc., 40, 465-472.

Miller, R.C., 1967: Notes on Analysis and Severe-Storm Forecasting Procedures of the Military Weather Warning Center, AWSTR 200, Air Weather Service (MAC), United States Air Force, Scott AFB, IL 62225, 162pp.

Miller, Robert C., 1972: Notes on Analysis and Severe-Storm Forecasting Procedures of the Air Force Global Weather Central. AWSTR 200 (Rev.), Air Weather Service (MAC), United States Air Force, Scott AFB, IL 62225, 190pp.

Monteith, J.L., 1973: Principles of Environmental Physics., American Elsevier, New York, 241pp.

Newton, C.W., 1963: Dynamics of severe convective storms. Severe Local Storms Meteor. Monogr., No. 27, Amer. Meteor. Soc., 33-58.

Newton, C.W., 1967: Severe convective storms. Advances in Geophysics, Vol. 12, Academic Press, 257-303.

NSSP Staff (National Severe Storms Project Staff Members, U.S. Weather Bureau), 1963: Environmental and thunderstorm structures as shown by National Severe Storms Project observations in Spring 1960 and 1961. Mon. Wea. Rev., 91, 271-292.

Ogura, Y. and Y. Chen, 1977: A life history of an intense mesoscale convective storm in Oklahoma. Jour. Atmos. Sci., 34, 1458-1478.

Ogura, Y., H.M. Juang, K.S. Zhang and S.T. Soong, 1982: Possible triggering mechanisms for severe storms in SESAME-AVE IV (9-10 May 1979). Bul. Amer. Meteor. Soc., 63(5), 503-515.

Orlanski, I., 1975: A rational subdivision of scales for atmospheric processes. Bul. Amer. Meteor. Soc., 56(5), 527-530.

Ortenburger, L.N., S.B. Lawson, and B.J. Patterson, 1985: Radiosonde Data Analysis III, Monthly Statistical Report, Tropospheric Ducting, Vol.3, Contract: MDA-904-84-C-6002, GTE Sylvania Inc., Electronic Systems Group, Western Division, Mountain View, CA, 94042.

Palmén, E. and C.W. Newton, 1969: Atmospheric Circulation Systems, Academic Press, 603pp.

Penman, H.L., 1956: Evaporation: An introductory survey. Netherlands Jour. of Agricultural Sci., 4, 9p.

Penn, Samuel, Charles Pierce, and James K. McGuire, 1955: The squall line and Massachusetts tornadoes of June 9, 1953. Bul. Amer. Meteor. Soc., 36(3), 109-122.

Peterson, R.A., 1979: A cross-sectional approach to three-dimensional analysis. Preprints Fourth Conference on Numerical Weather Prediction, Silver Springs, Amer. Meteor. Soc., 35-42.

Petterssen, S., 1956a: Weather Analysis and Forecasting, Vol. 1, 2ed., McGrawHill, New York. 428pp.

Petterssen, S., 1956b: Weather Analysis and Forecasting, Vol. 2, 2ed., McGrawHill, New York. 266pp.

Porter, J.M., L.L. Means, J.E. Hovde, and W.B. Chappell, 1955: A synoptic study on the formation of squall lines in the north central U.S. Bul. Amer. Meteor. Soc., 36(8), 390-396.

Ramaswamy, C., 1956: On the sub-tropical jet stream and its role in the development of large-scale convection. Tellus, 8, 26-60.

Reiter, E.R., 1963: Jet-Stream Meteorology, University of Chicago Press, Chicago, IL, 515pp.

Rhea, J.O., 1966: A study of thunderstorm formation along dry lines. Jour. Appl. Meteor., 5, 58-63.

Riehl, H., M.A. Alaka, C.L. Jordan and R.J. Renard, 1954: The jet stream. Meteorological Monographs, Amer. Meteor. Soc., 100pp.

Roe, Charlotte, and Joseph Vederman, 1952: September rains in the southwest United States. Mon. Wea. Rev., 80, 156-160.

Saxton, K.E. and A.T. Lenz, 1967: Antecedent retention indices predict soil moisture. Journal of the Hydrolics Division, Procedures of the American Society of Civil Engineers, July 1967.

Saucier, W.J., 1955: Principles of Meteorological Analysis, University of Chicago Press. Chicago, IL. 438pp.

Schaefer, J.T., 1973: The motion and morphology of the dryline, NOAA Technical Memorandum ERL NSSL-66, Norman OK, 81pp.

Schaefer, J.T., 1974a: The life cycle of the dryline. Jour. Atmos. Sci., 13, 444-449.

Schaefer, J.T., 1974b: A simulative model of dry line motion. Jour. Atmos. Sci., 31, 956-964.

Schaefer, J.T., 1975: Nonlinear biconstituent diffusion: A possible trigger of convection. Jour. Atmos. Sci., 32, 2278-2284.

Schaefer, J.T., 1976: Moisture features in the convective boundarylayer in Oklahoma. Quart. Jour. Roy. Meteor. Soc., 102, 447-450.

Schwartz, M.N., 1980: Synoptic and mesoscale stability analysis of the Red River Valley severe storm outbreak of 10 April 1979. M.S. Thesis, The Dept. of Meteor., The Pennsylvania State University, University Park, PA 16802, 94pp.

Shapiro, M.A., 1981: Frontogenesis and geostrophically forced secondary circulations in the vicinity of jet stream-frontal zone systems. Jour. Atmos. Sci., 38, 954-973.

Shapiro, M.A., 1982: Mesoscale Weather Systems of the Central United States, CIRES NOAA, University of Colorado. 78pp.

Showalter, A.K. and J.R. Fulks, 1943: Preliminary Report on Tornadoes: The Tornado, an Analysis of Antecedent Meteorological Conditions. U.S. Weather Bureau, Washington D.C., 162pp. Reprinted by U.S. Office of Naval Operations as its NAVAER 50-1R-41, 1950.

Showalter, A.K., 1953: A stability index for thunderstorm forecasting. Bul. Amer. Meteor. Soc., 34 (6), 250-252.

Silberstein, David Steven, 1983: An analysis of Southwest Asian elevated mixed layers over the Arabian Sea during the Summer Monsoon Experiment. M.S. Thesis, Dept. of Meteor., The Pennsylvania State University, University Park, PA 16802, 94pp.

Staley, D.O., 1965: Radiative cooling in the vicinity of inversions and the tropopause. Quart. Jour. Roy. Meteor. Soc., 96, 282-301.

Storm Data, May 1985, 27, No. 5, National Climatic Data Center, NOAA. (ISSN 0039-1972).

Storm Data, June 1985, 27, No. 6, National Climatic Data Center, NOAA. (ISSN 0039-1972).

Storm Data, October 1985, 27, No. 10, National Climatic Data Center, NOAA. (ISSN 0039-1972).

Sugg, A.L., and D.S. Foster, 1954: Oklahoma tornadoes. Mon. Wea. Rev., 82, 131-140.

Sun, W.Y. and Y. Ogura, 1979: Boundary-layer forcing as a possible trigger to a squall-line formation. Jour. Atmos. Sci., 36, 235-254.

Taggart K., R. Waganer, J. Campbell ,S. Wasserman, D. Witten, F. Makosky, and G. Forbes, 1985: Natural Disaster Survey Report to the Administrator. National Oceanic and Atmospheric Administration, NOAA, Severe Weather Branch, Silver Spring MD 20910, 69pp.

Tennekes, H., 1973: A model for the dynamics of the inversion above a convective boundary layer. Jour. Atmos. Sci., 30, 556-567.

Uccellini, L.W., 1975: A case study of apparent gravity wave initiation of severe convective storms. Mon. Wea. Rev., 103, 497-513.

Uccellini, L.W. and D.R. Johnson, 1979: The coupling of upper and lower tropospheric jet streaks and implications for the development of severe convective storms. Mon. Wea. Rev., 107, 682-703.

U.S. Weather Bureau, 1939: On synoptic conditions for tornadoes. Bul. Amer. Meteor. Soc., 20(2), 50-51.

Varney, B.M., 1926: Aerological evidence as to the causes of tornadoes. Mon. Wea. Rev., 54, 163-165.

Wagner, A. James, 1986: The 700mb circulation during 1985 over the northern hemisphere: A year of extremes. Weatherwise, 39, 16-20.

Warner, J., 1963: Observations relating to theoretical models of a thermal. Jour. Atmos. Sci., 20, 546-550.

Weisman, M.L. and J.B. Klemp, 1982: The dependence of numerically simulated convective storms on vertical wind shear and buoyancy. Mon. Wea. Rev., 110, 504-520.

Wessels, H.R.A., 1968: De zware windhozen van 25 juni 1967. Hemel en Dampkring, 66, 155-178.

Weston, K.J., 1972: The dryline of northern India and its role in cumulonimbus convection. Quart. Jour. Roy. Meteor. Soc., 98, 519-531.

Wetzel, P.J. and D. Atlas, 1981: Inference of precipitation through thermal infrared measurements of soil moisture. Precipitation measurements from space workshop report, D. Atlas and O.W. Thiele, eds., Goddard Laboratory for Atmospheric Sciences, Goddard Space Flight Center, Greenbelt, MD, 23, p. D-170 to D-172.

Wexler, H., 1961: A boundary layer interpretation of the low-level jet. Tellus, 13 369-378.

Whitney, L.F. Jr. and J.E. Miller, 1956: Destabilization by differential advection in the tornado situation of 8 June 1953. Bul. Amer. Meteor. Soc., 37(5), 224-229.

Williams, W.E., 1971: The relationship of some cirrus formations to severe local storms. Preprints Seventh Conference on Severe Local Storms, Boston MA, Amer. Meteor. Soc., 128-133.

Wills, T.G., 1969: Characteristics of the tornado environment as deduced from proximity soundings. Preprints Sixth Conference on Severe Local Storms, Boston MA, Amer. Meteor. Soc., 222-229.